(19) Canadian Intellectual Property Office
An Agency of Industry Canada

Office de la Propriété Intellectuelle du Canada
Un organisme d'Industrie Canada

(11) CA 2 467 329 (13) A1

(40) 14.11.2005
(43) 14.11.2005

(12)

(21) 2 467 329

(22) 14.05.2004

(51) Int. Cl.[7]: A61K 39/102, A61K 39/02, A61P 31/04, A61K 31/739

(71) NATIONAL RESEARCH COUNCIL OF CANADA, Montreal Road, OTTAWA, O1 (CA).

(72) COX, ANDREW (CA).
RICHARDS, JAMES C. (CA).

(74) MCKAY, MARGARET H.

(54) EPITOPES A LIPOPOLYSACCHARIDES DU NOYAU CENTRAL ET LEURS APPLICATIONS
(54) INNER CORE LPS EPITOPES AND USES THEREOF

(57)

The subject invention provides vaccines, vaccine components, and uses thereof suitable for providing immunity involving B-cell activating molecules derived from veterinary bacterial pathogens lipopolysaccharide (LPS), said molecules comprising one or more epitopes of the inner-core oligosaccharide portion of the lipopolysaccharide having the structure: <IMG> A Figure 1 Where R and R' are variable outer care structures.

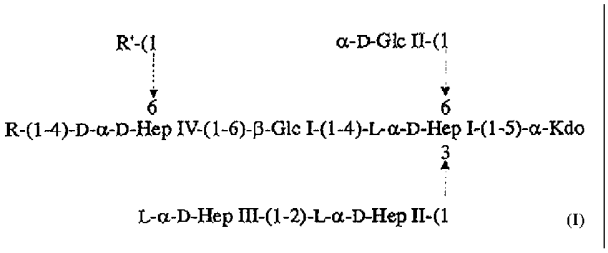

Office de la Propriété Intellectuelle du Canada
Un organisme d'Industrie Canada

Canadian Intellectual Property Office
An agency of Industry Canada

CA 2467329 A1 2005/11/14

(21) 2 467 329

(12) DEMANDE DE BREVET CANADIEN
CANADIAN PATENT APPLICATION

(13) A1

(22) Date de dépôt/Filing Date: 2004/05/14

(41) Mise à la disp. pub./Open to Public Insp.: 2005/11/14

(51) Cl.Int.^{7}/Int.Cl.^{7} A61K 39/102, A61K 31/739, A61P 31/04, A61K 39/02

(71) Demandeur/Applicant:
NATIONAL RESEARCH COUNCIL OF CANADA, CA

(72) Inventeurs/Inventors:
COX, ANDREW, CA;
RICHARDS, JAMES C., CA

(74) Agent: MCKAY, MARGARET H.

(54) Titre : EPITOPES A LIPOPOLYSACCHARIDES DU NOYAU CENTRAL ET LEURS APPLICATIONS
(54) Title: INNER CORE LPS EPITOPES AND USES THEREOF

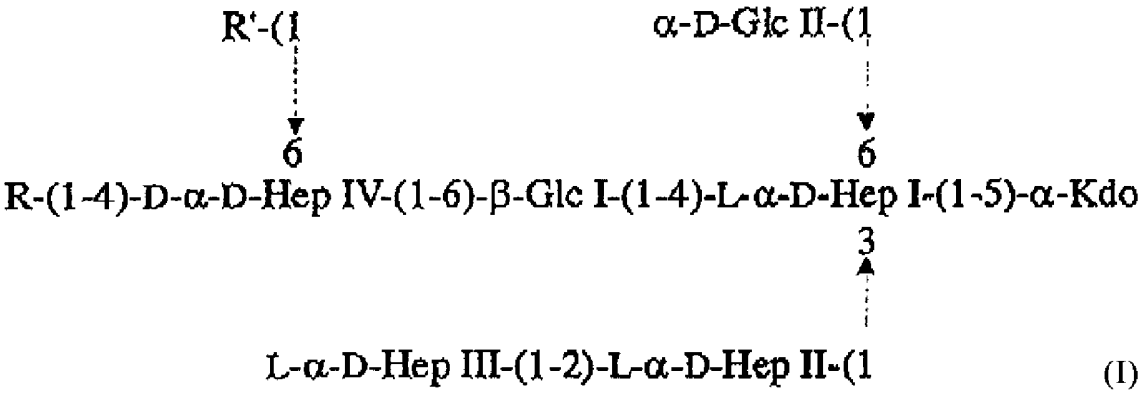

(I)

(57) Abrégé/Abstract:
The subject invention provides vaccines, vaccine components, and uses thereof suitable for providing immunity involving B-cell activating molecules derived from veterinary bacterial pathogens lipopolysaccharide (LPS), said molecules comprising one or more epitopes of the inner-core oligosaccharide portion of the lipopolysaccharide having the structure: (see formula I) A Figure 1 Where R and R' are variable outer core structures.

ABSTRACT

The subject invention provides vaccines, vaccine components, and uses thereof suitable for providing immunity involving B-cell activating molecules derived from veterinary bacterial pathogens lipopolysaccharide (LPS), said molecules comprising one or more epitopes of the inner-core oligosaccharide portion of the lipopolysaccharide having the structure:

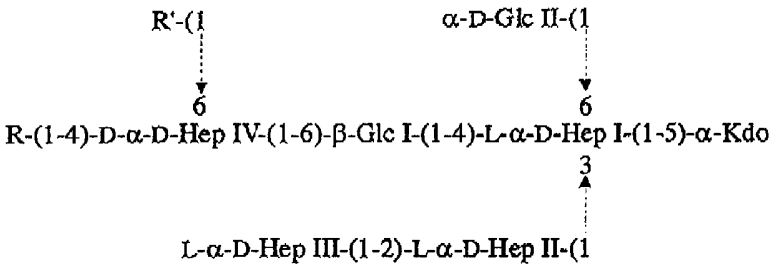

A Figure 1

Where R and R' are variable outer core structures.

Application number / numéro de demande: 2467329

Figures: 8, 10.

Pages: 25/92, 30/92.

Disclosure.

Unscannable items
received with this application
(Request original documents in File Prep. Section on the 10th floor)

Documents reçu avec cette demande ne pouvant être balayés
(Commander les documents originaux dans la section de préparation des dossiers au 10ème étage)

Title: **Inner Core LPS Epitopes and Uses Thereof**

Bacterial pathogens are a significant cause of economic loss in commercial farm operations as well as a health issue in a wide range of animal populations, including humans.

Three of the most common bacterial pathogens involved in veterinary diseases are *Mannheimia (Pasteurella) haemolytica (Mh), Actinobacillus pleuropneumoniae (App)* and *Pasteurella multocida (Pm). Mh* is primarily a bovine and ovine pathogen, *App* is a porcine pathogen and *Pm* is a multi-species pathogen including poultry, cattle and swine, and is also the causative agent of dog and cat bite infections in humans. Taken together they cause diseases resulting in major economic losses to the animal farming industry.

It would be useful to have a vaccine against pathogenic bacteria of concern.

Current practice involves using bacterins or crudely modified live strains as vaccines. Such approaches are not entirely satisfactory as effectiveness can be inadequate and there is a significant incidence of adverse effects.

The subject invention provides vaccines, vaccine components, and uses thereof suitable for providing immunity involving B-cell activating molecules derived from veterinary bacterial pathogens lipopolysaccharide (LPS), said molecules comprising one or more epitopes of the inner-core oligosaccharide portion of the lipopolysaccharide. The disclosure herein identifies and characterizes epitopes that are expressed on the LPS of bacterial veterinary pathogens across a range of disease causing isolates including but not necessarily limited to *Actinobacillus pleuropneumoniae (Ap), Mannheimia haemolytica (Mh)* and *Pasteurella multocida (Pm).*

There is identified herein a defined sub-unit antigen suitable for use in the manufacture of vaccines. Antigens which are vaccine candidates are preferably displayed on the surface of the bacteria in its natural state in order for the immune response to the vaccine antigen to subsequently target the live organism.

In this context veterinary organisms of interest contain surface exposed carbohydrate moieties that can be considered as vaccine candidates. These carbohydrate moieties include LPS and capsular polysaccharides. Capsular polysaccharides are repeating units of several carbohydrate residues directly linked to the bacterial surface whereas LPS consists of three regions, a lipid A region that links the LPS molecule to the bacterial surface via fatty acid residues, a relatively conserved core oligosaccharide region which links the lipid A region to the third region, the variable polysaccharide antigen (O-antigen). The heterogeneity of the capsular and O-antigenic polysaccharides from strain to strain would ordinarily preclude them as economically viable vaccine candidates due to their ability to provide coverage only to homologous strains. However, disclosed herein are carbohydrate structures useful as vaccine antigens.

The herein disclosed inner core LPS structure has been identified in *Ap*, *Mh* and *Pm*. This structure is useful as a vaccine candidate that provides broad coverage to all strains. The unexpected finding that all three species elaborate this identical structural unit, allows the preparation of multi-species vaccines based on this one conserved structure.

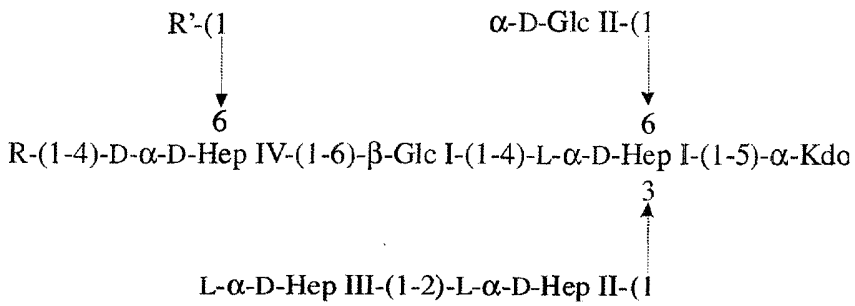

A Figure 1

Where R and R' are variable outer core structures. The structural analyses performed to characterize these conserved structures in each species are detailed in Examples 1, *Mh*; 2, *Ap* and 3 & 5, *Pm*. Example 1 describes the structural analysis of the serotype A1 LPS of *Pasteurella haemolytica*. Example 2 describes the structural analysis of the LPS from several serotypes of *Ap* whereby the structural relatedness of the inner core molecules of *Mh* and *Ap* was first identified. Example 3 describes the structural analysis of the LPS from the genome strain of *Pm* whereby the structural conservation of the inner core molecules of all three species was first identified. Example 4 provides a summary of core oligosaccharide structures elucidated from these veterinary pathogens illustrating the conservation of the inner core oligosaccharide molecule. Example 5 describes the conserved inner core structure of a second *Pm* strain.

Vaccines comprised of capsular polysaccharides are effective at preventing human disease caused by the homologous encapsulated bacteria. These carbohydrate antigens are often poorly immunogenic in humans due to a lack of T-cell dependent response. However, by conjugating the specific polysaccharide antigen to a suitable protein carrier, the immunogenicity of the carbohydrate antigen can be greatly enhanced over the polysaccharide alone. Glycoconjugate vaccines based on the specific capsular polysaccharide of type b *H. influenzae* (Hib), and type c *Neisseria meningitidis* e.g. ProHiBit, MenC, have already proven successful in the control of invasive Hib and meningococcal diseases.

The general strategy is to conjugate the conserved inner core LPS molecule in an appropriate manner to a suitable carrier molecule in order to elicit the desired immune response following immunisation of the host.

An immunogenic carrier protein is preferably selected from the group consisting of tetanus toxin/toxoid, cross-reacting material (CRM), NTHi high molecular weight protein, diphtheria toxin/toxoid, detoxified P. aeruginosa toxin A, cholera toxin/toxoid, pertussis toxin/toxoid, Clostridium perfringens exotoxins/toxoid, hepatitis B surface antigen, hepatitis B core antigen, rotavirus VP 7 protein, respiratory syncytial virus F and G proteins or other suitable carrier.

hepatitis B surface antigen, hepatitis B core antigen, rotavirus VP 7 protein, respiratory syncytial virus F and G proteins or other suitable carrier.

An adjuvant is preferably selected from the group consisting of Freund's adjuvant, alum and Ribi or any other pharmaceutically acceptable adjuvant.

In an embodiment of the invention there is provided a method of inducing or increasing immunity in an animal, fish or bird against a bacterial pathogen comprising administering a conserved inner core LPS molecule. In some instances the bacterial pathogen will be a variety of Mannheimia, Actinobacillus, or Pasteurella. In some instances the bacterial pathogen will be a veterinary organism of interest. In some instances the bacterial pathogen will be Actinobacillus suis. Administration may be by any suitable route, including injection, application to a mucous membrane, transdermal application, oral (preferably suitably coated), etc. In some instances the inner core LPS molecule will be linked or associated with a suitable carrier molecule. In some instances a suitable adjuvant will also be used. In some instances the inner core LPS will be co-administered with an antibacterial drug or another immune stimulation. In some instances the conserved inner core LPS molecule will be the inner core LPS of A Figure 1. In some instances the conserved inner core LPS molecule will be the inner core LPS of A Figure 1 without one or both R and R^1 as defined therein. In some instances the conserved inner core LPS will be at least one of the following:

a) $Hex_3\ Hep_5\ Kdo$

b) Hep-(1-6)-β-Glc-(1-4)-L,D-α-Hep$\begin{matrix}Q\\6\\3\\x\end{matrix}$-1-5-α-Kdo

c) Hep-(1-6)-β-Glc-(1-4)-L,D-α-Hep$\begin{matrix}Q\\6\\3\\x\end{matrix}$

d) Glc-(1-4)-L,D-α-Hep$\begin{matrix}Q\\6\\3\\x\end{matrix}$-1-5-α-Kdo

e) Glc-(1-4)-L,D-α-Hep (Q at 6, x at 3)

f) α Hep-(1-6)-β-Glc-(1,4)-L,D-α-Hep (x at 3)

g) α-Hep-(1-6)-β-Glc-(1-4)-L,D-α-Hep (Q at 6)

wherein:

Q is: α-Glc, and

X is: L,D-α-Hep (1) (L,D-α-Hep (2))

In some instances the conserved inner core LPS will be a variant of one or more molecules a-g, above or A Figure 1 (with or without R and R^1) wherein one or more terminal sugars appears as an isomer or has been modified to preserve it in a particular isomeric form.

In an embodiment of the invention there are provided the antigenic LPS-derived oligosacchardes described above free from covalent bonds to other oligosaccharides.

In an embodiment of the invention there is provided a method of making a vaccine comprising linking a conserved inner core LPS molecule or a portion and/or variant thereof to an immunogenic carrier protein. In some instances an adjuvant may be provided together with the LPS molecule-carrier protein.

Example

Embodiments of Antigen Preparation

1. Mutation of key glycosyltransferase genes in order to produce truncated LPS structure

Key LPS core biosynthetic genes have been identified in *Mh* and *App* (see figure below). These are *losB* in *Mh* and *lbgA* in *App*.

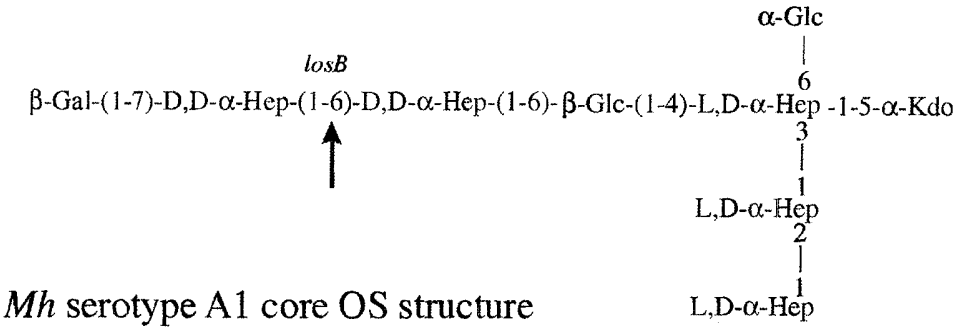

Mh serotype A1 core OS structure

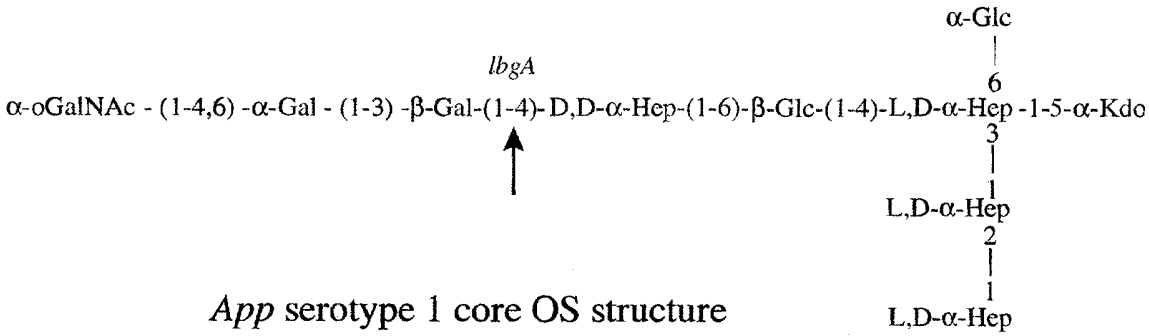

App serotype 1 core OS structure

Initially *losB* in *Mh* will be targeted because in this *Mh* strain there is a negligible amount of O-antigen present. In the *App* strain there is a considerable amount of O-antigen present that would be deleterious to the production of an immune response to the desired inner core antigen. The *losB* gene is cloned and then mutated by insertion of a chloramphenicol antibiotic resistance cassette into the cloned gene. This plasmid construct is transformed into the recipient *Mh* strain and either the plasmid is cured with concomitant migration of the mutated *losB* gene into the chromosome by homologous recombination or the plasmid is not maintained in the *Mh* host and lost with the concomitant migration of the mutated *losB* gene into the chromosome by homologous recombination. The LPS phenotype of the resulting mutant strain is confirmed by structural analysis.

2. Preparation of glycoconjugate vaccine from lipopolysaccharide of veterinary bacterial pathogens in readiness for immunisation studies

Strategy 1

De-acylation

LPS from the mutant strain that elaborates the target structure is de-acylated by dissolving in 4N KOH (~ 10 mg/ml.) and stirring at 125^{O}C for 30h. Solution is cooled to room temperature and neutralised with acetic anhydride, which serves to re-N-acetylate the amino groups created by this procedure. Precipitated salt is removed by centrifugation (9k, 15 min.) and supernatant applied to a Sephadex G-25 (or other suitable) column and eluted with pyridinium acetate buffer (or other suitable eluent). Carbohydrate-positive fractions will be pooled and freeze-dried and de-salted on a Sephadex G-50 column with water as eluent (if required). Carbohydrate-positive fractions are pooled and freeze-dried resulting in ~ 15 - 20% yield of KOH'd LPS. Quality control is performed by ^{1}H-NMR spectroscopy and ES-MS analysis. The resulting material is de-O-acetylated by treatment in 0.1M NaOH at room temperature for 2h and purified on a Sephadex G-25 (or other suitable) column in water, lyophilising, resulting in ~ 10% yield of KOH'd LPS.

Quality control is performed by ^{1}H-NMR spectroscopy and ES-MS analysis.

De-phosphorylation

The resulting material is de-phosphorylated by dissolving (~ 10 mg/ml.) in 0.1M NH_4HCO_3 buffer with alkaline phosphatase (Aldrich Cat. # P-6772) (~ 200 units alk.P / mg KOH'd LPS) and stirring at 54^{O}C for ~ 16h. Solution is heated to 100^{O}C for 5 min., cooled and centrifuged at 14K for 10 min. Supernatant is freeze-dried. Resulting material is de-salted on a Sephadex G-25 (or other suitable) column in water, lyophilising, resulting in ~ 10% yield of KOH'd alk. P'd LPS. Quality control is performed by ^{1}H-NMR and CE-ES-MS analysis confirming de-phosphorylation of the KOH treated LPS.

Amination

Resulting aldehydo functional group is aminated by dissolving the dried carbohydrate (2mg) in 50ul of DMSO and adding 400ul of 2M NH_4Oac in MeOH and 24mg of $NaCNBH_3$ dissolved in 100ul of MeOH at pH 8.3 at $50^{O}C$ for 72h. The MeOH is evaporated under N_2 and the product lyophilised and purified on a Sephadex G-25 (or other suitable) column in water, lyophilising, resulting in ~ 10% yield of KOH'd alk. P'd aminated LPS. Quality control is performed by ^{1}H-NMR and CE-ES-MS analysis confirming amination of the KOH treated LPS.

Attachment of linker molecule

A linker molecule (squarate) is attached to the resulting amino group by dissolving the dried carbohydrate (2mg) in 100ul of H_2O and adding 900ul of MeOH and 10ul of squarate at pH 8 (adjust with triethylamine (~1ul)) for 2h at room temperature, monitoring the pH every .5h. The MeOH is evaporated under N_2 and the product lyophilised and purified on a Sephadex G-25 (or other suitable) column in water, lyophilising, resulting in ~ 10% yield of KOH'd alk. P'd aminated squarated LPS. Quality control is performed by ^{1}H- and ^{13}C-^{1}H-NMR and CE-ES-MS analysis confirming attachment of the squarate linker.

Conjugation to protein carrier

~ 15 mg of a suitable protein is linked to a 25 x molar excess of the squarate linked carbohydrate in 1ml of 0.02M sodium borate buffer by stirring at room temperature for 72h at pH 9.2. Every 24h an aliquot is removed and examined by MALDI-MS, HPLC and SDS-PAGE with Western blotting with a carbohydrate specific monoclonal antibody (Mab). The final reaction mixture is purified down a Sepharose 6B column with PBS (50mM sodium phosphate, 100mM NaCl, pH 7.5) to achieve separation of free from conjugated carbohydrate. The fractions corresponding to the product peak are concentrated in an Amicon ultra-15 10K spin column. The final volume of conjugate is quantified for protein by the BCA assay and for carbohydrate by the PhOH / H_2SO_4 method, to give the molar ratio of carbohydrate to protein.

Strategy 2

De-acylation

LPS from strain that elaborates target structure is de-acylated by dissolving in 4N KOH (~ 10 mg/ml.) and stirring at 125^{O}C for 30h. Solution is cooled to room temperature and neutralised with 4N HCl, in order to preserve the amino groups created in the lipid A region by this procedure. Precipitated salt is removed by centrifugation (9k, 15 min.) and supernatant applied to a Sephadex G-25 (or other suitable) column and eluted with pyridinium acetate buffer (or other suitable eluent). Carbohydrate-positive fractions are pooled and freeze-dried and de-salted on a Sephadex G-50 column with water as eluent (if required). Carbohydrate-positive fractions will be pooled and freeze-dried resulting in ~ 15 - 20% yield of KOH'd LPS. Quality control is performed by ^{1}H-NMR spectroscopy and ES-MS analysis.

Attachment of linker molecule

A linker molecule (squarate) is attached to the resulting amino groups by dissolving the dried carbohydrate (2mg) in 100ul of H_2O and adding 900ul of MeOH and 10ul of squarate at pH 8 (adjust with triethylamine (~1ul)) for 2h at room temperature, monitoring the pH every .5h. The MeOH is evaporated under N_2 and the product lyophilised and purified on a Sephadex G-25 (or other suitable) column in water, lyophilising, resulting in ~ 10% yield of KOH'd squarated LPS. Quality control is performed by ^{1}H- and ^{13}C-^{1}H-NMR and CE-ES-MS analysis confirming attachment of the squarate linker.

N-acetylation

Any free amino groups remaining following the linker attachment are acetylated by treating the freeze-dried carbohydrate (~10mg/ml) with an aqueous solution of 1%

acetic anhydride (v/v) in 10% MeOH (v/v), for 1h at room temperature. The resulting solution is evaporated under N_2 and the product lyophilised and purified on a Sephadex G-25 (or other suitable) column in water, lyophilising, resulting in ~ 10% yield of N-acetylated KOH'd squarated LPS. Quality control is performed by CE-ES-MS analysis confirming N-acetylation.

Conjugation to protein carrier

Performed as described above.

3. Glycoconjugate vaccine Immunisation strategies

Balb/C mice are immunised sub-cutaneously with glycoconjugates derived from either strategy that contain 10ug of carbohydrate and adjuvant three times at three-week intervals. Sera produced are examined for cross reactivity within and between species and subsequently for functional activity. Subsequently mice are challenged following immunisation for evidence of protection by vaccination. Vaccinations observed to provide a significant level of protection and/or to reduce the duration and/or extent of infection for all *App*, *Mh*, and *Pm* strains.

4. Other studies

Monoclonal antibodies (Mabs) are raised in mice to the targeted LPS structure. These Mabs are examined for cross-reactivity within and between strains of the targeted species. Subsequently the Mabs are examined in mice for functional activity in passive protection and other assays.

Fig. 1. Proton NMR spectrum at 600 MHz of the core oligosaccharide component from *M. haemolytica* serotype A1 LPS in D_2O (300 K, pH 3). The HOD resonance is at 4.756 ppm. Resonances in the anomeric region up from 4.4 ppm are labelled along with the Kdo methylene resonances. The determined structure designated as A1 and nomenclature for the residues are also shown. Heterogeneity due to partial truncation of the backbone oligosaccharide is indicated by dotted arrows at linkage sites. In the text, the minor component for f due to heterogeneity is indicated by f'. Hep_I, Hep_{II}, and Hep_{III} are L-D-heptose while Hep_{IV} and Hep_V are D-D-heptoses. Other residues have the D-configuration.

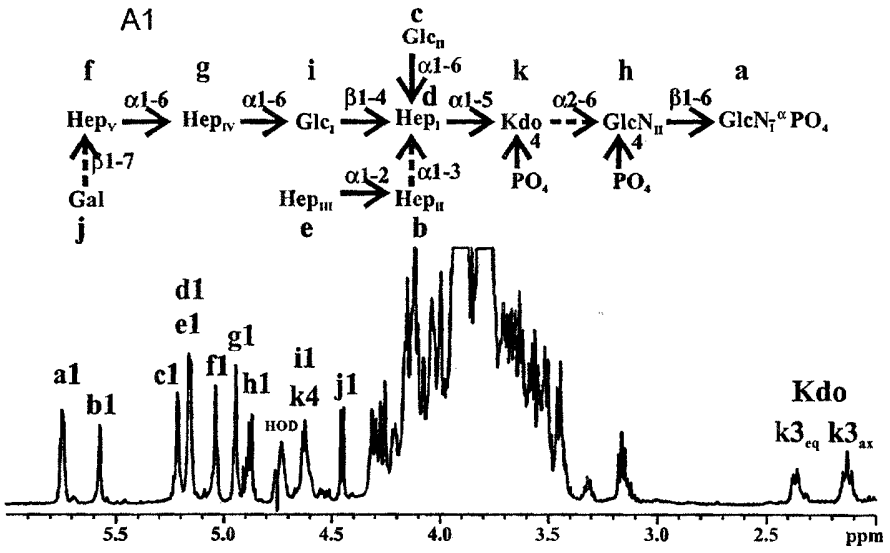

Example 1

Analysis of the LPS of *M. haemolytica* serotype A1 revealed Hex_3Hep_5Kdo as the major core oligosaccharide component. This was determined by 1D 1H NMR and FAB-MS analysis of the oligosaccharide fraction obtained following mild acid hydrolysis (1% HOAc, 100°C, 3 h) of the LPS sample. The core oligosaccharide was found to contain D-glucose, D-galactose, L-D-heptose, and DD-heptose in a molar ratio of 2:1:3:2 in the major fraction as determined by GLC–MS analysis of their alditol acetate and 2-butyl glycoside derivatives. The D-Gal residue was found to be a terminal nonreducing moiety from methylation analysis and was absent in the minor component of the core oligosaccharide fraction, that had the composition of Hex_2Hep_5Kdo. The occurrence of Kdo in the LPS was established by colorimetric analysis.

Treatment of *M. haemolytica* LPS with anhydrous hydrazine followed by strong alkali afforded water-soluble, deacylated LPS oligosaccharides. The deacylated LPS sample was representative of the intact backbone oligosaccharide of the native material containing core and lipid A oligosaccharide moieties. This was confirmed by electrospray ionization ESI-MS which gave molecular ions corresponding to

$Hex_3Hep_5Kdo_1HexN_2(H_2PO_3)_3$ as the major oligosaccharide component (see *Experimental section*). Figure numbers refer to each Example.

From the proton spectrum (Fig. 1) and HMQC and COSY spectra (Fig. 2), 10 anomeric ^1H NMR resonances were observed, as well as methylene proton resonances. The anomeric resonances were labeled a–j in decreasing order of their ^1H NMR chemical shifts and $k3_{eq}$ and $k3_{ax}$ assigned to the methylene protons of Kdo. The integral for the b1 and de1 and j1 anomeric peaks were 40% less than those for the

Fig. 2. 2D NMR experiments for A1 showing the HMQC spectrum of the anomeric region (*a*), and the COSY (*b*) and NOESY (*c*) spectra of the anomeric and ring region. The arrow indicates the position of the b2 resonance observed near k5.

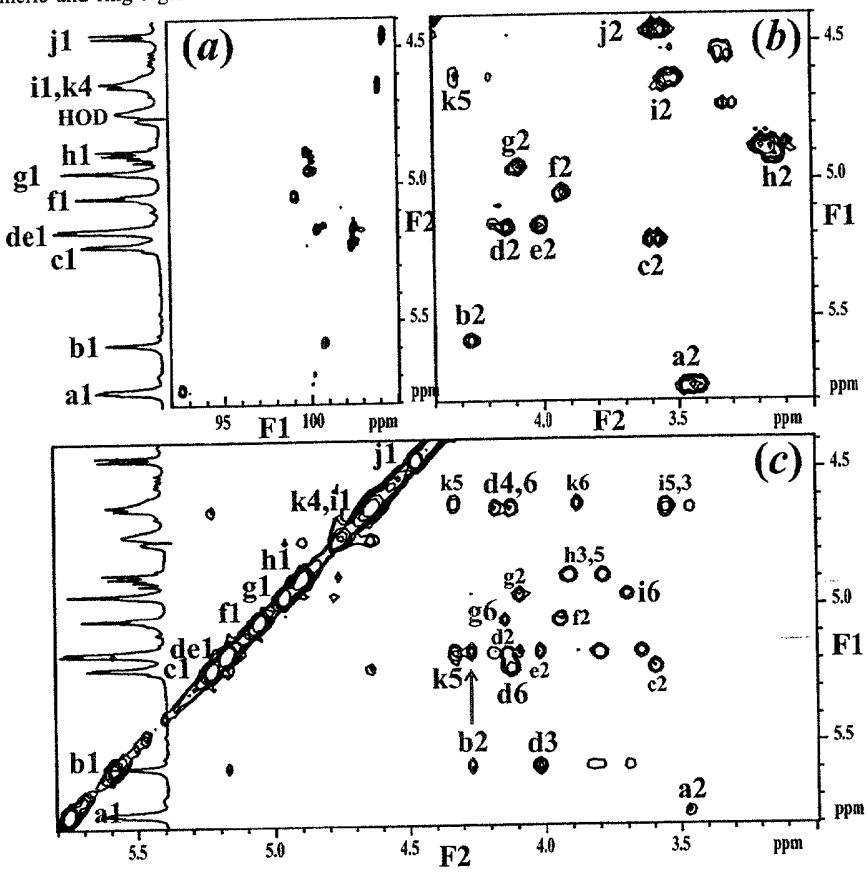

other anomeric resonances confirming heterogeneity in the sample. There was also some heterogeneity at h1 with the appearance of a downfield doublet at 4.91 ppm near h1.

Standard homo- and hetero-nuclear 2D-NMR analyses was undertaken. From the COSY spectrum in Fig. 2, the H-2 resonances could be located. It was realized that for residues **b**, **d**, **e**, **f**, and g, $J_{1,2}$ was small, typical of *manno*-heptoses, and that a 2D-TOCSY could not be used to transfer magnetization from H-1 past H-2. From the HMQC spectrum in Fig. 3, the H-2 of the heptose residues overlapped with other resonances making 2D-TOCSY difficult to analyze for these residues. The 2D-NOESY spectrum also showed an unusually high number of NOEs especially for the b1, de1 resonances. Also, there was overlap of several resonances in the anomeric region. Hence, due to the complexity of the spectra and heterogeneity of the sample, 1D selective methods were used to extract spectral parameters that could not be obtained using standard 2D methods, thus permitting the resolution of the structure and conformational analysis. HMQCTOCSY and HMBC experiments were also very important in determining the complete assignments, especially for the heptose units. Using this approach, the complete assignment for the ^{1}H and ^{13}C NMR chemical shifts for the major backbone oligosaccharide (A1) was possible (Table 1).

The Kdo-$GlcN_{II}$-$GlcN_{I}$ sequence and partial assignments are known from previous studies (65) and are consistent with the assignments made here. The 1D-TOCSYs for residues **a** and **h** permitted assignment of the resonances and measurement of proton coupling constants (Fig. 4*a*, 4*b*). Location of phosphate groups was confirmed from a ^{31}P HMQC experiment as done previously (65). Assignment of the ^{13}C NMR chemical shifts was then made from HMQC, HMQC-TOCSY, and HMBC spectra. This information led to the definition of residues **a** and **h** as the α-D-GlcN and ß-D-GlcN pyranosyl units of the lipid A moiety. Most of the proton, $_{31}P$ and $_{13}C$ NMR chemical shifts were similar to those previously reported in a similar structural element (65). In the 1D-TOCSY for h1, the h'5 peak at 3.62 ppm is due to hydrolysis of the Kdo-(2-6)-β-D-$GlcN_{II}$ glycosidic linkage. After several months in solution, the linkage was completely hydrolyzed with h'6 and h'6 appearing at 3.82 and 3.92 ppm,

respectively. The sharp anomeric signal at 3.91 ppm was also found to be due to h'1 of this disaccharide.

For Kdo, the H-4 and H-5 resonances were assigned from 1D-TOCSY experiments with selective excitation of H-3_{eq} or H-3_{ax}. The H-4 resonance is shifted downfield due to a phosphate group at C-4, confirmed by a ^{31}P HMQC. A small $J_{5,6} < 1$ Hz impeded the TOCSY transfer past H-5 (Fig. 4*c*). However, a strong NOE is observed between k4 and k6 in Fig. 2*c* in accord with the X-ray structure of Kdo (66). 1D NOESY-TOCSY(k4, k6) was used to complete the assignment

Fig. 3. Selected plots from the heteronuclear ^{1}H-^{13}C 2D NMR spectra of A1. (*a*) In the HMQC spectrum of the ring region some assignments are labelled where possible. (*b*) In the HMQC-TOCSY spectrum, the C7-H7s-C6-H6, C4-H4-C5-H5 TOCSY correlations and those for b2 are labelled. (*c*) In the HMBC spectrum, the H1-C1-O1-Cx inter-glycosidic correlations are shown for the anomeric proton resonances along with their intra-residue correlations.

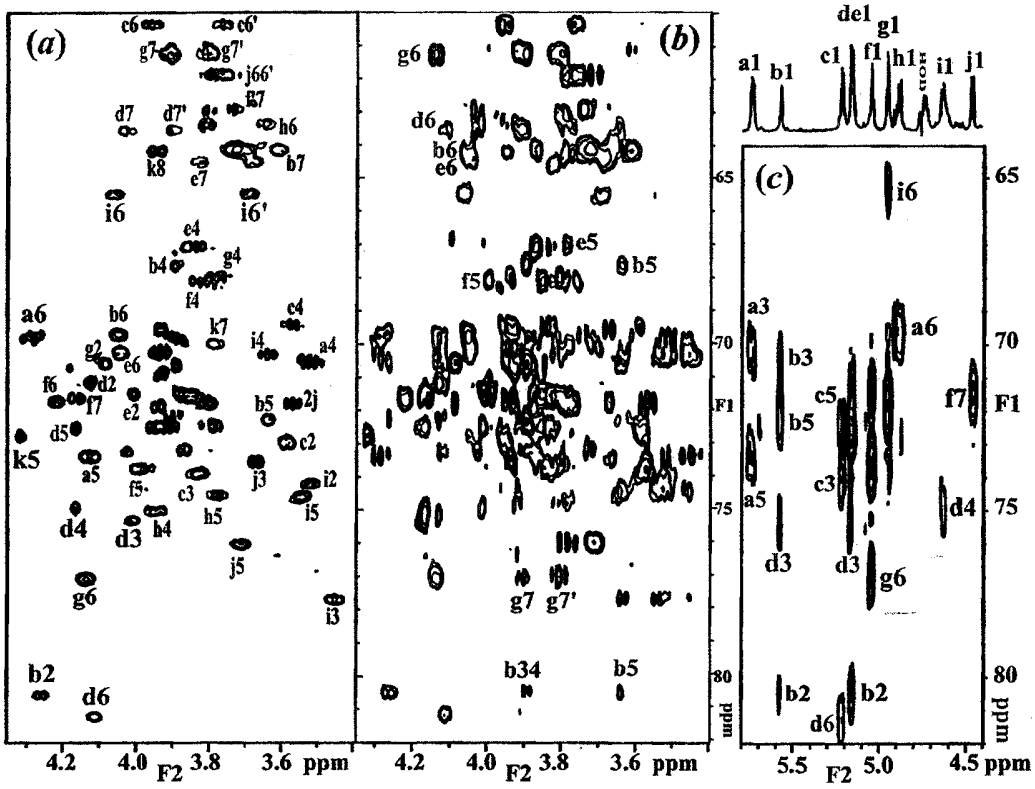

(Fig. 4*d*). As shown later, for the HepI-(1-5)-Kdo linkage, the d1-k7 NOE was also observed, typical of a substitution at C-5 of Kdo (67). Using this NOE, the Kdo resonances detected from the 1D-NOESY-TOCSY (de1, k7) (Fig. 4*e*) had the same chemical shifts and similar multiplet patterns as those found in the previous experiment, thus confirming the Kdo ^{1}H NMR assignments. The ^{13}C NMR assignments for Kdo where then obtained from the HMQC spectrum and confirmed from the HMQC-TOCSY spectrum.

Residue **i** was determined to be 6-substituted ß-D-glucose denoted as Glc_I. The anomeric resonance for residue **i** overlapped with the H-4 resonance of Kdo. In the 1D-TOCSY for these two overlapping resonances, it was possible to distinguish the resonances for residue **i** because of the small $J_{5,6}$ coupling constant for Kdo (Fig. 4*c*). All resonances up to H-6s could be detected and coupling constants of the multiplets could be measured. Due to its ß-D configuration the i1-i3 and i1-i5 NOE were also observed in the NOESY spectrum (Fig. 2 and Fig. 5*f*). ^{13}C NMR assignments for Glc_I were then obtained from the HMQC spectrum and confirmed with the HMQC-TOCSY spectrum. From a comparison with chemical shifts of terminal glucose (68, 69), a glycosidation down-field shift of 3.7 ppm was observed for the C-6 resonance, indicating its substitution at that position. A substantial shift of –2.2 ppm was also observed for C-5. The rotamer distribution about the C-5—C-6 bond could be determined from the H-5 multiplet observed for the i1-i5 NOE in Fig. 5*f*. It was apparent that both $J_{5,6}$ and $J_{5,6'}$ had small values <2 Hz since the H-5 multiple appeared as a doublet dominated by the large $J_{4,5}$ coupling of 10 Hz. This showed that both H-6 and H-6′ were gauche to H-5 with the O6-C6-C5-O5 = –60° rotamer being preferred in solution.

Residue **c** was determined to be a terminal α-D-glucose denoted as Glc_{II}. From the 1D-TOCSY for c1 (Fig. 4*f*) resonances up to H-5 were detected, indicating that residue **c** was an α-glucose based on the measured proton coupling constants. From the HMQC spectra and comparison with chemical shifts of terminal glucose model compounds (68, 69), all the ^{1}H and ^{13}C NMR assignments could be completed.

The terminal galactose, residue **j**, denoted as Gal, was identified from the 1D-TOCSY of j1 and resonances up to H-4 were observed (Fig. 4*j*). To get past the small $J_{4,5}$ coupling constants and identify H-5, the 1D-TOCSY-NOESY (j1, j4) was done (Fig. 4*h*). From the HMQC spectra and comparison with chemical shifts of terminal galactose model compounds (68, 69), all the ^{1}H and ^{13}C NMR assignments were completed.

To assign the heptose residues, model compounds were synthesized to obtain accurate ^{1}H and ^{13}C NMR chemical shifts and *J*H,H values. These were crucial in assigning the terminal heptose units by chemical shifts comparisons. Also,

Table 1. NMR chemical shifts (ppm) of the core oligosaccharide component from *Mannheimia (Pasteurella) haemolytica* serotype A1 LPS.

Residue	δ_C / δ_H	C-1 H-1	C-2 H-2	C-3 H-3 H-3′	C-4 H-4	C-5 H-5	C-6 H-6 H-6′	C-7 H-7 H-7′	C-8 H-8 H-8′
Hep_I		100.3	71.1	75.3	74.9	72.5	81.2	63.5	
D		5.17	4.13	4.01	4.17	4.17	4.11	4.02	
								3.89	
Hep_{II}		100.7	80.5	70.6	67.6	72.2	69.6	64.1	
B		5.57	4.26	3.89	3.90	3.64	4.05	3.70	
								3.60	
Hep_{III}		102.5	71.5	71.5	67.0	72.4	70.2	64.5	
E		5.16	4.01	3.87	3.83	3.78	4.04	3.83	
								3.68	
Hep_{IV}		99.8	70.5	71.7	67.9	71.8	77.0	61.2	
G		4.95	4.08	3.81	3.78	3.94	4.14	3.91	
								3.80	
Hep_V		99.0	70.8	71.5	68.1	73.7	71.7	71.6	
F		5.04	3.93	3.85	3.82	3.99	4.22	4.16	
								3.85	
Hep_V		99.0	70.8	71.5	68.3	73.7	72.8	62.9	
f′		5.04	3.93	3.85	3.77	3.97	4.05	3.79	
								3.73	
Glc_I		104.0	74.2	77.7	70.2	74.6	65.5		
I		4.64	3.51	3.45	3.64	3.54	4.06		
							3.69		
Glc_{II}		102.4	72.9	73.9	69.3	72.4	60.3		
C		5.22	3.58	3.83	3.58	3.95	3.96		
							3.76		
Gal		104.3	71.7	73.5	69.5	76.0	61.8		
J		4.46	3.56	3.67	3.93	3.71	3.80		
							3.76		
$GlcN_I$		92.6	54.8	70.2	70.5	73.4	69.7		
A		5.75	3.45	3.93	3.51	4.13	4.28		
							3.89		
$GlcN_{II}$		99.7	56.3	72.2	75.0	74.6	63.4		
H		4.88	3.17	3.90	3.94	3.78	3.81		
							3.64		
Kdo			99.7	34.5	70.8	72.7	73.2	69.9	64.2
K				2.37	4.61	4.32	3.87	3.78	3.94
				2.13					3.73

Note: Measured at 600 MHz (^{1}H) in D_2O, 25°C and pH 3 from HMQC and HMBC data with the CH_3 signal of external acetone set at 2.225 ppm for ^{1}H NMR and 31.07 ppm for ^{13}C NMR. Average error of ±0.2 ppm for δ_C and ±0.02 ppm for δ_H. The minor component for f due to heterogeneity is indicated by f′. The CH_2 spin systems, (H, H′), are in decreasing order of chemical shifts. For Kdo, H-3 and H-3′ are assigned to H-3_{eq} and H-3_{ax}.

upon glycosidation, the ^{13}C NMR resonance of the substituted carbon experiences a substantial down-field glycosidation shift (56, 57). The proton spectra for D-D-heptose and D-L-heptose are shown in Fig. 6. In solution both the α and ß forms are present for each compound. Their ^{1}H NMR spectra were assigned using 1D-TOCSY experiments. To obtain accurate coupling constants and chemical shifts, spin simulations of the proton spectra were done. The simulated spectra are shown in Fig. 6. The simulated spectra reproduced exactly the observed spectra, especially the strong coupling for H-3-H- in D-α-L-heptose (Fig. 6*b*). ^{13}C NMR chemical shifts were assigned using HMQC. The NMR data for the heptose monosaccharides are given in Table 2. The chemical shifts for L-D-heptose are the same as those of D-Lheptose since they are enantiomers of each other.

Residues **b**, **d**, **e**, **f**, and **g** in A1 were identified as heptoses from their narrow anomeric resonance due to the small $J1,2$ coupling and lack of transfer of magnetization beyond H-2 from H-1 in a TOCSY experiment. All the heptoses in A1 had the α-D configuration since the only intra-residue NOE from H-1 was to H-2 (Fig. 2). 1D-TOCSY-TOCSY (H-1, H-2) was used to assign all the heptose residues. The first TOCSY step from H-1 transfers the magnetization to H-2 and further transfer is impeded due to the small $J_{1,2}$ value of 1.8 Hz. However, the second step at H-2 will transfer the magnetization further to higher spins due to the larger $J_{2,3}$ value of 3 Hz. However, for L-D-heptose, transfer of magnetization stops at H-5 due to the small $J_{5,6}$ value of 1.6 Hz. For D-D-heptose, transfer of magnetization is less impeded due to a large $J_{5,6}$ value of 3.2 Hz. However, relaxation

Fig. 4

Fig. 4. 1D selective experiments for assignment of the non heptose residues in A1. (*a*) 1D TOCSY (a1, 180 ms); (*b*) 1D TOCSY (h1, 180 ms); (*c*) 1D TOCSY (i1 k4, 180 ms); (*d*) 1D NOESY-TOCSY (i1 k4, 400 ms; k6, 180 ms); (*e*) 1D NOESY-TOCSY (de1, 400 ms; g3 k7, 180 ms); (*f*) 1D TOCSY (c1, 180 ms); (*g*) 1D TOCSY (j1, 180 ms); and (*h*) 1D TOCSY-NOESY (j1, 180 ms; j4, 400 ms). Minor components for f and h due to heterogeneity are indicated by f′ and h′, respectively. The resonance for the first selective step is underlined and the one for second selection step is doubly underlined, where applicable. Selected resonances in the anomeric region are indicated on the left of the spectra.

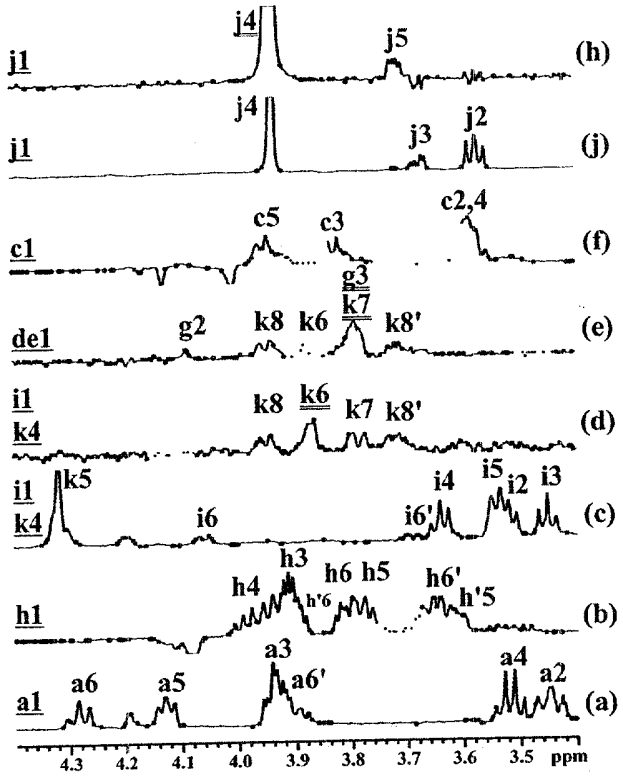

effects can also impede transfer of magnetization and one cannot use a lack of transfer beyond H-5 as proof of L-D-heptose identification.

Residue **b** was determined to be the 2-substituted L-α-D-heptose denoted as Hep_{II}. The 1D-TOCSY-TOCSY (b1, b2) identified resonances at 3.64 ppm and 3.9 ppm (Fig. 7*a*). The multiplet pattern at 3.64 ppm was indicative of a H-5 resonance while those at 3.9 ppm were similar to the strongly coupled H-3 and H-4 resonances observed in the monosaccharide (Fig. 6*b*). To identify H-6 a 1D-TOCSYNOESY (b2, b5) was done (Fig. 7*b*). In the first TOCSY step for b2, the a6 resonance was also irradiated but the second step only selected the b5 resonance. NOEs from b2 were observed on b3 and b6 along with an inter-residue NOE on d2. Once b6 was located, the HMQC-TOCSY from the C-7-H-7s-C-6-H-6 was used to assign the H-7 and H-7′ resonances (Fig. 3*b*). Assignments for the other resonances were then obtained from the HMQC spectrum and confirmed from the HMQC-TOCSY and HMBC spectra (Fig. 3). Comparison of chemical shifts with those of L-α-Dheptose indicated a 9 ppm

down-field shift for C-2 and an up-field shift of –0.8 ppm for C-3 indicative of a substitution at C-2. The C-4 to C-7 chemical shifts were within 0.6 ppm of those of the monosaccharide.

Fig. 5

Fig. 5. 1D selective experiments to detect dipolar interactions in A1. 1D NOESY spectra of the resonances in the anomeric region with a 200 ms mixing time for b1, c1, de1, f1, g1, i1/k4 and a 1D ROESY (f1, 500 ms) for j1 in (*a*)–(*g*), respectively. The selected anomeric resonances and the linkage are indicated on the left of the spectra.

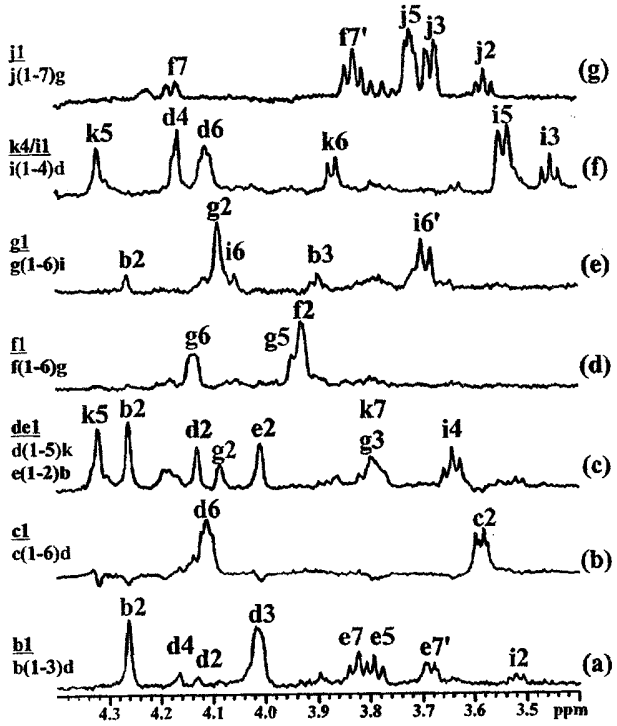

Residue **e** was determined to be a terminal L-α-D-heptose denoted as Hep_{III}. Although the d1 and e1 resonances overlap, this is of no concern since their H-2 resonances did not overlap. The 1D-TOCSY-TOCSY (de1, e2) identified the e3, e4, and e5 spins (Fig. 7*c*). From the b1 NOE in Fig. 5*a*, the e5 resonance was also observed. The high digital resolution of the 1D selective experiments permits accurate matching of resonances between different experiments due to the observation of their multiplet pattern. In Fig. 5*a*, the b1-e7 and b1-e7′ NOEs were also observed. As seen later, these NOEs are due to the close proximity of b1 proton to the e5 and the e7 and e7′ protons. The H-6 resonance was located in the HMQC-TOCSY from C-7-H-7s-C-6-H-6. ^{1}H and ^{13}C NMR assignments were completed with HMQC and HMQCTOCSY. ^{1}H and ^{13}C NMR chemical shifts of residue **e** were similar to those of L-α-D-heptose.

Residue **d** was identified as a 3,4,6-trisubstituted L-α-Dheptose denoted as Hep_I. The 1D-TOCSY-TOCSY (de1, d2) identified a narrow multiplet at 4.17 and a broader one at 4.01 ppm (Fig. 7*d*). The multiplets at 4.01 ppm and 4.17 ppm (d2) were also observed in the 1D-NOESY for b1 (Fig. 5*a*). The resonance at 4.17 ppm was also observed in

Table 2. NMR data for D-L-heptose and D-D heptose monosaccharides.

Heptose	δ_C δ_H $J_{H,H}$	C-1 H-1 $J_{1,2}$	C-2 H-2 $J_{2,3}$	C-3 H-3 $J_{3,4}$	C-4 H-4 $J_{4,5}$	C-5 H-5 $J_{5,6}$	C-6 H-6 $J_{6,7}$	C-7 H-7 $J_{6,7'}$	H-7' $J_{7,7'}$
D-α-L-		95.00[a]	71.45	71.36	67.05	71.81	69.63	63.84	
		5.166	3.914	3.838	3.845	3.749	4.024	3.689	3.652
		1.8	3.1	10.0	9.7	1.6	7.3	5.5	−11.7
D-β-L-		94.74[b]	72.02	74.09	66.69	75.43	69.53	63.57	
		4.866	3.927	3.649	3.788	3.329	3.98	3.713	3.695
		1.0	3.2	10.0	9.8	1.8	7.5	5.8	−11.7
D-α-D-		94.86[a]	71.32	71.38	68.35	73.42	72.72	62.75	
		5.151	3.905	3.812	3.756	3.865	4.018	3.797	3.708
		1.8	3.4	9.4	10.1	3.2	3.3	7.6	−12.0
D-β-D-		94.79[b]	71.84	74.11	68.16	77.22	72.623	62.58	
		4.851	3.921	3.622	3.682	3.423	4.025	3.788	3.725
		1.1	3.3	9.5	9.9	3.3	3.4	7.4	−12.0

Note: Measured at 600 MHz (^1H) in D_2O at 25°C from ^1H spin simulations and from the ^{13}C spectra (150 MHz) with the CH_3 signal of acetone set at 2.225 ppm for ^1H NMR and 31.07 ppm for ^{13}C NMR. δ_C and δ_H are in ppm with an average error of ±0.005 ppm for δ_C and ±0.003 ppm for δ_H. $J_{H,H}$ values are in Hz with an average error of ±0.2 Hz. H-7 and H-7′ are in decreasing g order of chemical shifts.

[a] $^1J_{C1,H1}$ = 171 ± 1 Hz.

[b] $^1J_{C1,H1}$ = 160 ± 1 Hz measured from the undecoupled ^{13}C NMR spectrum.

Fig. 6. Proton spectra of heptose monosaccharides. Resolution enhanced spectrum of D-L-heptose at 600 MHz in D_2O, 300 K (*a*) and its simulated spectrum for the α (*b*) and β forms (*c*). Resolution enhanced spectrum of D-D-heptose at 600 MHz in D_2O, 300 K (*d*) and its spin simulated spectra for the α (*e*) and β forms (*f*). The anomerics and H-5β resonances are not shown. Note that strong coupling for the H-3, H-4 and virtual coupling for H-5 resonances are reproduced correctly for (*b*).

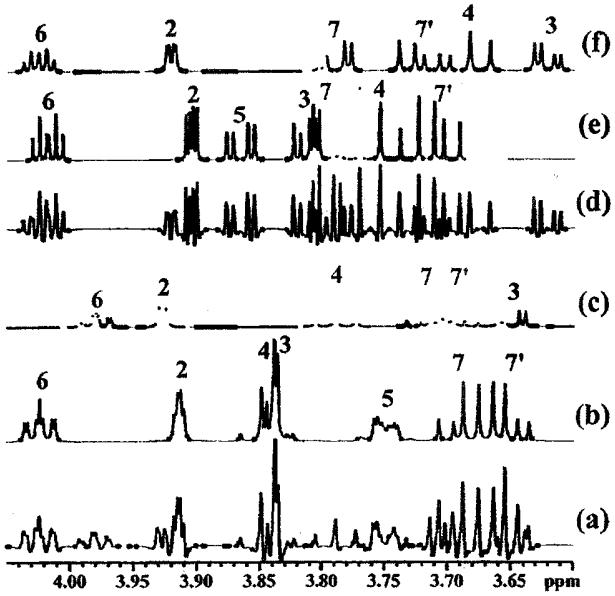

the 1D-NOESY for i1 (Fig. 5*f*). In the HMQC spectrum two narrow crosspeaks at (δc, δh) (74.9, 4.17), (72.5, 4.17) and a broader one at (75.3, 4.01) were identified. HMQC-TOCSY correlations were also observed between these crosspeaks. From a comparison of the ^{13}C NMR chemical shifts with those of the α-D-heptopyranoses in Table 2, it was obvious that the crosspeaks at (74.9, 4.17) and (75.3, 4.01) were subject to a ^{13}C NMR down-field glycosidation shift. Since these three crosspeaks are from d3, d4, or d5, only the d5 crosspeak will not experience a large glycosidation shift since substitutions on heptose cannot occur at C-5. Hence, the crosspeak at (72.5, 4.17) was assigned to (C-5, H-5). The crosspeak at (75.3, 4.01) was assigned to (C-3, H-3) based on the HMBC (d3, d1) and (d3, b1) correlations. The crosspeak at (74.9,

4.01) was thus assigned as (d4, d1), consistent with the observation of the HMBC (d4, i1) correlation and (i1, d4) NOE (Fig. 3 and Fig. 5*f*). The d6 resonance was assigned from the 1D-NOESY from i1, since for the GlcI-(1-4)-HepI linkage, a strong NOE to H-6 is also expected only if residue **d** is L-D-heptose. The d6 resonance was also observed for the 1D-NOESY for c1 (Fig. 5*b*). The H-7 and H-7′ resonances were located from the HMQCTOCSY (C-7, H-6) crosspeak (Fig. 3) and from 1DNOESY-TOCSY (i1, d6) (not shown). Comparison of chemical shifts with those of L-α-D-heptose indicated a 3.9, 7.9, and 11.6 ppm down-field glycosidation shift for C-3, C-4, and C-6, respectively.

As shown below, there should be a 4,6-disubstituted L-α-D-heptose (**d′**) present due to heterogeneity on the branching heptose (Fig. 1). From the HMQC and COSY spectra for the anomeric region, no separate signal could be observed either for the H-1 or H-2 due to overlap with other resonances. It is suspected that the proton chemical shifts of d′1 were the same as the one for d1, and that d′2 had a similar chemical shift to e2.

Residue **g** was determined to be a 6-substituted D-α-Dheptose denoted as Hep_{IV}. The 1D-TOCSY-TOCSY (g1, g2) identified the g3, g4, and g5 spins (Fig. 7*e*). The multiplet pattern at 3.94 was indicative of a H-5 resonance. To identify H-6, an 1D-TOCSY-NOESY (g2, g5) was acquired (Fig. 7*f*). NOEs from g2 were observed on g3 and g6 along with a putative inter-residue NOE on i6. Once g6 was located, the HMQC-TOCSY from the C-7-H-7s-C-6-H-6 (Fig. 3*b*) and 1D-NOESY-TOCSY (f1, g6) (Fig. 7*g*) were

Fig 7.

Fig. 7. 1D selective experiments for assignment of the heptose residues in A1. (*a*) 1D TOCSY-TOCSY (b1, 75 ms; b2, 75 ms) to detect b3, b4 and b5; (*b*) 1D TOCSY-NOESY (b2, 150 ms; b5, 400 ms) to detect the b5-b6 and b5-b3 NOEs. Note also the strong b5-d2 NOE due to the b(1-3)d linkage; (*c*) 1D TOCSY-TOCSY (de1, 75 ms; e2, 75 ms) to detect e3, e4 and e5; (*d*) 1D TOCSY-TOCSY (de1, 75 ms; d2, 75 ms) to detect d3, d4 and d5; (*e*) 1D TOCSY-TOCSY (g1, 90 ms; g2, 150 ms) to detect g3 to g5; (*f*) 1D TOCSY-NOESY (g2, 150 ms; g5, 400 ms) showing the g5-g6 and g5-g3 NOEs and g5-i6 NOE in accord with the g(1-6)i linkage; (*g*) 1D NOESY-TOCSY (f1, 400 ms; g6 180 ms) to detect the g7 resonances from the f1-g6 interglycosidic NOE in accord with the f(1-6)g linkage; (*h*) 1D TOCSY-TOCSY (f1, 90 ms; f2, 150 ms) for detection of f and f' resonances up to H-6. Note the clear multiplet pattern for f5 and f'5; (*i*) 1D TOCSY (f6, 40 ms) to detect the f7 resonances only due to the short spin lock time. The resonance for the first selective step is underlined and the one for second selection step is doubly underlined, where applicable. Selected resonances in the anomeric region are indicated on the left of the spectra.

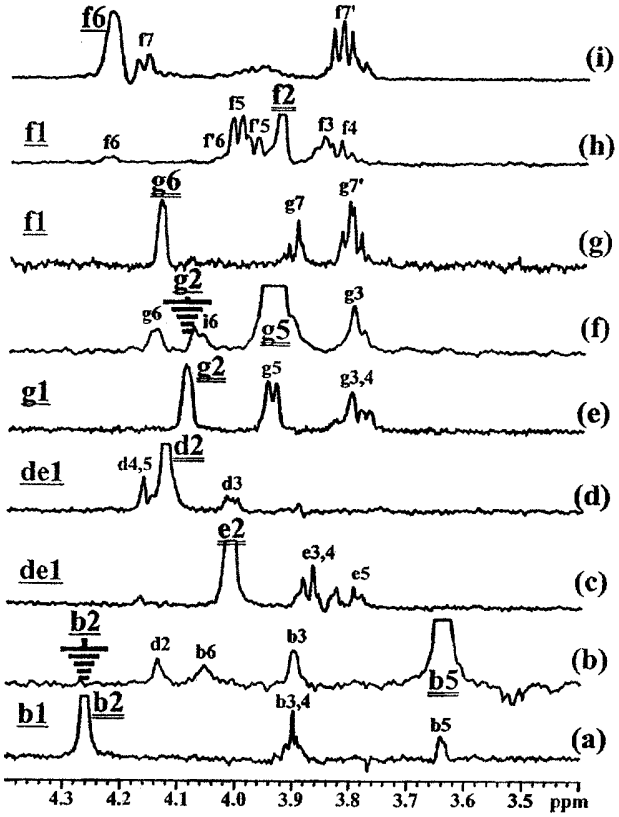

used to assign the H-7 and H-7' resonances. Assignments for the other resonances were then obtained from the HMQC spectrum and confirmed with the HMQC-TOCSY spectrum (Fig. 3). In the 1D-NOESY (f1), the g6 and g5 resonances were observed (Fig. 5*d*). The NOE f1-g5 NOE can only be possible if residue **g** is a D-D-

heptose from molecular modeling studies (see below). Comparison of chemical shifts with those of D-α-D-heptose indicated a 4.3 ppm down-field shift for C-6.

Residue **f** was determined to be a 7-substituted D-α-D-heptose and denoted as HepV. The 1D-TOCSY-TOCSY (f1, f2) identified spins up to f6 indicating that residue **f** was a D-D-heptose. The f5 multiplet pattern was quite clear. From a 1D-TOCSY starting on f6, the f7, and f7′ resonances were identified. The ^{13}C NMR assignments were then obtained from the HMQC spectrum and confirmed with the HMQCTOCSY spectrum. Comparison of chemical shifts with those of α-D-D-heptose indicated a 8.8 ppm down-field shift for C-7. A terminal D-α-D-heptose, denoted **f** ′, was only detected due to heterogeneity at this linkage site. As seen in the 1D-TOCSY-TOCSY (f1, f2), the f ′5 and f ′6 resonance can be detected, along with crosspeaks in the HMQC and HMQC-TOCSY spectra which correspond to those of a terminal D-α-D-heptose similar to those for D-α-D-heptose in Table 2.

The sequence of the core octasaccharide was established from the 1D-NOESY spectrum for the anomeric resonances presented in Fig. 5 and from the HMBC spectrum of the anomeric proton resonances (Fig. 3*c*). Inter-residue NOEs were also observed in 1D-TOCSY-NOESY experiments in Fig. 7*b* and 7*f*. The results are tabulated in Table 3 and the structure shown in Fig. 1. From integration of the anomeric resonances and appearance of new resonances with time, the linkage sites where heterogeneity occurs were determined. The k(2-6)h linkage and the b(1-3)d linkage hydrolyzed over a period of months in solution at pH 3, while the j(1-7)f linkage was stable.

An unusually large number of long-range NOEs were observed spanning up to five sequential residues. For an α-D sugar, the H-1-H-2 intra-residue NOE is expected. For a β-Dsugar, the H-1-H-3 and H-1-H-5 intra-residue NOEs are expected. The H-1-C-1-O-1-C-*x*-H-*x* interglycosidic NOEs are expected for (1-*x*) linkage. Inter-residue anomeric NOEs between two linked sugars on the H-*x* ± 1 and H-*x* ± 2 can also occur. Other inter-residue NOEs, not in the vicinity of the glycosidic linkage, are deemed to be long-range NOEs as listed in Table 3.

To explain the large number of long-range NOEs, conformational analysis was done using the Metropolis Monte Carlo (MMC) method to vary the glycosidic linkage angles and sample the multiple conformations of the molecule. Using this method for the inner core oligosaccharide with Kdo at the reducing end, it was found that all the observed long-range NOEs could be explained by the close proximity of the e-b branch to the g-i branch. These longrange NOEs were possible due to restriction of the inner core residues brought about by the three branching points on Hep_I.

A minimum energy conformer obtained from the calculation is shown in Fig. 8. The various interproton distances measured from these coordinates are given in Table 3. As can be observed the occurrence of most NOEs can be explained by the short inter-proton distances. The long-range NOEs for g1-b2 and g1-b3 are not consistent with distances obtained from the molecular model drawn in Fig. 8. Although there is restriction due to the 3,4,6)-Hep_I substitution pattern, there is flexibility about the glycosidic linkage and this must be taken into account. As shown in Fig. 9 for the g1-b2 and g1-b3 distances, multiple conformations having short inter-proton distances are sampled consistent with the

Fig. 8. Molecular model of a minimum-energy conformer obtained from a MMC calculation of the inner core heptasaccharide of A1. Oxygens are depicted as the larger spheres and hydroxyl protons are removed. Relevant protons are labelled. Note the close proximity of the e-b branch to the g-i branch and the close proximity of the exocyclic chain of residue e to the anomeric proton of residue b consistent with the long range NOEs observed. Also, note the differences in orientation of the exocyclic chain between L-D heptose (residues d, b, e) and D-D heptose (residue g).

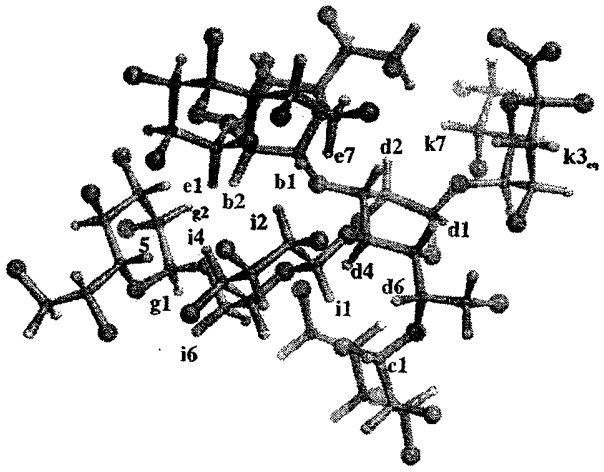

Table 3. HMBC and NOE data for A1 and distances from a minimum energy conformer of the core heptasaccharide shown in Fig. 8.

Linkage	HMBC H-1-C-*x*	Intra-residue NOE	*r* (Å)	Inter-residue NOE	*r* (Å)	Long range NOE	*r* (Å)
b(1-3)d	b1-d3	b1-b2	2.6	b1-d3	2.6	b1-e5	3.3
		b5-b3	2.5	b1-d4	3.7	b1-e7	2.9
		b5-b6	2.4	b5-d2	2.3	b1-e7′	2.6
				k3ax-d5	3.2	b1-i2	2.2
c(1-6)d	c1-d6	c1-c2	2.4	c1-d6	2.0	c1-i1	2.4
d(1-5)k		d1-d2	2.6	d1-k5	2.2		
				d1-k7	2.9		
e(1-2)b	e1-b2	e1-e2	2.6	e1-b2	2.1	e1-g2	4.2
				e1-b1	2.8	e1-g3	2.3
						e1-i4	2.0
f(1-6)g[a]	f1-g6	f1-f2	2.6	f1-g6	2.5		
				f1-g5	2.6		
g(1-6)i	g1-i6	g1-g2	2.6	g1-i6	2.6	g1-b2	4.2
		g5-g3	2.6	g1-i6′	2.6	g1-b3	4.9
		g5-g6	2.5	g5-i6	3.0		
i(1-4)d	i1-d4	i1-i3	2.6	i1-d4	2.8	i1-c1	2.4
		i1-i5	2.4	i1-d6	2.1		
j(1-7)f[a]	j1-f7	j1-j2	3.1	j1-f7	2.7		
		j1-j3	2.7	j1-f7′	2.5		
		j1-j5	2.4				

[a]For the j and f residues in the Gal-(1-7)-Hep_V-(1-6)-Hep_{IV} sequence (j-f-g), the average distances from MMC calculations are given.

observed NOEs. The same situation was applicable for all the other long-range and inter-residue NOEs. The long-range NOEs for g1-b2 and g1-b3 and e1-i4 span four residues with mobility about the three glycosidic (ϕ, ψ) angles for a total of 6 df. The long-range NOEs between e1-g2 and e1-g3 that

Fig. 9. Variation of inter-proton distances (r) vs. macro move in a MMC calculation of the inner core heptasaccharide of A1 for b1-e5, b1-e7, e1-i4, e1-g2, g1-b2, g1-b3 in (a)–(g), respectively. Occurrences of interproton distances in the 2–4 Å range are consistent with the observed long range b-e, e-i, and e-g NOEs.

Fig 9

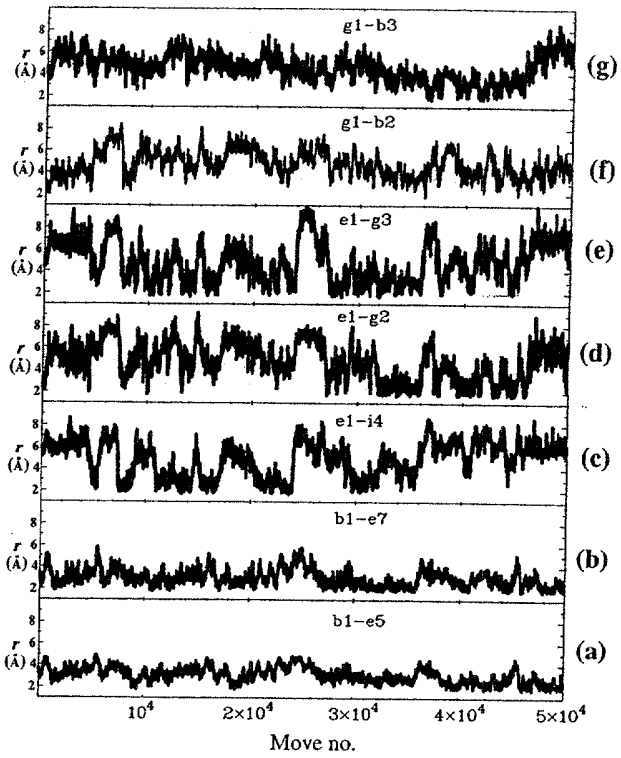

span five residues (e-b-d-i-g) vary even more due to 8 df about the glycosidic angles, not counting possible flexibility about the C-5—C-6 bond for the g(1-6)i linkage. The b1-e5, b1-e7, and b1-e7′ are dependent on mobility about the e(1-2)b glycosidic bond and rotation about C-6-C-7 of residue **e**. In all cases, the occurrence of multiple conformations that have short inter-proton distances is consistent with the observed inter-residue and long-range NOEs.

In the present study it was established that the lipid A region of the *M. haemolytica* A1 LPS molecule contains a bis-4,4′-phosphorylated β-1,6 linked D-glucosamine disaccharide moiety. The nature and substitution patterns of the fatty acyl groups attached to this disaccharide have not been reported. The fully acylated LPS molecule makes up the outer most leaflet of the bacterial membrane and is essential for maintaining membrane integrity. The glycose portion of the molecule typically extends out and away from the plane defined by the bacterial membrane. The LPS oligosaccharide portion is important in virulence (70) and is involved in eliciting host immune responses (17). To gain a perspective of the relative sizes and orientation of the core oligosaccharide and membrane-anchoring lipid A regions of this LPS

molecule, a molecular model was constructed using the lipid A fatty acid substitution pattern found in a related organism, *Haemophilus influenzae*. This is shown in Fig. 10. The *H. influenzae* lipid A has been reported (71) to have six fatty acyl groups in which the amide group (C-2) and C-3 hydroxyl groups of the reducing glucosamine residue are acylated by 3-hydroxytetradecanoic acid while the C-2′ amide and C-3′ hydroxyl groups of the nonreducing residue are acylated by 3-tetradecanoyloxytetradecanoic acid.[2] As observed in Fig. 10, due to the inner core which provides a fairly rigid structure, the glycose portion projects out from the lipid A moiety which defines the bacterial membrane. More mobility was observed for the terminal residues, especially for the terminal Gal residue. In the NOESY spectrum in Fig. 2, no NOEs for the anomeric resonance were observed consistent with increased mobility of this residue.

The core structures of several LPS have been found to be highly branched (3) and this can result in well-defined conformations for the inner core. In a previous study, the LPS of *Moraxella catharrhalis* was found to adopt an unusual conformation in which a very rare *anti* conformer (72) was observed (73). For a highly branched 3,4,6-trisubstituted Dglucose residue in this LPS molecule, a dihedral angle (C-1′-O-1′-C-4-H-4) near 180° was detected for β-D-Glc*p*-(1–4)-DGlc*p* linkage to the branched glucose unit.

The results of the present study have provided a detailedpicture of the structure of the LPS core oligosaccharide region of *M. haemolytica* serotype A1. We have previously shown that the oligosaccharide region of *M. haemolytica* LPS is immunogenic in mice, sheep, and cattle and that eight of the 12 *M. haemolytica* serotypes (i.e., serotypes A1, A5, A6, A7, A8, A12, A14, and A16) share common core oligosaccharide determinants (17). The core oligosaccharides from serotypes A1 and A8 show almost identical ^{1}H NMR spectra (17) establishing the presence of a common basal structure. Based on the results of the present study it is apparent that the *O*-chain deficient LPS elaborated by *M. haemolytica* serotype A8 lacks the terminal Gal unit in the core oligosaccharide, a residue which possibly provides a site for *O*-chain attachment (16). An understanding of LPS structural differences among *M. haemolytica* serotypes could provide the basis for a vaccine against *M.*

haemolytica bovine pasturellosis. Serotype A1 is the principal microorganism responsible for this disease, accounting for 30% of total cattle deaths globally (11). The use of a less virulent serotype or antigens thereof in a vaccine formulation could provide an effective disease management strategy.

Experimental for Example 1

Preparation of LPS from *M. haemolytica*

Pasteurella (Mannheimia) haemolytica serotype A1 (NRCC 4212) was obtained from the Veterinary Infectious Diseases Organization (VIDO), Saskatoon, SK, Canada. LPS was extracted and purified from fermenter-grown bacteria culture by the hot aqueous phenol method as previously described in Severn, 1993.

Deacylation of LPS to give backbone oligosaccharides

Backbone oligosaccharide was prepared as previously described in Severn, 1996 by modification of the deacylation procedure of Holst et al. Ester-bound fatty acids were removed from the lipid A of the LPS by treatment of a sample (400 mg) with anhydrous hydrazine at ambient temperature (20 mL, 37°C, 30 min). Excess hydrazine was destroyed by addition of acetone (three volumes) to the cooled reaction mixture (0°C). The precipitated *O*-deacylated LPS product was isolated by centrifugation (5000 rpm, 10 min), washed with acetone, and lyophylized from water. Removal of *N*-acyl groups was achieved by heating the *O*-deacylated sample (200 mg) in aq KOH (4 M, 10 mL) at 100°C for 20 h. The reaction mixture was cooled (0°C), neutralized with 4 M HCl, and the precipitated fatty acids removed by centrifugation (12 000 × g, 30 min). The supernatants were filtered in an Amicon concentration cell with a 500-molecular-weight-cutoff membrane (Amicon; YC05) and washed with deionized water until the eluant was free of chloride ions (as determined with aq $AgNO_3$). The dialyzed material was lyophylized to give deacylated LPS (ca. 80 mg). The oligosaccharide was purified by anion-exchange chromatography on DEAE A-25 (Severn, 1996). The backbone oligosaccharide fraction (ca. 50 mg) showed a doubly charged ion at *m/z* 1124.8 in the positive ion ESI-MS as the major ion which corresponded to a composition of Hex_3Hep_5 Kdo $HexN_2(H_2PO_3)_3$ (M, 2246.9). MS–MS of the doubly charged ion gave characteristic

fragments at *m/z* 500 ($HexN_2(H_2PO_3)_2$) and 801 ($KdoHexN_2(H_2PO_3)_2$) corresponding to deacylated lipid A and the Kdo-P substituted units, respectively.

D*-glycero-*L*-manno-*Heptose

The heptose was prepared by the condensation of Dgalactose with nitromethane in alkaline methanol Sawden, 1960. The crystalline 1-deoxy-1-nitro-D-*glycero*-L-*manno*-heptitol obtained

Fig. 10. Molecular model of the LPS of *M. haemolytica* A1 constructed using a lipid A having the fatty acyl substitution patterns reported for LPS from *H. influenzae*. The lipid A moiety is colored with the atoms C in black, O in red, and H in white. The sugar moiety is colored with Kdo in gray, heptoses in red or purple, glucose in green, and galactose in blue. The PO_4 groups are yellow. Hydroxyl protons have been removed.

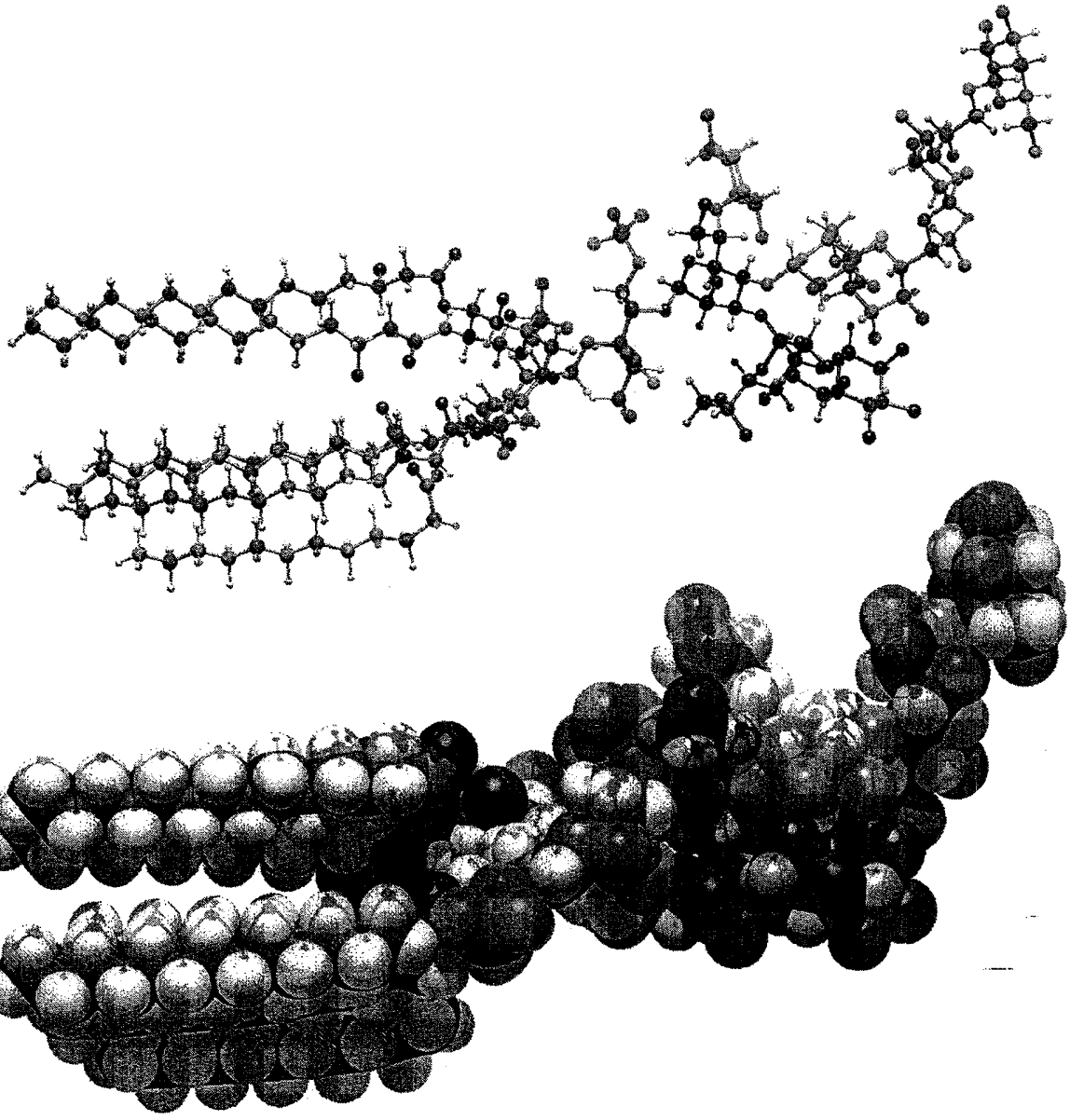

from the aqueous solution of the deionized products (mp 158°C, 21% yield) was converted to its sodium salt. On treatment with dilute sulphuric acid (35°C), followed by deionization with Rexyn 101(H^+) and Amberlite A4(OH^-) ion-exchange resins, the solution was lyophilized to give the heptose as a syrup (80% yield). The product was fractionated by cellulose column chromatography using butan-1-ol–water (1:10 v/v) as the eluant. Fractions containing the heptose were concentrated to dryness under reduced pressure. The D-*glycero*-L-*manno*-heptose having $[\alpha]_D$ –14° (*c* 0.2, water) was pure by paper chromatography and its reduced ($NaBH_4$) and acetylated product on GLC gave a single peak corresponding in retention time with that of authentic hepta-*O*-acetyl-D-*glycero*-L-*manno*-heptitol, establishing its purity.

D*-glycero-*D*-manno-*Heptose

The heptose was prepared from D-altrose via its condensation with nitromethane to yield 1-deoxy-1-nitro-D-*glycero*-D*manno*- heptitol (mp 109°C, $[\alpha]_D$ –7.0° (*c* 1.1, EtOH), 27% yield)) whose aqueous sodium salt solution on slow dropwise addition to stirred 20% (v/v) sulfuric acid maintained at 0°C was converted to D-*glycero*-D-*manno*-heptose Hulyalkar, 1963. The reaction mixture was neutralized with sat. $Ba(OH)_2$ solution, filtered, passed through Rexyn 101(H^+) and Duolite A4(OH^-) ion-exchange resins to remove residual ionic material, and was concentrated to a syrup (92% yield). The heptose product, as indicated by paper chromatography, was contaminated with altrose and unchanged 1-deoxy-1-nitro-D-*glycero*-D-manno-heptitol (ca. 2 to 3%). The product was purified by cellulose column chromatography using butan-1-ol–water (1:10 v/v) as the mobile phase. The D-*glycero*-D-*manno*mannose had [α]D +22° (*c* 2, MeOH). A reduced ($NaBH_4$) and acetylated sample on GLC gave a single peak corresponding to authentic hepta-*O*-acetyl-D-*glycero*-D-*manno*-Dheptitol indicating the identity and purity of the synthesized heptose.

Electrospray mass spectrometry

Samples were analyzed on a VG Quattro triple quadrupole mass spectrometer (Micromass, Manchester, U.K.) fitted with an electrospray ion source. Backbone oligosaccharide was dissolved in acetonitrile–water (approx. 1:2 v/v) containing 0.5% acetic acid. Injection volumes were 10 μL and the flow rate was set at 4 mL min^{-1}.

The electrospray tip voltage was typically 2.7 kV and the mass spectrometer was scanned from *m/z* 50 to 2500 with a scan time of 10 s. For MS–MS experiments, precursor ions were selected using the first quadrupole and fragment ions formed by collisional activation with argon in the RF-only quadrupole cell, were mass analyzed by scanning the third quadrupole. Collision energies were typically 60 ev (laboratory frame of reference).

Nuclear magnetic resonance

NMR spectra were performed on a Bruker AMX 600, AMX 500, or a Varian Inova 600 spectrometer using standard software. All measurements were made at 300 K and at pH 3, containing 10 mg of sample dissolved in 0.6 mL of D_2O. Measurements were done at pH 3 to improve resolution of the proton spectrum as done previously (Cox, 1996). Acetone was used as an internal or external reference at 2.225 ppm for ^{1}H spectra and 31.07 ppm for ^{13}C spectra. Standard homo- and heteronuclear correlated 2D techniques were used for general assignments of the core oligosaccharide: COSY, TOCSY, NOESY, triple quantum homonuclear correlated experiment, HMQC, HMQC-TOCSY, and HMBC and ^{31}P HMQC (Uhrin, 1994). Spin simulations for the heptose monosaccharides were performed with standard Varian software. Accurate chemical shifts and coupling constants were obtained from the parameters used to perform the spin simulation and not from the peak listing of the spectra.

Selective 1D-TOCSY, 1D-NOESY, 1D-TOCSY-TOCSY, 1D-TOCSY-NOESY, and 1D-NOESY-TOCSY experiments were performed for complete residue assignment and for determination f inter-residue ^{1}H-^{1}H nuclear Overhauser enhancements. The nomenclature used to describe the use of the 1D selective sequences will be 1D EXP (spin, mixing time) and 1D EXP1-EPX2 (spin1, mixing time; spin2, mixing time), where EXP, EXP1, and EXP2 stand for either TOCSY or NOESY. Also, in the figures, the selected resonances are underlined. A doubly underlined resonance means that this resonance was selected as the second selection step. As shown in Fig. 1, all the residues are labeled by letters and the spins are labeled by the atom number, so that a1 refers to the H-1 resonance of residue **a**.

On the AMX spectrometers, selective excitation was achieved by means of half-Gaussian pulses. The mixing time used for a TOCSY depended on the spin system. Usually a range of mixing times (spin lock times) from 30 to 180 ms was used to assign the spin system. The mixing time for a 1D-NOESY depended on the correlation time of the molecule and internal motion about the glycosidic linkage. NOESY mixing times were in the range from 150 to 400 ms. To detect inter-residue NOEs for the terminal Gal residue, a 1D-ROESY experiment was done with a mixing time of 500 ms. For the doubly selective experiments, the selective pulses were kept as short as possible to avoid loss of signal intensity due to relaxation effects. Each part was optimized one at a time. The 1D-TOCSY could be carried out in a matter of minutes. The 1D-NOESY took from minutes to hours depending on the magnitude of the NOE. Some doubly selective experiments took up to 12 h. The 1D-TOCSYTOCSY and 1D-TOCSY-NOESY were the most efficient. As the sample degraded with time, some experiments were also performed on an Inova 600 spectrometer making use of pulse field gradients.

Molecular modeling

The conformational analysis was done using the Metropolis Monte Carlo method as previously described (Peters, 1993). The PFOS potential was used (80). Minimized coordinates for the monosaccharides were obtained using MM3 (92) available from the Quantum Chemistry Program Exchange (QCPE). The minimum energy conformation for each disaccharide was used as the starting conformation. Starting from the Kdo at the reducing end, calculations were performed for various oligosaccharides up to the complete structure. For the inner core octasaccharide, 5×10^4 macro moves were used with a step length of 5° for the glycosidic linkage and a temperature of 1×10^3 K resulting in an acceptance ratio of 0.36. The molecular model for the inner core octasaccharide was generated using the minimum energy conformer. Distances were extracted from the saved coordinates at each macro move. The complete LPS with lipid A was generated using the lipid A structure (Wang, 1996) and the minimum energy conformer for the Kdo linkage. Molecular drawings were done using Schakal97 from E. Keeler, University of Freiburg, Germany.

EXAMPLE 2

Investigation of A. pleuropneumoniae Serotype 5a

Sugar analysis of the column-fractionated LPS revealed glucose (Glc), galactose (Gal), *N*-acetyl- glucosamine (GlcNAc), D-*glycero*-D-*manno*-heptose (DD-Hep), and L-*glycero*-D-*manno*-heptose (LD-Hep) in the approximate ratio of 2 : 1.5 : 1 : 2 : 3 respectively. The core OS was purified following gel filtration chromatography fractionation of the acid hydrolysate as described in the materials and methods and a fraction enriched in core OS and relatively free from O-antigen was obtained and subjected to sugar analysis which revealed; Glc, Gal, DD-Hep, and LD-Hep in the ratio of 2 : 1 : 2 : 3 respectively. As the capsular polysaccharide of serotype 5b contains *N*-acetyl-D-glucosamine and a ketose residue we suspected that the LPS had some capsule (CPS) contamination and that the fractionated core OS sample was devoid of CPS due to the sensitivity of the ketosidic bond in the CPS to the acid hydrolysis conditions employed to obtain the core OS. Additionally the relatively low amount of galactose, the only O-antigen residue, suggested that the fraction examined was primarily core OS without significant O-antigen extension.

LPS-OH was prepared and fractionated by gel filtration chromatography. A fraction eluting at a volume consistent with containing a low proportion of O-antigen was analysed by CE-ES-MS (Example 2, Table 1). A simple mass spectrum was observed corresponding to a molecule of 2537 amu consistent with a composition of 2Hex, 5Hep, Kdo, P, Lipid A-OH. CE-MS/MS analysis (data not shown) on the doubly charged ion, *m/z* 1268, gave two singly charged peaks at *m/z* 951 and 1584, confirming the size of the O-deacylated lipid A as 952 amu and the core OS as 1584. The O-deacylated lipid A species (952 amu) consists of a disaccharide of N-acylated (3-OH C 14:0) glucosamine residues, each residue being substituted with a phosphate molecule. ES-MS and CE-ES-MS analyses of the fractionated OS sample revealed a mass of 1505 Da, consistent with a composition of 2Hex, 5Hep, Kdo (Ex. 2, Table 1) (Ex. 2, Fig. 1). The CE-ES-MS spectrum of a later eluting core OS fraction had a mass of 1562, 57 amu higher than the major glycoform (Ex. 2, Table 1). This mass corresponds to the amino acid glycine as has been recently observed in the LPS of *Neisseria meningitidis* and *Haemophilus influenzae*. CE-ES-MS/MS analyses located

this glycine residue on the second heptose residue (Hep II) from the Kdo molecule (data not shown).

Methylation analysis was performed on the core OS in order to determine the linkage pattern of the molecule. Analysis on a fraction corresponding to core OS alone revealed the presence of approximately equimolar amounts of terminal Glc, 6-substituted Glc, terminal DD-Hep, terminal LD-Hep, 6-subsituted DD-Hep, 2-substituted LD-Hep and 3,4,6-tri-substituted LD-Hep. Analysis of an earlier fraction of the OS, containing predominantly O-antigen, revealed the presence of 6-substituted Gal (the O-antigenic component) confirming the linkage pattern of the O-antigen.

In order to elucidate the exact locations and linkage patterns of the OS, NMR studies were performed on the OS fraction enriched for the absence of O-antigen (Fig. 2a). The assignment of ^{1}H resonances of the OS was achieved by COSY and TOCSY experiments. Example 2 Fig. 3 shows a series of selective 1D-TOCSY experiments from the anomeric ^{1}H-resonance of each residue in the OS. In the course of the NMR analysis it became apparent that the *Ap* 5a OS was structurally related to the structure of *Mannheimia haemolytica* core OS and assignment of the *Ap* 5a OS spectra was aided by reference to this ^{1}H NMR data (Example 2, Table 2).

In the selective spectra of the *Ap* 5a OS, spin systems arising from heptose residues (Hep I, (Fig. 3a), Hep II, (Fig. 3b), Hep III, (Fig. 3c), Hep IV (Fig. 3d) and Hep V, (Fig. 3e),) were readily identified from their anomeric ^{1}H resonances at 5.11 (Hep I), 5.70 (Hep II), 5.17 (Hep III), 4.96 (Hep IV) and 5.03 (Hep V) ppm coupled with the appearance of their spin systems which pointed to *manno*-pyranosyl ring systems. The heterogeneity observed for the anomeric protons of Hep I and Hep II (Fig. 2a) was due to rearrangements of the Kdo residue on acid hydrolysis. The remaining residue in the α-anomeric region at 5.21 ppm (Glc II) was determined to be *gluco*-pyranose sugar, based upon the appearance of its spin system (Fig. 3f). The remainder of the anomeric resonances in the low field region (4.45 – 6.00 ppm) of the spectrum were all attributable to β-linked residues by virtue of their anomeric ^{1}H resonances and in the case of resolved residues their high $J_{1,2}$ (~ 8 Hz) coupling constants. One of the resonances at 4.66 ppm (Glc I) was assigned to the *gluco*-configuration from the appearance of the spin system (Fig. 3g). The remaining

resonance in the low-field region at 4.49 (Gal I) ppm was assigned to a *galacto*-pyranosyl residue from the appearance of the characteristic spin system to the H-4 resonance in a TOCSY experiment (Fig. 3h). The Kdo spin system was also accessed in this experiment as the H-6 ^{1}H resonance of Kdo at 4.48 ppm was also irradiated and revealed the H-4 and H-5 ^{1}H resonances at 4.10 and 4.21 ppm respectively. However the spin system of Kdo was difficult to completely determine due to rearrangements of the Kdo residue on core hydrolysis and the very low intensity levels of the methylene H-3 protons probably due to deuterium exchange. However, the spin system was further assigned in another 1-D TOCSY experiment from the H-3 axial proton at 1.92 ppm, revealing ^{1}H resonances for the equatorial proton at 2.08 ppm and the H-4 proton at 4.10 ppm (data not shown).

The sequence of the glycosyl residues in the OS was determined from the inter-residue ^{1}H-^{1}H NOE measurements between anomeric and aglyconic protons on adjacent glycosyl residues and confirmed and extended the methylation analysis data. The linkage pattern for the *Ap* 5a OS was determined in this way (Fig. 4) (Table 2). Thus the occurrence of intense transglycosidic NOE connectivities between the proton pairs Hep III H-1 and Hep II H-2 (Fig. 4a) and Hep II H-1 and Hep I H-3 (Fig. 4b) established the sequence and points of attachment of the three LD-heptose residues. This linkage pattern is commonly encountered in the inner core OS from *M. haemolytica* and *H. influenzae*. Furthermore, inter-residue NOE's between the anomeric protons Hep III H-1 and Hep II H-1provided confirmation of the 1,2-linkage[16]. Examination of NOE connectivities from H-1 of Glc I illustrated that this glucose residue was connected to Hep I at the 4-position by virtue of inter-residue NOE's to Hep I H-4 and Hep I H-6 (Fig. 4c). The appearance of an inter-residue NOE to H-6 is a common occurrence for 4-substituted heptose residues. The occurrence of a long range NOE connectivity between H-1 of Glc I and H-1 of Glc II suggested that the α-configured glucose residue (Glc II) was substituting Hep I at the 6-position as has been observed previously for the OS from *M. haemolytica*. Examination of NOE connectivities from H-1 of Glc II confirmed that this glucose residue was connected to Hep I at the 6-position by virtue of inter-residue NOE's to Hep I H-6 (Fig. 4d). Similarly to Glc I a long-range NOE connectivity was observed between the anomeric ^{1}H resonances of Glc I and Glc II. The linkage positions of the remaining heptose residues (Hep IV and Hep V) were deduced as follows.

Examination of NOE connectivities from H-1 of Hep IV revealed that this heptose residue was connected to Glc I at the 6-position by virtue of inter-residue NOE's to Glc I H-6 and H-6' (Fig. 4e). Finally, Hep V was determined to be substituting Hep IV at the 6-position by virtue of a NOE connectivity from Hep V H-1 to Hep IV H-6 (Fig. 4f). Additionally, NMR analysis of OS from serotype 5a enabled the point of attachment of the O-chain galactose residue to be identified. A fraction that contained just one galactose residue was utilised for this purpose. NOE connectivities from the anomeric ^{1}H-resonance included intra-connectivities to H-3 and H-5 at 3.68 and 3.93 ppm and an inter-connectivity to 3.93 ppm (Fig. 5a). Selective 1-D experiments were then utilised to identify the spin-system of the proton resonance at 3.93 ppm. A 1D NOESY-TOCSY experiment from the H-1 proton of Gal I in the NOESY step followed by selective excitation of the resonance at 3.93 ppm in the TOCSY step confirmed the connectivity of the resonance at 3.93 ppm to a resonance at 4.06 ppm (Fig. 5b). A 1-D TOCSY experiment from the anomeric proton resonance of the Hep III residue at 5.16 ppm utilising a 150 ms mixing time revealed the H-4 and H-5 proton resonances of this spin-system at 3.82 ppm (Fig. 3c). This resonance was then selectively irradiated in a NOESY step that revealed the Hep III H-6 resonance at 4.06 ppm thus confirming the 7-position of the Hep III residue as the point of attachment of the O-chain (Fig. 5c). Confirmatory data was obtained from a ^{13}C-^{1}H HMBC experiment which identified a cross-peak from the anomeric ^{1}H-resonance of the O-chain galactose residue at 4.48 ppm that correlated with a ^{13}C-resonance at 70.3 ppm (Fig. 5d), which in a ^{13}C-^{1}H HSQC experiment was found to correlate to the proton resonance at 3.93 ppm (Fig. 5e), which appeared as positive peak in a ^{13}C-^{1}H HSQC spectrum indicative of a $-CH_2-$ group, confirming the 7-position of a heptose residue as the point of O-chain attachment. This conclusion was confirmed by methylation analysis on a fraction that contained just one galactose residue that indicated the presence of a 7-substituted LD-Hep residue; this permethylated alditol acetate derivate was not observed following methylation analysis of a core OS fraction devoid of O-chain.

Investigation of A. pleuropneumoniae Serotype 5b

All analyses of LPS, LPS-OH and OS from serotype 5b were identical or very similar to the previous analyses described for serotype 5a (Tables 1 and 2; Fig. 2b).

Investigation of A. pleuropneumoniae Serotype 2

Sugar analysis of the intact LPS revealed the presence of Glc, DD-Hep, LD-Hep, Rha, Gal, GlcNAc and GalNAc in the approximate ratio 8 : 2 : 2 : 1 : 2 : 1 : 2 consistent with the presence of O-antigen and capsular polysaccharide in this material. Sugar analysis of the fractionated acid hydrolysate revealed the presence of Glc, Rha, Gal and GalNAc in an early eluting fraction, in the approximate ratio 2 : 1 : 1 : 1 consistent with a fraction enriched for O-antigen. A later fraction enriched for the absence of O-antigen revealed the presence of only Glc, DD-Hep and LD-Hep in the approximate ratio of 3 : 2 : 3 consistent with the absence of O-antigen from this core OS fraction.

LPS-OH was prepared and fractionated by gel filtration chromatography. A fraction eluting at a volume consistent with containing a low proportion of O-antigen was analysed by CE-ES-MS in the negative ion mode (Example 2 Table 1). A simple mass spectrum was observed corresponding to a molecule of 2700 amu consistent with a composition of 3Hex, 5Hep, Kdo, P, Lipid A-OH with minor amounts of a second molecule indicated with a mass of 80 amu lower, consistent with the absence of a phosphate residue. CE-MS/MS analysis (data not shown) on the triply charged ion *m/z* 899 gave a singly charged peak at *m/z* 951 confirming the size of the O-deacylated lipid A as 952 amu for the major molecule of mass 2700 amu. CE-ES-MS analyses of the fractionated core OS sample enriched for absence of the O-antigen revealed a mass of 1667 Da, consistent with a composition of 3Hex, 5Hep, Kdo (Example 2, Table 1). Mass spectrometric analyses therefore indicated that the core OS of serotype 2 contained an additional glucose residue than the core OS from serotypes 5a and 5b.

Methylation analysis of the core OS fraction enriched for absence of O-antigen revealed the presence of terminal Glc, 6-substituted Glc, terminal DD-Hep, terminal LD-Hep, 2-substituted DD-Hep, 2-substituted LD-Hep, 4,6-di-subsituted

DD-Hep, and 3,4,6-tri-substituted LD-Hep in the approximate ratio 6 : 3 : 3 : 2 : 1 : 2 : 3 : 2. The main discrepancy between the methylation data for the serotype 2 and 5b OS was the replacement of the mono-6-substituted DD-Hep with a 4,6-di-substituted DD-Hep tentatively identifying the 4-position of the internal DD-Hep residue as the point of attachment of the additional glucose residue. The ratio of terminal glucose residues, identified by methylation analyses, between serotypes 2 and 5b is also consistent with the presence of an additional terminal glucose residue in the core OS of serotype 2.

^{1}H-NMR data (Table 2, (Fig. 2c)) corroborated the mass spectrometric and methylation analyses data, confirming that the core OS of serotype 2 was identical to that found for serotype 5b but with the identification of an additional terminal α-configured glucose residue (Glc III). NOE data defined the point of attachment of the Glc III residue at the 4-position of Hep IV by virtue of an inter NOE connectivity from the ^{1}H resonance of the anomeric proton of Glc III at 4.53 ppm to the ^{1}H resonance of the 4 position of Hep IV at 3.96 ppm (data not shown). A NOE connectivity was also observed to the 6-position of Hep IV as has been observed previously for 4-substituted heptose residues.

Investigation of A. pleuropneumoniae Serotype 1

Sugar analysis of the column-fractionated LPS revealed the presence of Rha, Glc, Gal, GlcNAc, DD-Hep and LD-Hep in an approximate ratio of 1 : 3 : 1 :0.5 : 1 : 3. The identification of Rha and GlcNAc suggested some O-antigenic components were still present in this fraction[20]. Sugar analysis of a core OS fraction enriched for absence of O-antigen revealed Glc, Gal, DD-Hep, and LD-Hep in the ratio 2 : 1.5 : 1 : 3. Sugar analysis on earlier fractions containing full length O-antigen revealed Rha, Glc and GlcNAc in an approximate ratio of 2 : 1 : 1 consistent with the published structure for the O-antigen of this serotype.

LPS-OH was prepared and fractionated by gel filtration chromatography. A fraction eluting at a volume consistent with containing a low proportion of O-antigen was analysed by ES-MS and CE-ES-MS in the negative ion mode (Table 1). A simple mass spectrum was observed corresponding to a molecule of 2874 amu consistent

with a composition of 4Hex, HexNAc, 4Hep, Kdo, P, Lipid A-OH with minor amounts of a second molecule indicated with a mass of 123 amu higher, consistent with the presence of an additional phosphoethanolamine residue and a third molecule with a mass of 80 amu lower, consistent with the absence of a phosphate residue. CE-MS/MS analysis (data not shown) on the triply charged ion *m/z* 957 gave a singly charged peak at *m/z* 951 confirming the size of the O-deacylated lipid A as 952 amu for the major molecule of mass 2874 amu and a doubly charged ion at *m/z* 959 corresponding to the core OS. ES-MS and CE-ES-MS analyses on several core OS fractions enriched for absence of the O-antigen revealed a mass of 1840 Da, consistent with a composition of 4Hex, HexNAc, 4Hep, Kdo (Table 1). CE-MS/MS analysis in positive ion mode on the doubly charged ion at *m/z* 930 revealed singly charged ions consistent with the presence of the following groups of residues in serotype 1 core OS including, HexNAc *m/z* 204, Hex-Hex-HexNAc *m/z* 528, Hep-Hex-Hex-HexNAc *m/z* 720 (Fig. 6). Mass spectrometric analyses therefore indicated that the core OS of serotype 1 contained one DD-Hep residue less than the core OS from serotypes 5a and 5b, but contained and an additional 2 Hex's and a HexNAc residue. However the absence of evidence for HexNAc in sugar analysis of core OS enriched for the absence of O-antigen was initially confusing.

Methylation analysis on a core OS fraction enriched for absence of O-antigen revealed the presence of terminal Glc, 6-substituted Glc, 3-substituted Gal, terminal LD-Hep, 4,6-disubstituted Gal, 4-subsituted DD-Hep, 2-substituted LD-Hep and 3,4,6-trisubstituted LD-Hep in approximately equimolar amounts. Once again the absence of any evidence for a HexNAc residue was perplexing.

The mass spectrometric, sugar and methylation analyses data were therefore consistent with the inner core structure observed for serotypes 2, 5a and 5b and ^{1}H NMR data corroborated these inferences (Fig. 2d) (Table 2). ^{1}H NMR data also enabled identification of the additional core OS residues not present in the core OS from serotypes 2, 5a and 5b. An α-configured galactose residue (Gal II) was assigned at 5.18 ppm by virtue of a characteristic spin system to the H-4 ^{1}H resonance in a TOCSY experiment. A β-configured galactose residue (Gal I) was identified at 4.55 ppm by virtue of the ^{1}H resonance of its anomeric proton and from the appearance of its characteristic spin system. An α-configured N-acetyl hexosamine residue

(HexNAc) was assigned at 4.88 ppm by virtue of the ^{1}H resonance of its H-2 proton at 4.34 ppm correlating to a ^{13}C chemical shift of 52.6 ppm in a ^{13}C-^{1}H HSQC experiment (Fig.7a). The ^{13}C chemical shift being consistent with a nitrogen substituted carbon atom. However it was very difficult to access the spin system of this HexNAc residue beyond the H-2 proton, and the chemical shift of the H-2 proton seemed to be of considerably low-field. Inter-residue NOE connectivities established the linkage pattern between the anomeric proton of the Gal I residue at 4.55 ppm and the 4-position of Hep IV at 3.94 ppm. In a similar way a NOE connectivity between the anomeric proton of the Gal II at 5.18 ppm and the 3-position of the Gal I residue at 3.79 ppm established this linkage. However, inter-residue NOE connectivities between the anomeric proton of the HexNAc residue at 4.88 ppm and the 4-position of the Gal II residue at 4.25 ppm and the 6-position of this residue at 4.12 and 4.01 ppm suggested that the HexNAc residue was substituting the Gal II residue at both the 4 and 6-positions, consistent with the methylation analysis data but nonetheless confusing (Fig. 7c). FAB-MS of the methylated OS gave further insight in to the sequence of the sugars of this portion of the OS. The *m/z* of the A-type primary glycosyl oxonium ions and secondary ions (loss of methanol) observed were as follows, 464→432 (Hex, HexNAc)$^{+}$, 668→636 (Hex_2, HexNAc)$^{+}$, 916→884 (Hex_2, HexNAc, Hep)$^{+}$, 1120→1088 (Hex_3, HexNAc, Hep)$^{+}$, 1368 (Hex_3, HexNAc, Hep_2)$^{+}$, 1572→1540 (Hex_4, HexNAc, Hep_2)$^{+}$, and 1865→1833 (Hex_3, HexNAc, Hep_4)$^{+}$. This FAB data was consistent with the NOE and positive ion CE-ES-MS/MS data, but the lack of evidence for a terminal HexNAc residue was confusing but in agreement with the sugar analysis and methylation analysis data. The lack of definitive data for the HexNAc residue therefore prompted more sophisticated NMR studies to attempt to identify the nature of the presumed HexNAc residue and confirm the linkage pattern for this region of the core OS from serotype 1.

A series of selective 1D experiments from the H-1 ^{1}H-resonance of the HexNAc residue at 4.88 ppm with mixing times ranging from 30 – 150 ms revealed the H-2 ^{1}H-resonance at 4.34 ppm and weak signals assigned to H-3 at 4.13 ppm and H-4 at 3.36 ppm. To confirm these inferences and complete assignment of this HexNAc residue further selective experiments were performed. A 1-D TOCSY experiment was obtained from the H-4 ^{1}H-resonance at 3.36 ppm, which confirmed

the H-2 and H-3 assignments and identified the H-5 and H-6, 6' resonances at 3.93, 3.66 and 3.64 ppm respectively (Fig. 7d). A 1-D NOESY experiment was obtained from the H-2 ^{1}H-resonance at 4.34 ppm, which confirmed the H-3 and H-4 assignments (Fig. 7e). A 1-D NOESY experiment was obtained from the H-4 ^{1}H-resonance at 3.36 ppm, which confirmed the H-2, H-3, H-5 and H-6, 6' assignments (Fig. 7f). The coupling constants were determined from these experiments and found to be $J_{1,2}$ 4.8 Hz, $J_{2,3}$ 1.0 Hz, $J_{3,4}$ 9.7 Hz, $J_{4,5}$ 1.4 Hz, $J_{5,6}$ 6.5 Hz, $J_{5,6'}$ 6.5 Hz and $J_{6,6'}$ -12 Hz . A 2D-^{13}C-^{1}H-HSQC NMR spectrum was performed (Fig. 7e) which identified the ^{13}C chemical shifts for the C-1 to C-6 positions on the HexNAc molecule as 101.1 ppm, 52.6 ppm, 68.5 ppm, 70.0 ppm, 70.7 ppm and 64.1 ppm respectively. This data was initially confusing, however a search of an in-house carbohydrate database identified a similar set of data for an open-chain N-acetyl galactosamine residue found in the core OS from *Proteus* species[21,22]. The identification of an open-chain residue although surprising, was consistent with the sugar, methylation and FAB analysis data as such a residue would be sensitive to the hydrolysis conditions employed for the sugar and methylation analyses and the formation of a glycosyl oxonium ion for the terminal residue, in FAB analysis, would be precluded by the open-chain configuration of this residue.

Structural analysis of the core OS's from the 1, 2, 5a and 5b serotypes was therefore complete and had identified a conserved inner core structure in all strains with different decoration beyond this conserved structure as illustrated in Fig. 8.

Structural analysis of core oligosaccharides from serotypes 1, 2, 5a and 5b representing core types I, II, II and II, revealed a relatively conserved structure. The inner core OS was identical for each strain consisting of a trisaccharide of L-*glycero*-D-*manno*-heptose residues linked to a Kdo residue. In each serotype the proximal heptose residue (Hep I) was substituted at the 3-position by the second L-*glycero*-D-*manno*-heptose residue (Hep II) of the L-*glycero*-D-*manno*-heptose trisaccharide, at the 4-position by a β-glucose residue (Glc I) and at the 6-position by an α-glucose residue (Glc II). A D-*glycero*-D-*manno*-heptose residue (Hep IV) was found at the 6-position of the Glc I residue in each strain. A second D-*glycero*-D-*manno*-heptose residue (Hep V) substitutes Hep IV at the 6-position in serotypes 2, 5a and 5b. The

only difference between serotypes 2 and 5a, 5b was an additional glucose residue linked to the 4-position of the Hep IV residue in serotype 2. There was a striking similarity between these OS structures and that found previously for the OS from *M. haemolytica* serotype A1[14]. The only difference between the 5b, 5a OS structures and *M. haemolytica* serotype A1core OS was the absence of the additional terminal galactose residue at Hep V found in *M. haemolytica* A1 OS. In serotype 1 there is no Hep V residue, Hep IV is alternatively substituted at the 4-position by a trisaccharide of α-GaloNAc-(1-4,6)-α-Gal-(1-3)-β-Gal-, wherein the HexNAc residue was of the rarely encountered open-chain configuration. The structural arrangement identified as the initial trisaccharide extension from Hep I in serotype 1 is identical to that previously found for *Haemophilus ducreyi* strain 2665 LPS[23], however the serotype 1 LPS has a different extension beyond the Gal I residue when compared to the DD-Hep interrupted lacto-N-neotetraose structure found in *H. ducreyi*.

A structural explanation has therefore been attained for the SDS-PAGE observation of two core types in *Ap* LPS. Serotypes 2, 5a and 5b of core type II have very similar LPS structures differing only by an additional glucose residue in serotype 2. However serotype 1 of core type I has lost a DD-Hep residue, but gained two hexoses and a novel open chain HexNAc residue. To investigate if this novel open chain HexNAc residue was found in other core type I serotypes LPS from serotypes 6, 9 and 11 were examined. Evidence for the open chain HexNAc was seen by both MS and NMR studies (data not shown) in serotypes 9 and 11 but not in serotype 6. Closer examination of SDS-PAGE profiles that had been used to categorise core types revealed that serotype 6 had both LPS migration patterns of the two core types and therefore it is possible that the serotype 6 strain we examined only had a core type II profile.

Little data is available on the genetic control of LPS biosynthesis in *Ap*. A recent paper by Galarneau et al identified three genes following transposon mutagenesis that appeared to be involved in the biosynthesis of the core OS region of *Ap* serotype 1 LPS. These genes were tentatively identified as glycosyltransferases based on homology to other glycosyltransferases. The three genes were postulated to be *lbgB*, an α-1,6-DD-heptosyltransferase, *lbgA* a β-1,4-galactosyltransferase and a hexose or N-acetyl-hexosamine transferase. The former two genes, *lbgAB*, are

consistent with the structure identified here in serotype 1 core OS, and have the same locus arrangement as found in *H. ducreyi* LPS. Another paper by Rioux et al identified a gene *galU*, the structural gene for UTP-α-D-glucose-1-phosphate uridyltransferase. SDS-PAGE of LPS isolated from a serotype 1 *Ap galU* mutant strain had an altered migration pattern of the core-lipid A region, and this mutant strain was less adherent to pig tracheal cells and was less virulent in pigs, suggesting that an alteration in the nature or presentation of the core OS region could have an effect on the virulence of this animal pathogen.

The identification of a novel open chain HexNAc residue was of interest. This structure has only previously been identified in two Proteus species and recently in *Shewanella oneidensis* and its significance is unknown. As found in the existing literature, the open chain residue identified here was found to concurrently di-substitute the neighbouring residue at the 4- and 6-positions, so this could be a common arrangement for such residues.

The identification of a DD-Hep residue in the oligosaccharide extension from Hep I has been observed before for several strains including *M. haemolytica, H. ducreyi* and non-typable *H. influenzae*. In *M. haemolytica* two DD-Hep residues were observed, whereas in *H. ducreyi* and *H. influenzae* only one DD-Hep residue was found. In *Ap* both scenarios exist, with serotypes 2 and 5a, 5b having two DD-Hep residues and serotype 1 having just one DD-Hep residue in the oligosaccharide extension from Hep I. The tri-LD-heptosyl inner core group has also been observed previously in *M. haemolytica*, *H. ducreyi* and *H. influenzae*. The 3,4,6-trisubstituted Hep I residue found here for all strains of *App* studied has been observed before in *M. haemolytica* LPS, however *H. ducreyi* LPS only elaborates the 3,4-di-substituted Hep I residue as also found in *H. influenzae*.

The identification of the 7-position of the Hep III residue as the point of attachment of the O-antigen galactose residue in serotype 5a was of interest and consistent with the observation that three variously truncated core oligosaccharide mutants in serotype 1 still elaborated an O-antigen[24], as the anticipated function of the three mutated gene products would not interfere with the biosynthesis of the inner

core LD-heptosyl trisaccharide unit and therefore the acceptor for O-antigen attachment would still be present in the mutant LPS core oligosaccharide.

This study has structurally characterised the core oligosaccharide region of several strains of *Ap*, representative of the two core types, identifying a conserved inner-core structure and a novel outer-core constituent. This region is known to be involved in adherence of *Ap* and is therefore implicated in virulence. This study will therefore better enable future studies on the relevance of the structure of the core oligosaccharide region of *Ap* LPS to the potential virulence of this organism.

MATERIALS and METHODS – EXAMPLE 2

Media and Growth conditions

Ap serotypes 1 (strain 4074), 2 (strain 4226), 5a (strain K17) and 5b (strain L20) were initially grown overnight on chocolate agar plates at 37°C and growths were used to inoculate 1 L of brain-heart infusion (BHI) medium supplemented with ∃ NAD (Sigma N-7004) to a final concentration of 5ug/ml, haemin (Sigma H-2250) to a final concentration of 5ug/ml and 1% glucose (10g). Cultures were then incubated at 37°C at 200 rpm for 6 hours and used to inoculate 23 L BHI medium (supplemented as above) in a 28 L NBS fermenter. The cultures were then grown at 37°C, with 24 $lmin^{-1}$ aeration and stirring at 200 rpm for 18 hours. Cells were killed (2% phenol w/v, for 4 hours) and harvested by using a Sharples continuous centrifuge (~40g wet weight).

Isolation and purification of lipopolysaccharide

The lipopolysaccharide (LPS) was isolated from the dried cell mass by the hot water/phenol method (Westphal, 1965), following washing of the dried cell mass with organic solvents for serotypes 5a and 5b (Masoud, 1997). The aqueous phase was dialyzed against water and lyophilised and in the case of serotype 2 the LPS was isolated from the extensively dialysed phenol phase (Altman, 1987). The dried sample was dissolved in water to give a 1-2% solution (w/v) and treated with

deoxyribonuclease I (DNase) (0.01 mg/ml) and ribonuclease (RNase) (0.01 mg/ml) for 3 hrs at 37°C, then treated with proteinase K (0.01 mg/ml) for 3hrs. The dialysed, dried sample was dissolved in water to make a 1 % solution and ultracentrifuged (5hrs, 100,000 g). The LPS pellet was redissolved in water and lyophilised, purified by gel-filtration on a column of Bio-Gel P-2 (1 cm X 100 cm) with water as eluent and fractions containing sugar were pooled and lyophilised. Purified LPS was treated with anhydrous hydrazine with stirring at 37°C for 1 hr to prepare O-deacylated LPS (LPS-OH). The reaction was cooled in an ice bath and gradually cold acetone (-70°C, 5 vols.) was added to destroy excess hydrazine and the precipitated LPS-OH was isolated by centrifugation. The sample was then purified down a Bio-Gel P-2 column as described above. The core oligosaccharide (OS) was isolated by treating the purified LPS with 1 % acetic acid (10mgml^{-1}, 100°C, 1.5 hr) with subsequent removal of the insoluble lipid A by centrifugation (5000 g). The lyophilised OS was further purified down a Bio-Gel P-2 column with individual fractions lyophilised.

Analytical methods

Sugars were determined as their alditol acetate derivatives (Sawardeker, 1965) by GLC-MS. Samples were hydrolysed for 4 hrs using 4 M trifluoroacetic acid at 100°C. The hydrolysate was reduced ($NaBD_4$) overnight in H_2O and acetylated with acetic anhydride at 100°C for 2h using residual sodium acetate as catalyst. The GLC-MS was equipped with a 30 M DB-17 capillary column (180°C to 260°C at 3.5°C/min) and MS was performed in the electron impact mode on a Varian Saturn II mass spectrometer. Methylation analysis was carried out by the NaOH / DMSO /methyl iodide procedure (Ciucanu, 1994) and analysed by GLC-MS as above.

Mass spectrometry

ESI-MS was performed in the negative ion mode on a VG Quattro Mass Spectrometer (Micromass, Manchester, U.K.) by direct infusion of samples in 25% aqueous acetonitrile containing 0.5% acetic acid. Capillary electrophoresis (CE)-ESI-MS was performed on a crystal Model 310 (CE) instrument (AYI Unicam) coupled to an API 3000 mass spectrometer (Perkin-Elmer/Sciex) via a microIonspray interface. A sheath solution (isopropanol-methanol, 2:1) was delivered at a flow rate of 1 μL/min to a

low dead volume tee (250 μm i.d., Chromatographic Specialties). All aqueous solutions were filtered through a 0.45-μm filter (Millipore) before use. An electrospray stainless steel needle (27 gauge) was butted against the low dead volume tee and enabled the delivery of the sheath solution to the end of the capillary column. The separations were obtained on about 90 cm length bare fused-silica capillary using 10 mM ammonium acetate/ammonium hydroxide in deionized water, pH 9.0, containing 5% methanol. A voltage of 20 kV was typically applied at the injection. The outlet of the capillary was tapered to ca. 15 μm i.d. using a laser puller (Sutter Instruments). Mass spectra were acquired with dwell times of 3.0 ms per step of 1 *m/z* unit in full-mass scan mode. The MS/MS data were acquired with dwell times of 1.0 ms per step of 1 *m/z* unit. Fragment ions formed by collision activation of selected precursor ions with nitrogen in the RF-only quadrupole collision cell, were mass analyzed by scanning the third quadrupole.

Nuclear Magnetic Resonance

NMR experiments were acquired on Varian Inova 400, 500 and 600 MHz spectrometers using a 5mm or 3mm triple resonance (^{1}H, ^{13}C, ^{31}P) probe. The lyophilised sugar sample was dissolved in 600 μL (5mm) or 140 μL (3mm) of 99% D_2O. The experiments were performed at 25°C with suppression of the HOD (deuterated H_2O) signal at 4.78 ppm. The methyl resonance of acetone was used as an internal reference at 2.225 ppm for ^{1}H spectra and 31.07 ppm for ^{13}C spectra. Standard homo and heteronuclear correlated 2D pulse sequences from Varian, COSY, TOCSY, NOESY, ^{13}C-^{1}H HSQC, ^{13}C-^{1}H HSQC-TOCSY and ^{13}C-^{1}H HMBC, were used for general assignments. Selective 1D-TOCSY with a Z-filter and 1D-NOESY experiments and 1-D analogues of 3-D NOESY-TOCSY and TOCSY-NOESY experiments were performed for complete residue assignment and for the determination of ^{1}H-^{1}H nuclear Overhauser enhancements (Brisson, 2002). The pulse width of the selective pulses was 30-80 Hz. Mixing times of 30-150 ms were used for the 1D-TOCSY experiments. Mixing times of 400-800 ms were used for the 1D-NOESY experiments.

The inclusions of a reference to a document or disclosure is neither an admission nor a suggestion that it is relevant to the patentability of anything disclosed herein.

1. W.B. Severn and J.C. Richards. Carbohydr. Res. 240, 277 (1993).
2. A.D. Cox, J.R. Brisson, V. Varma, and M.B. Perry. Carbohydr. Res. 290, 43 (1996).
3. W.B. Severn, R.F. Kelly, J.C. Richards, and C. Whitfield. J. Bacteriol. 178, 1731 (1996).
4. O. Holst, U. Zahringer, H. Brade, and A. Zamojski. Carbohydr. Res. 215, 323 (1991).
5. J.C. Sowden and D.R. Strobach. J. Am. Chem. Soc. 82, 954 (1960).
6. R.K. Hulyalkar, J.K.N. Jones, and M. B. Perry. Can. J. Chem. 41, 1490 (1963).
7. D. Uhrin, J.R. Brisson, L.L. MacLean, J.C. Richards, and M.B. Perry. J. Biomol. NMR, 4, 615 (1994).
8. T. Peters, B. Meyer, P. Stuike, R. Somorjai, and J. R. Brisson. Carbohydr. Res. 238, 49 (1993).
9. I. Tvaroska and S. Perez. Carbohydr. Res. 149, 389 (1986).
10. Y. Wang and R.I. Hollingsworth. Biochemistry, 35, 5647 (1996).
11. Brisson, J. –R., Crawford, E., Uhrin, D., Kheiu, N. H., Perry, M.B., Severn, W. B., and Richards, J. C. *Can. J. Chem.* 2002, 80, 949-963.
12. Masoud, H., Moxon, E. R., Martin, A., Krajcarski, D., and Richards, J. C. *Biochemistry* **1997**, *36*, 2091-2103.
13. Altman, E., Brisson, J.-R., Bundle, D. R., and Perry, M. B. *Biochem. Cell. Biol.* **1987**, *65*, 876-889.
14. Westphal, O. & Jann, K. Bacterial lipopolysaccharide. *Methods Carbohydr. Chem.* **1965**, *5*, 88-91.
15. Sawardeker, D.G., Sloneker, J. H., & Jeanes, A. *Anal. Chem.* **1965**, *37*, 1602-1604.
16. Ciucanu, I. & Kerek, F. *Carbohydr. Res.* **1994**, *131*, 209-217.

17. Brisson, J.R., Sue, S.C., Wu, W.G., McManus, G., Nghia, P.T., & Uhrin, D. In *NMR spectroscopy of glycoconjugates* (Jimenez-Barbero, J. & Peters, T., Eds), Wiley-VCH, Weinhem, 2002; pp 59-93.

18. Brisson, J.-R., Crawford, E., Uhrin, D., Khieu, N. H., Perry, M. B., Severn, W. B., and Richards, J. C. (2002) The core oligosaccharide component from *Mannheimia (Pasteurella) haemolytica* serotype A1 lipopolysaccharide contains L-*glycero*-D-*manno* and D-*glycero*-D-*manno*-heptoses. Analysis of the structure and conformation by high-resolution NMR spectroscopy. *Can. J. Chem.* **80**, 949-963.

19. Schweda, E. K. H., Sundstrom, A. C., Eriksson, L. M., Jonasson, J. A., and Lindberg, A. (1994) Structural studies of the cell envelope lipopolysaccharides from *Haemophilus ducreyi* strain ITM 2665 and ITM 4747. *J. Biol. Chem.* **269**, 12040-12048.

FIGURE LEGENDS (Numbers refer to figures in Example 2

Figure 1. Negative ion electrospray mass spectrum of *Ap* serotype 5a core OS.

Figure 2. Anomeric regions of the ^{1}H- NMR spectra of the core OS from *Ap* serotypes a) 5a; b) 5b; c) 2; d) 1. The spectra were recorded in D_2O at pH 7.0 and 25 ^{O}C.

Figure 3. Ring regions of the selective 1D-TOCSY NMR spectra of the core OS from *Ap* serotype 5a residues a) Hep I; b) Hep II; c) Hep III; d) Hep IV; e) Hep V; f) Glc II; g) Glc I; h) Gal I. Letter designations for each residue are as indicated in Table 2. The spectra were recorded in D_2O at pH 7.0 and 25 ^{O}C with mixing times of 150ms for the heptose residues and 90ms for the hexose residues.

Figure 4. Ring regions of the selective 1D-NOESY NMR spectra of the core OS from *Ap* serotype 5a residues a) Hep III; b) Hep II; c) Glc I; d) Glc II; e) Hep IV; f) Hep V. Letter designations for each residue are as indicated in Table 2.The spectra were recorded in D_2O at pH 7.0 and 25 ^{O}C with a mixing time of 400ms.

Figure 5. Determination of the location of the O-chain Gal I residue of the core OS from *Ap* serotype 5a. a) 1D-NOESY NMR spectrum from the anomeric ^{1}H-resonance of Gal I; b) 1D-NOESY-TOCSY spectrum from the anomeric ^{1}H-resonance of Gal I residue in the NOESY step and from the H-7 ^{1}H-resonance of the Hep III residue in the TOCSY step; c) 1D- TOCSY-NOESY spectrum from the anomeric ^{1}H-resonance of Hep III residue in the TOCSY step and from the H-4 / H-5 ^{1}H-resonances of the Hep III residue in the NOESY step. d) Region of the ^{13}C -^{1}H-HMBC NMR spectrum indicating the HMBC from the anomeric ^{1}H-resonances of Gal I and Glc I. e) Region of the ^{13}C -^{1}H-HSQC NMR spectrum indicating the ^{13}C -cross-peaks from the H-7 ^{1}H-resonance of Hep III, the H-2 ^{1}H-resonance of Hep V and the H-3 ^{1}H-resonance of Hep II. The spectra were recorded in D_2O at pH 7.0 and 25 ^{o}C.

Figure 6. Positive ion capillary electrophoresis-electrospray mass spectrum of the core OS from *Ap* serotype 1. Product ion spectrum from *m/z* 930^{2+}.

Figure 7. Identification of the open-chain N-acetylgalactosamine residue of the core OS from *Ap* serotype 1. a) Ring region of the 2D-^{13}C-^{1}H-HSQC NMR spectrum of the core OS from *Ap* serotype 1. b) Ring region of the ^{1}H-NMR spectrum of the core OS from *Ap* serotype 1. c) 1-D NOESY spectrum from the H-1 ^{1}H-resonance of the GalNAc residue. d) 1-D TOCSY spectrum from the H-4 ^{1}H-resonance of the GalNAc residue. e) 1-D NOESY spectrum from the H-2 ^{1}H-resonance of the GalNAc residue. f) 1-D NOESY spectrum from the H-4 ^{1}H-resonance of the HexNAc residue. The spectra were recorded in D_2O at pH 7.0 and 25 ^{o}C. The assignments of the resonances are as indicated (i, GalNAc; j, Gal II).

Figure 8. Structural representation of an embodiment of the core oligosaccharides from *Ap* serotypes 1, 2, 5a and 5b. For serotype 1; R is α-GaloNAc-(1-4,6)-β-Gal II-(1-3)-β-Gal I, and R' is H where o indicates open-chain configuration. For serotype 2; R is β-Glc III, and R' is D-α-D-Hep V. For serotypes 5a and 5b; R is H and R' is D-α-D-Hep V.

Example 2, Fig.1

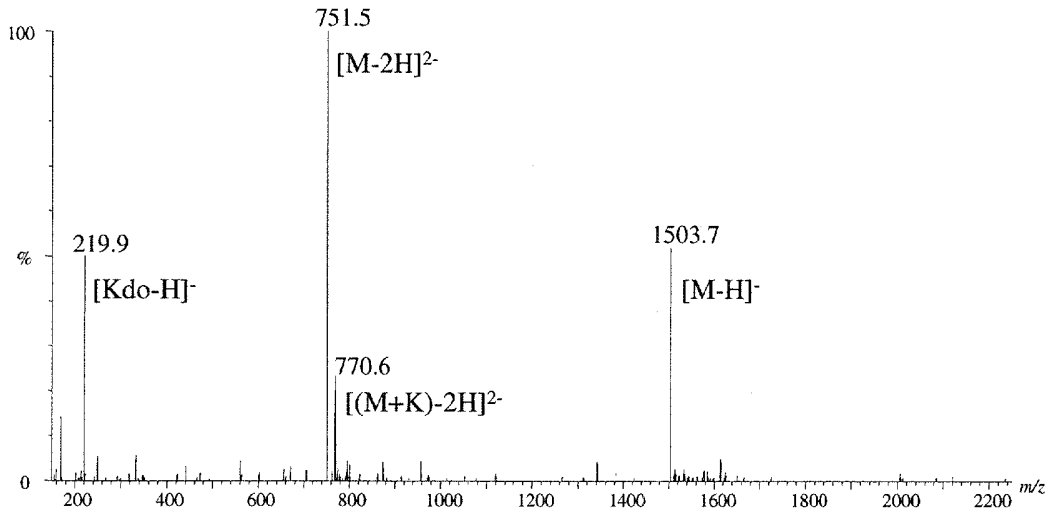

Example 2, Fig. 2

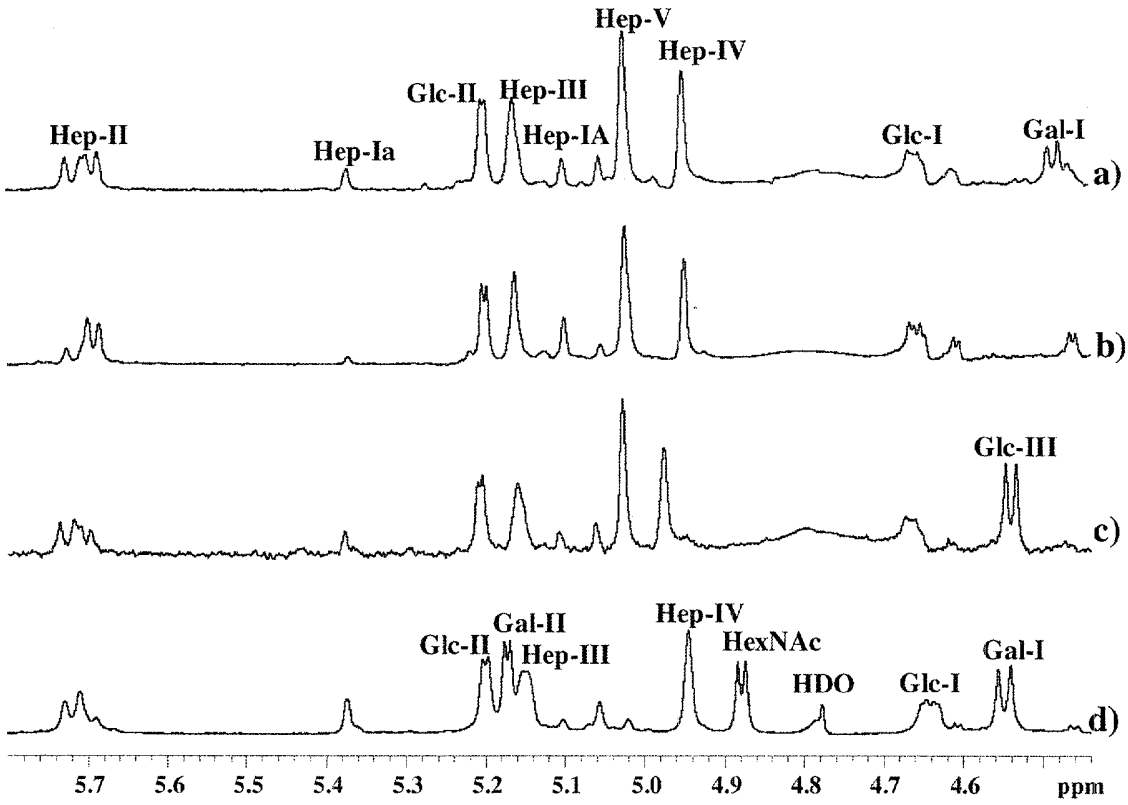

Example 2, Fig. 3

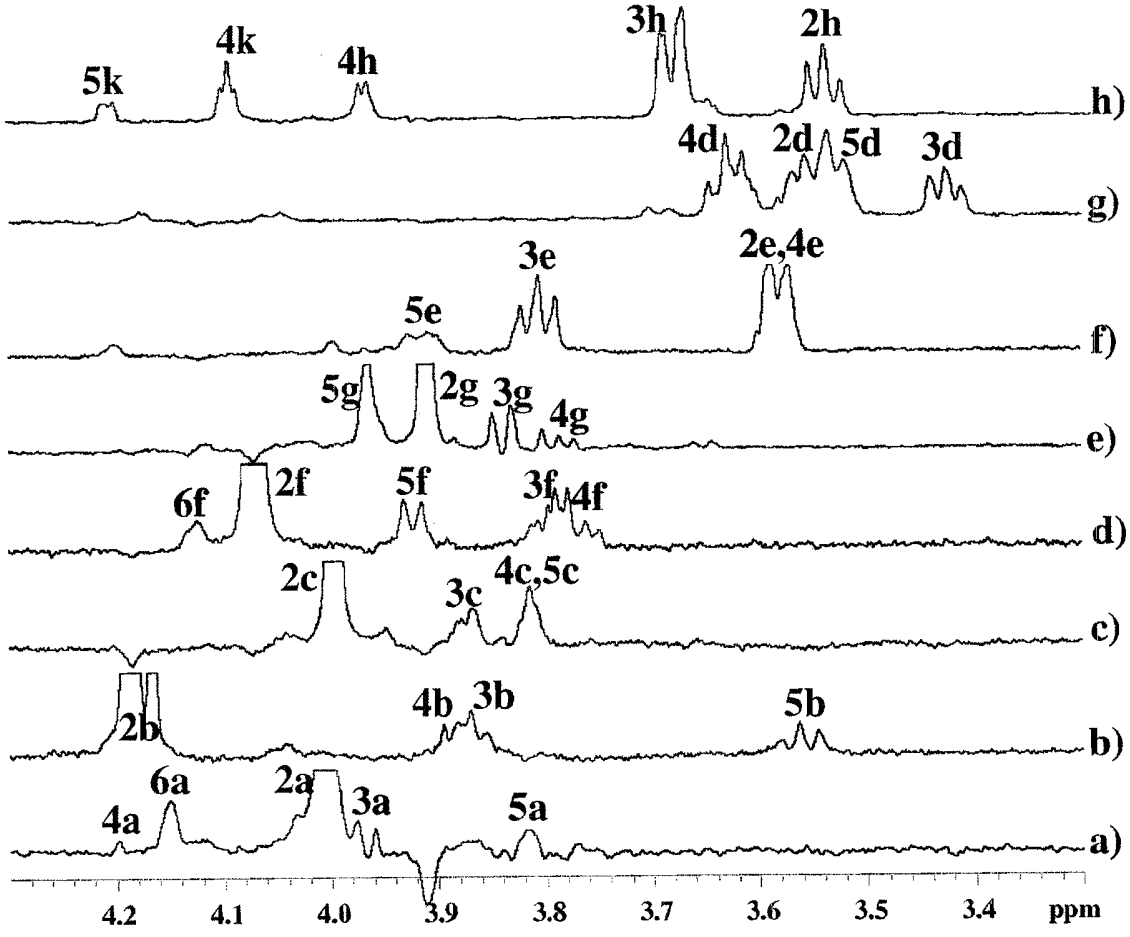

Example 2, Fig.4

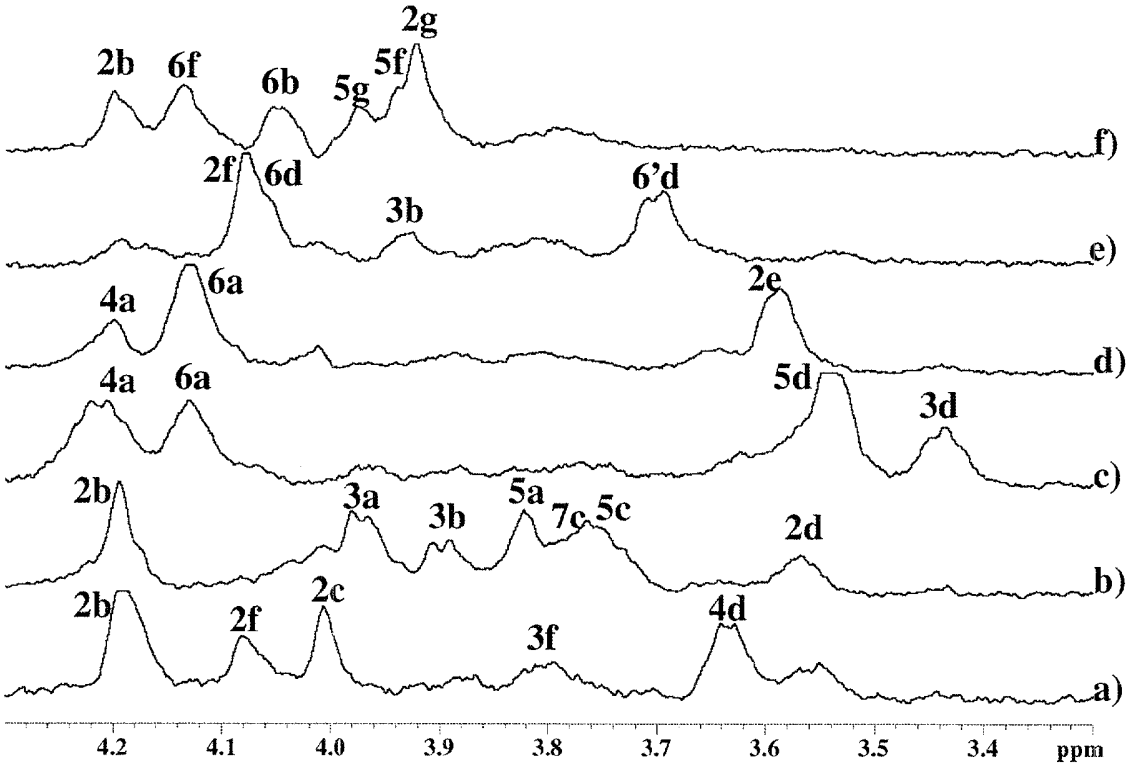

Example 2, Fig. 5

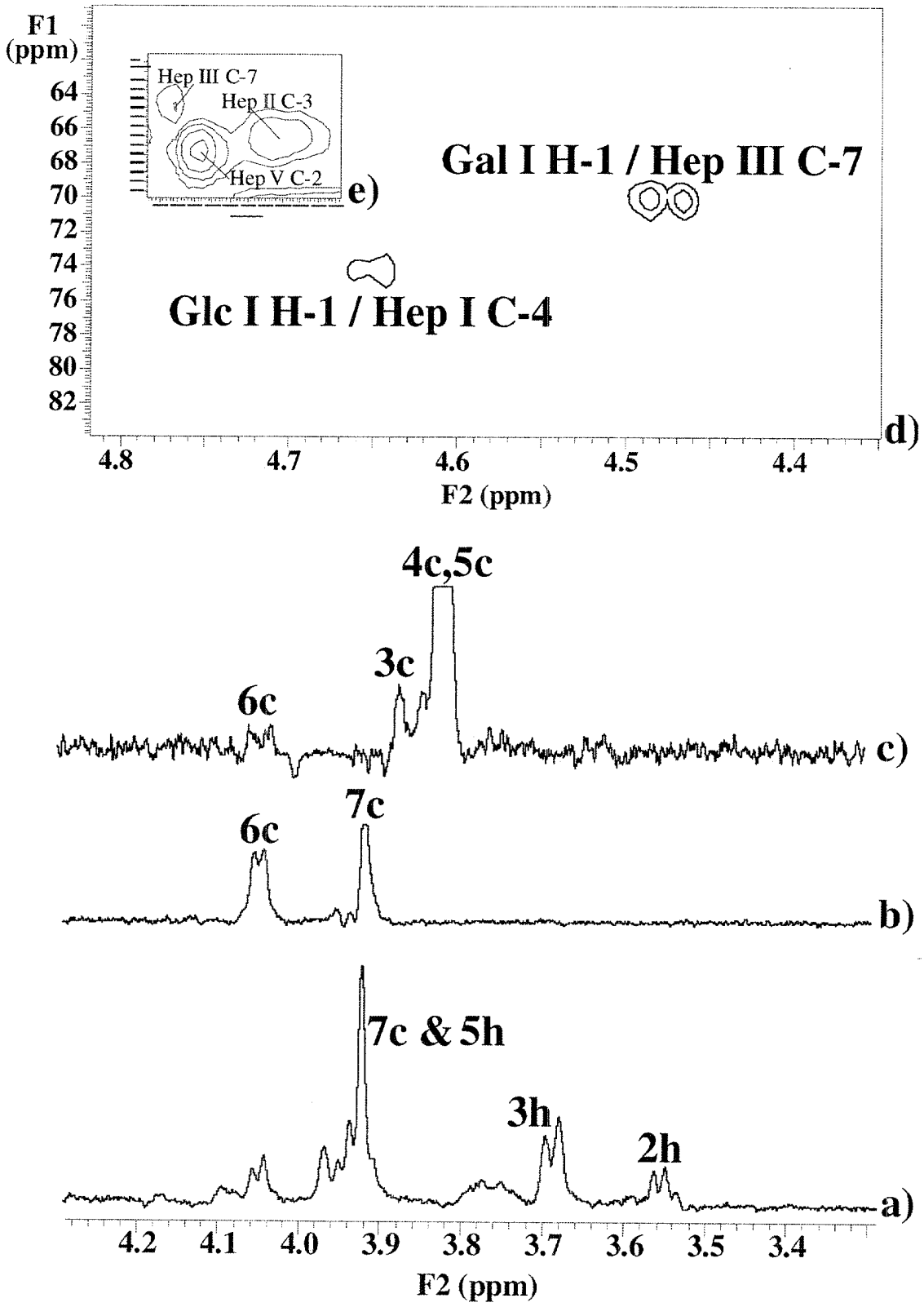

Example 2, Fig.6

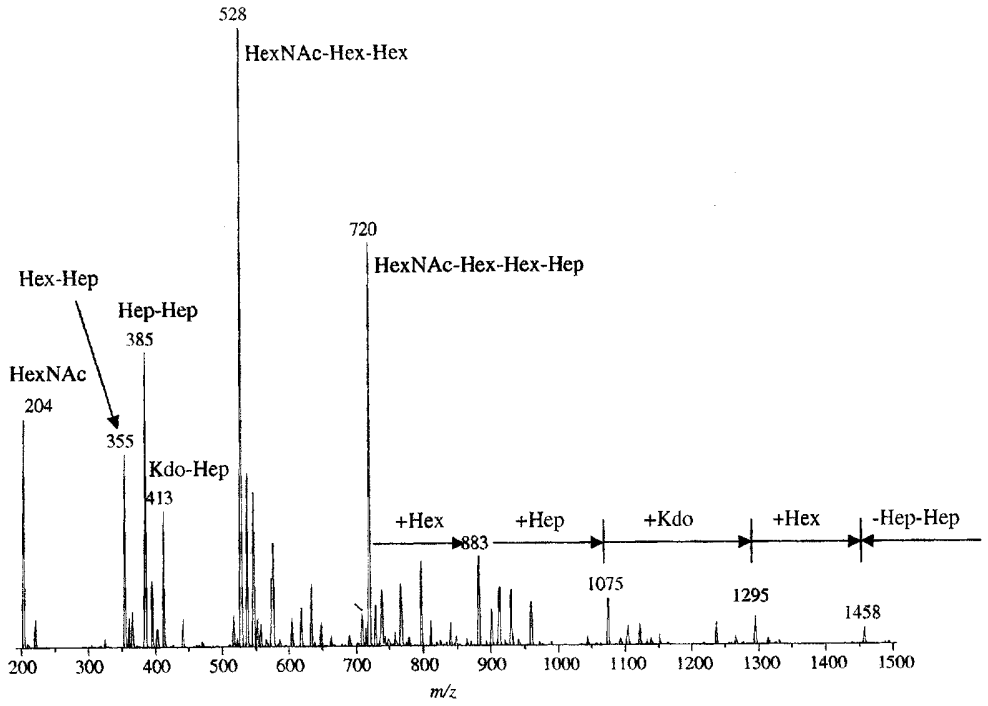

Example 2, Fig.7

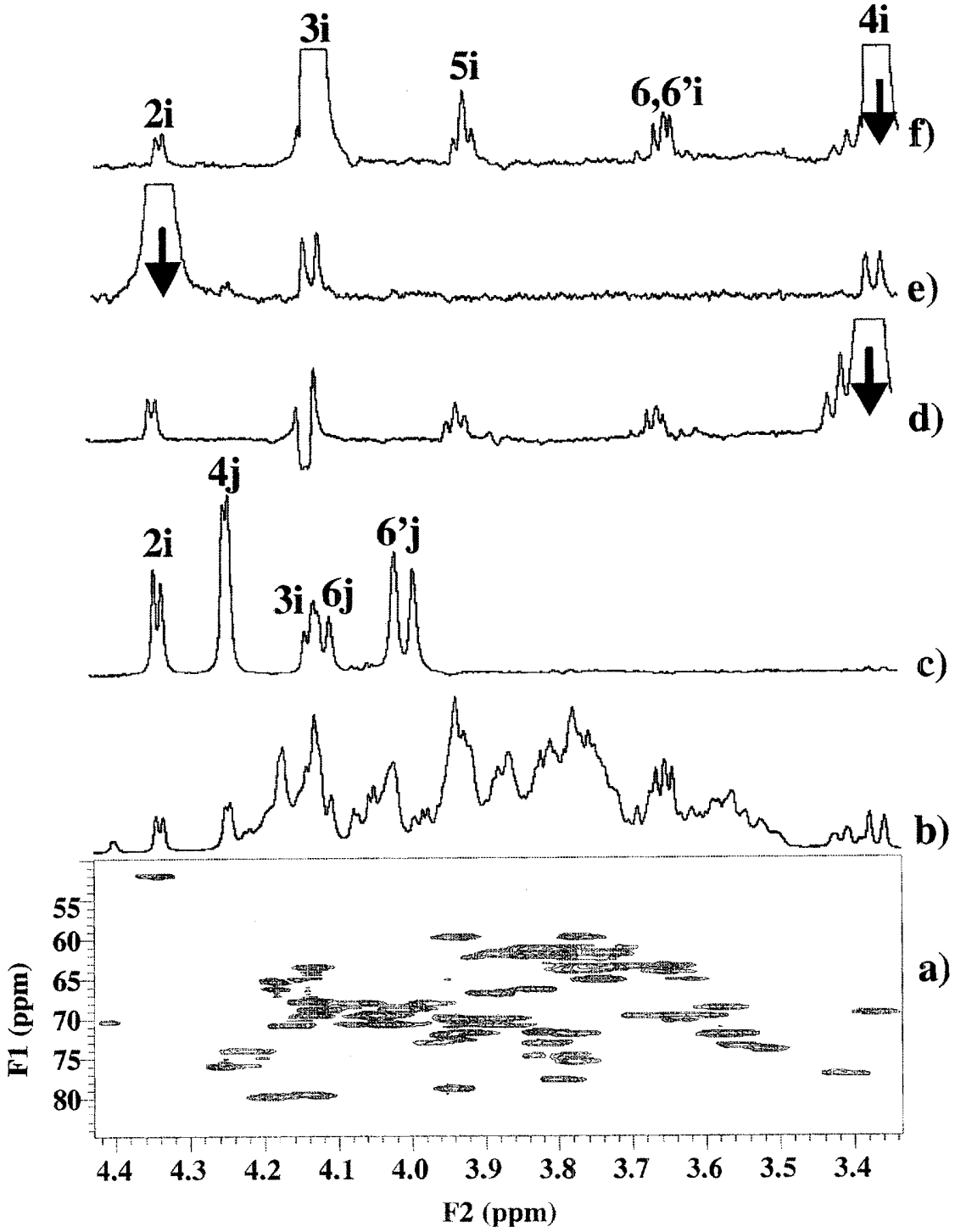

Example 2, Fig.8

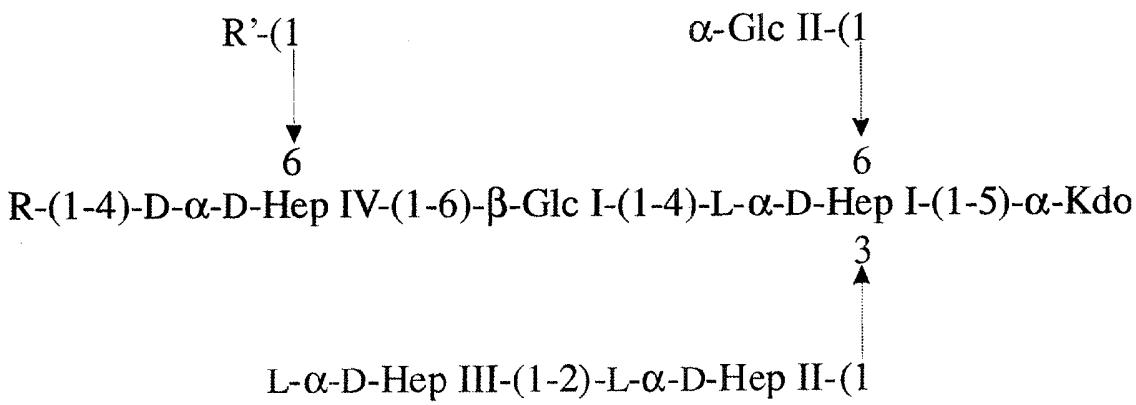

Example 2,

Table 1: Negative ion ES-MS and CE-ES-MS data and proposed compositions of *O*-deacylated LPS and core oligosaccharides from *A. pleuropneumoniae* serotypes 1, 2, 5a and 5b. Average mass units were used for calculation of molecular weight based on proposed composition as follows: Hex, 162.15; HexNAc, 203.19; Hep, 192.17; Kdo, 220.18; P, 79.98; PEtn, 123.05; Gly, 57.05. *O*-deacylated lipid A (Lipid A-OH) is 952.00.

Serotype	Observed Ions (*m/z*) $(M-2H)^{2-}$	$(M-3H)^{3-}$	Molecular Mass (Da) Observed	Calculated	Proposed Composition
1	1396	930	2794	2792.7	*HexNAc, 4Hex, 4Hep, Kdo, Lipid A-OH*
O-deac	1436	957	2874	2872.6	*HexNAc, 4Hex, 4Hep, Kdo, P, Lipid A-OH*
	1497	998	2997	2995.7	*HexNAc, 4Hex, 4Hep, Kdo, P, PEtn, Lipid A-OH*
Core OS	919	-	1840	1840.7	**HexNAc, 4Hex, 4Hep, aKdo**[a]
	928		1858	1858.7	**HexNAc, 4Hex, 4Hep, Kdo**
2	1309	872	2620	2620.5	**3Hex, 5Hep, Kdo, Lipid A-OH**
O-deac	1349	899	2700	2699.5	**3Hex, 5Hep, Kdo, P, Lipid A-OH**
Core OS	832	-	1667	1667.5	**3Hex, 5Hep, Kdo**
5a O-deac	1268	845	2537	2537.4	**2Hex, 5Hep, Kdo, P, Lipid A-OH**
Core OS	752		1505	1505.3	**2Hex, 5Hep, Kdo**
	780		1562	1562.3	**2Hex, 5Hep, Kdo, Gly**
5b O-deac	1268	845	2537	2537.4	**2Hex, 5Hep, Kdo, P, Lipid A-OH**
Core OS	752	-	1505	1505.3	**2Hex, 5Hep, Kdo**
	780		1562	1562.3	**2Hex, 5Hep, Kdo, Gly**

[a] The major ion corresponded to the molecular ion – 18 (loss of H_2O).

Example 2, Table 2: ^{1}H- and ^{13}C-NMR chemical shifts for the core OS from *Actinobacillus pleuropneumoniae* serotypes 1, 2, 5a and 5b.

	H-1	H-2	H-3	H-4	H-5	H-6	H-7	NOE's Inter	NOE's Intra	NOE's Long Range
Inner Core[a] Serotypes 1, 2, 5a, 5b										
Kdo (k)	-	-	2.08 1.92	4.10	4.21	4.48	nd			
Hep-I (a)	5.11 (98.9)	4.01 (71.2)	3.97 (73.7)	4.21 (74.7)	3.79 (72.6)	4.13 (80.3)	3.88 3.73 (62.9)	4.20 Kdo H-5	4.01 H-2	
Hep-I (A)	5.37 (101.3)	4.08 (71.2)	3.95 (73.5)	4.22 (74.6)	3.78 (72.6)	4.13 (80.3)	3.88 3.73 (62.9)	nd	4.00 H-2	
Hep-II (b)	5.70 (100.2)	4.19 (80.5)	3.87 (70.7)	3.89 (67.5)	3.55 (72.7)	4.04 (70.3)	3.76 3.74 (64.2)	5.15 Hep III H-1 3.97 Hep I H-3	4.19 H-2 3.87 H-3	3.79 Hep I H-5 3.82 Hep III H-5 3.77 Hep III H-7a 3.56 Glc I H-2
Hep-III[b] (c)	5.17 (102.3)	4.00 (71.5)	3.88 (71.6)	3.82 (67.1)	3.82 (72.4)	4.06 (70.2)	3.93 3.93 (70.3)	5.70 Hep II H-1 4.19 Hep II H-2	4.00 H-2	4.08 Hep IV H-2 3.80 Hep IV H-3 3.63 Glc I H-4
Hep-III[c]	5.17	4.00	3.88	3.82	3.82	4.04	3.77	5.70 Hep II H-1	4.00 H-2	4.08 Hep IV H-2

	(c)	(102.3)	(71.5)	(71.6)	(67.1)	(72.4)	(70.2)	3.62 (64.6)	4.19 Hep II H-2		3.80 Hep IV H-3 3.63 Glc I H-4
	β-Glc (Glc-I) (d)	4.66 (104.0)	3.56 (74.1)	3.43 (77.8)	3.63 (70.3)	3.54 (74.5)	4.06 3.70 (65.5)	-	4.21 Hep I H-4 4.13 Hep I H-6	3.54 H-5 3.43 H-3	5.21 Glc II H-1
	α-Glc (Glc-II) (e)	5.21 (102.6)	3.58 (72.8)	3.81 (73.8)	3.59 (69.3)	3.92 (72.4)	3.96 3.76 (60.2)	-	4.13 Hep I H-6	3.58 H-2	4.66 Glc I H-1
	Outer Core **Serotypes 5a, 5b**										
	Hep-IV (f)	4.96 (99.8)	4.08 (70.5)	3.80 (71.7)	3.78 (68.1)	3.93 (71.9)	4.13 (77.0)	3.90 3.80 (61.2)	4.06 Glc I H-6a 3.70 Glc I H-6b	4.08 H-2	
	Hep-V (g)	5.03 (99.0)	3.92 (70.8)	3.84 (71.5)	3.79 (68.2)	3.97 (73.7)	4.02 (73.1)	3.79 3.74 (63.0)	4.13 Hep IV H-6 3.93 Hep IV H-5	3.92 H-2 3.97 H-5	4.19 Hep II H-2 4.04 Hep II H-6 3.93 Hep IV H-5
	β-Gal (Gal-I) (h)	4.49 (104.2)	3.55 (71.6)	3.68 (73.4)	3.97 (69.5)	3.93 (74.5)	3.75 3.61 (65.7)	-	3.93 Hep III H-7a 3.93 Hep III H-7b	3.68 H-3 3.93 H-5	

Serotype 2

Hep-IV	4.96 (99.5)	4.13 (70.3)	3.90 (70.6)	3.96 (78.0)	4.05 (70.3)	4.30 (75.4)	3.97 3.82 (60.9)	4.06 Glc I H-6a 3.70 Glc I H-6b	4.14 H-2
Hep-V	5.02 (98.6)	3.88 (70.7)	3.82 (71.5)	3.78 (68.1)	3.97 (73.9)	4.00 (73.0)	3.80 3.74 (62.8)	4.30 Hep IV H-6 4.05 Hep IV H-5	3.88 H-2
β-Glc (Glc III)	4.53 (103.4)	3.33 (74.0)	3.51 (76.4)	3.41 (70.4)	3.51 (77.0)	3.95 3.74 (61.6)	-	3.96 Hep IV H-4 4.30 Hep IV H-6 4.05 Hep IV H-5	3.51 H-3 3.52 H-5

Serotype 1

Hep-IV[d]	4.95 (99.7)	4.13 (70.2)	3.94 (70.7)	3.94 (79.5)	3.94 (72.9)	4.17 (66.9)	3.83 3.80 (61.9)	4.15 Glc I H-6a 3.74 Glc I H-6b	4.13 H-2
β-Gal (Gal-I)	4.55	3.67	3.79	4.17	4.17	3.87	-	3.94 Hep IV H-4	3.79 H-3

		(103.9)	(70.3)	(78.4)	(65.9)	(71.6)	3.75 (62.4)			4.17 H-5
	α-Gal (Gal-II)	5.18	3.97	4.06	4.25	4.13	4.12	-	3.79 Gal I H-3	3.97 H-2
	(j)	(97.3)	(68.8)	(68.7)	(76.7)	(64.2)	4.01 (69.5)			
	α-GalNAc	4.88	4.34	4.13	3.36	3.93	3.66	-	4.25 Gal II H-4	4.34 H-2
	Open chain	(101.1)	(52.6)	(68.5)	(70.0)	(70.7)	3.64		4.12 Gal II H-6a	
	(i)						(64.1)		4.01 Gal II H-6b	

[a]; Inner core data derived from serotype 5a; letter designation of residues as indicated in parentheses. Chemical shifts from other serotypes inner core residues were virtually identical

[b]; Data for substituted Hep III residue in serotypes 5a and 5b

[c]; Data for terminal Hep III residue of serotypes 1 and 2

[d]; For serotype 1 ^{1}H-resonances, Glc I H-6a and H-6b are 4.15 and 3.74 ppm respectively.

Example 3

Investigation of P. multocida strain Pm70

Sugar analysis of the purified LPS revealed glucose (Glc), galactose (Gal) and L-*glycero*-D-*manno*-heptose (LD-Hep) in the approximate ratio of 4 : 2 : 3 respectively. Small amounts of *N*-acetyl- glucosamine (GlcNAc) and *N*-acetyl- galactosamine (GalNAc) were also identified.

LPS-OH was prepared and fractionated by gel filtration chromatography and analysed by CE-ES-MS (Example 3). A simple mass spectrum was observed with one major triply charged ion of *m/z* 1173.8 corresponding to a molecule of 3525 amu consistent with a composition of 2HexNAc, 4Hep, 6Hex, PEtn, Kdo, P, Lipid A-OH with low amounts of ions consistent with the loss or gain of one PEtn residue from the major species. CE-MS/MS analysis (data not shown) on the triply charged ion *m/z* 1173.8 gave a singly charged peak of *m/z* 951 and a doubly charged ion of *m/z* 1236.5, confirming the size of the O-deacylated lipid A as 952 amu and the core OS as 2475. The O-deacylated lipid A basal species (952 amu) consists of a disaccharide of N-acylated (3-OH C 14:0) glucosamine residues, each residue being substituted with a phosphate molecule. ES-MS and CE-ES-MS analyses of the fractionated OS sample revealed a mass of 2492 Da, consistent with a composition of 2HexNAc, 4Hep, 6Hex, PEtn, Kdo (Example 3 Table 1) (Example 3 Fig. 1). CE-ES-MS/MS analyses in positive ion mode was performed on the core OS in order to obtain information as to the location of some of the functional groups in the OS molecule. MS/MS analysis on the doubly charged ion at *m/z* 1246.5^{2+} revealed several product ions (Example 3, Fig. 2). Dominant were the singly charged ions corresponding to a HexNAc residue at 204.5^{+}, and two HexNAc residues at 407.5^{+}. Other product ions were also identified and correspond to the compositions indicated in Example 3 Fig. 2. Following precursor ion scanning for an ion with *m/z* 316 (which corresponds to a Hep-PEtn group) the PEtn moiety of the core OS was localized to a heptose residue (Hep) of the inner core by virtue of the identification of hydrated doubly charged ions of *m/z* 817.5^{2+} (3Hex, 4Hep, Kdo, PEtn), 898.5^{2+} (4Hex, 4Hep, Kdo, PEtn), 979.5^{2+} (5Hex, 4Hep, Kdo, PEtn), 1059.5^{2+} (6Hex, 4Hep, Kdo, PEtn) and 1263.5^{2+} (2HexNAc, 6Hex, 4Hep, Kdo, PEtn) (Example 3, Fig. 3). Precursor ion scanning for an ion with *m/z* 407 (which corresponds to a HexNAc-HexNAc group) revealed a

singly charged ion of 893^+ that corresponds to a composition of 3Hex, 2HexNAc (data not shown). These two precursor ion experiments therefore suggested an inner core composition of 3Hex, 4Hep, Kdo, PEtn with an outer core extension of 3Hex and 2HexNAc residues.

Methylation analysis was performed on the core OS in order to determine the linkage pattern of the molecule revealing the presence of terminal Glc, terminal Gal, 6-substituted Glc, 4-substituted Glc, 4-substituted Gal, 3-substituted Gal, terminal LD-Hep, 2-substituted LD-Hep, 4,6-disubsituted LD-Hep, and 3,4,6-tri-substituted LD-Hep in the approximate molar ratio of 2 : tr : 1: 1 : 1: 1 : 1 : tr : 1 : tr.

In order to elucidate the exact locations and linkage patterns of the OS, NMR studies were performed on the OS fraction that gave the most resolved and homogeneous spectrum (Example 3, Fig. 4). The assignment of ^{1}H resonances of the OS was achieved by COSY and TOCSY experiments with reference to the structurally related core OS from *Mannheimia haemolytica* and *Actinobacillus pleuropneumoniae* (Brisson, *et al*, 2002, Example 2) (Example 3, Table 2).

In the ^{1}H spectrum of the Pm70 OS, spin systems arising from heptose residues (Hep I, Hep II, Hep III and Hep IV) were readily identified from their anomeric ^{1}H resonances at 5.04 (Hep I), 5.76 and 5.85 (Hep II), 5.10 and 5.23 (Hep III) and 4.96 (Hep IV) ppm coupled with the appearance of their spin systems which pointed to *manno*-pyranosyl ring systems. The heterogeneity observed for the anomeric protons of Hep II and Hep III was thought to be due to the presence or absence of the PEtn moiety as inferred from the two H-2 resonances observed for each H-1 resonance of Hep II at 4.29 and 4.19 ppm, the former resonance consistent with substitution of the Hep II residue at the 3-position with PEtn (see below) and the latter shift consistent with the absence of PEtn. Additionally, inter-residue NOE's from the anomeric resonances of each Hep II residue at 5.76 and 5.85 ppm were observed to 5.10 and 5.23 ppm respectively, consistent with the heterogeneity of Hep III being due to the presence or absence of PEtn at Hep II. The □-configurations were evident for the heptosyl residues from the occurrence of intra-residue NOE's between the H1 and H2 resonances only. Two of the remaining residues in the □-anomeric region at 5.21 ppm (Glc II) and 5.08 ppm (GlcNAc) were determined to be *gluco*-

pyranose sugars, based upon the appearance of their spin systems. The *gluco*-configured residue at 5.08 ppm was determined to be an amino sugar by virtue of its ^{1}H resonance of its H-2 proton at 4.22 ppm correlating to a ^{13}C chemical shift of 49.5 ppm in a ^{13}C-^{1}H HSQC experiment. The ^{13}C chemical shift being consistent with a nitrogen substituted carbon atom. The remaining residue in the □-anomeric region at 4.94 ppm (Gal II) was determined to be a *galacto*-pyranose sugars, based upon the appearance of its characteristic spin system to the H-4 resonance in a TOCSY experiment. The remainder of the anomeric resonances in the low field region (4.45 – 6.00 ppm) of the spectrum were all attributable to □-linked residues by virtue of their anomeric ^{1}H resonances and in the case of resolved residues their high $J_{1,2}$ (~ 8 Hz) coupling constants. Resonances at 4.64 ppm (Glc I), 4.69 ppm (Glc III) and 4.69 ppm (Glc IV) were assigned to the *gluco*-configuration from the appearance of their spin systems. The remaining resonances in the low-field region at 4.52 ppm (Gal I) and 4.73 ppm (GalNAc) were assigned to *galacto*-pyranosyl residues from the appearance of characteristic spin systems to the H-4 resonances in a TOCSY experiment. The *galacto*-configured residue at 4.73 ppm was determined to be an amino sugar by virtue of its ^{1}H resonance of its H-2 proton at 4.11 ppm correlating to a ^{13}C chemical shift of 51.0 ppm in a ^{13}C-^{1}H HSQC experiment. The ^{13}C chemical shift being consistent with a nitrogen substituted carbon atom. Signals for the CH_2 protons of the PEtn moiety were observed at 3.27 and 4.16 ppm that correlated to characteristic ^{13}C chemical shifts of 40.1 and 62.2 ppm respectively in a ^{13}C-^{1}H HSQC experiment. Additionally characteristic signals for acetyl groups of the amino sugars were observed at 2.06 and 2.03 ppm that correlated to ^{13}C chemical shifts of 22.4 and 22.1 ppm respectively in a ^{13}C-^{1}H HSQC experiment.

The sequence of the glycosyl residues in the OS was determined from the inter-residue ^{1}H-^{1}H NOE measurements between anomeric and aglyconic protons on adjacent glycosyl residues and confirmed and extended the methylation analysis data. The linkage pattern for the Pm70 OS was determined in this way (Example 3, Fig. 4 and Table 2). Thus the occurrence of intense transglycosidic NOE connectivities between the proton pairs Hep III H-1 and Hep II H-2, Hep II H-1 and Hep I H-3 and Hep I H-1 and Kdo H-5 established the sequence and points of attachment of the three LD-heptose residues. This linkage pattern is commonly encountered in the inner core OS from

Haemophilus influenzae and *Mannheimia haemolytica*. Furthermore, inter-residue NOE's between the anomeric protons Hep III H-1 and Hep II H-1provided confirmation of the 1,2-linkage. Examination of NOE connectivities from H-1 of Glc I illustrated that this glucose residue was connected to Hep I at the 4-position by virtue of inter-residue NOE's to Hep I H-4 and Hep I H-6. The appearance of an inter-residue NOE to H-6 is a common occurrence for 4-substituted heptose residues. The occurrence of a long range NOE connectivity between H-1 of Glc I and H-1 of Glc II indicated the □-configured glucose residue (Glc II) was substituting Hep I at the 6-position. Examination of NOE connectivities from H-1 of Glc II confirmed that this glucose residue was connected to Hep I at the 6-position by virtue of inter-residue NOE's to Hep I H-6. Similarly to Glc I a long-range NOE connectivity was observed between the anomeric ^{1}H resonances of Glc I and Glc II. Examination of NOE connectivities from H-1 of Hep IV revealed that this heptose residue was connected to Glc I at the 6-position by virtue of inter-residue NOE's to Glc I H-6a and H-6b. This inner core glycose structure has been observed previously for both *Mannheimia haemolytica* and *Actinobacillus pleuropneumoniae*, however in both these cases the HepIV residue was of the D-*glycero*-D-*manno* configuration, whereas here the HepIV residue is of the L-*glycero*-D-*manno* configuration. The linkage pattern of the outer core residues was deduced from the NOE connectivities in conjunction with the methylation analysis data. The two *gluco*-configured residues with their anomeric proton resonances at 4.69 ppm showed inter-NOE connectivities to the H-4 and H-6 proton resonances of the Hep IV residue at 4.14 and 4.30 ppm, consistent with the 4,6-disubstituted L,D-heptose residue observed in methylation analysis and similar to the arrangement of HepIV observed in *Actinobacillus pleuropneumoniae* serotype 2 (St. Michael *et al*, 2004). By virtue of the intensity of the NOE connectivities it could be determined that Glc III was linked to HepIV at the 4-position and Glc IV was linked to HepIV at the 6-position. An inter-NOE connectivity from the anomeric proton resonance of Gal I at 4.52 ppm to the H-4 proton resonance of Glc IV suggested that Gal I substituted Glc IV at the 4-position, confirmed by methylation analysis that had resolved two 4-linked hexose residues i.e. a 4-linked glucose and a 4-linked galactose residue. An inter-NOE connectivity from the anomeric proton resonance of Gal II at 4.94 ppm to the H-4 proton resonance of Gal I suggested that Gal II substituted Gal I at the 4-position, consistent with the two 4-linked hexose residues observed by methylation analysis. An inter-NOE connectivity from the

anomeric proton resonance of GalNAc at 4.73 ppm to the H-3 proton resonance of Gal II suggested that GalNAc substituted Gal II at the 3-position, confirmed by methylation analysis that had identified a 3-linked hexose residue. Finally, an inter-NOE connectivity from the anomeric proton resonance of GlcNAc at 5.08 ppm to the H-3 proton resonance of GalNAc suggested that GlcNAc substituted GalNAc at the 3-position, consistent with MS/MS identification of a HexNAc-HexNAc disaccharide. Confirmation of the 3-position of Hep II as the location of PEtn substitution was obtained from ^{31}P-^{1}H-HSQC and ^{31}P-^{1}H-HSQC-TOCSY experiments. The HSQC experiment identified a cross-peak from the phosphorus signal to the proton resonance at 4.39 ppm which had been assigned to the 3-position of the Hep II residue and this was confirmed and extended in the HSQC-TOCSY experiment which revealed the H-2 and H-1 proton resonances of Hep II at 4.29 and 5.85 ppm respectively.

Example 3

DISCUSSION

Structural analysis of the oligosaccharide of the Pm70 genome strain of *Pasteurella multocida* has revealed a structure with similarities to the previously determined LPS core oligosaccharide structures for the related species *Mannheimia haemolytica* (Brisson *et al*, 2000), *Actinobacillus pleuropneumoniae* (Example 2), *Haemophilus ducreyi* (Schweda *et* al, 1994) and *Haemophilus influenzae* (Cox *et al*, 2001a). In each case the core OS contains an identically linked tri-heptosyl unit that is attached to a Kdo residue. Interestingly in *Pm* the 3-position of the HepII residue is substituted in the majority of cases with a PEtn residue, whereas *App*, *Hd* and *Mh* do not contain a PEtn residue and *Hi* elaborates a PEtn residue at the 6-position of Hep II. The substitution pattern at the Hep I residue of *Pm* is identical to that found for the veterinary pathogens *App* and *Mh* with two glucose residues at the 4- and 6-positions, whereas the Hep I residue in *Hi* and *Hd* is only substituted at the 4-position. Additionally the glucose residue at the 4-postion of Hep I is consistently substituted at the 6-postion with a heptose residue in the three veterinary pathogens, *Hd* and in some strains of *Hi*. However in *Pm* (and in some strains of *Hi*) the heptose residue substituting the glucose residue is L-*glycero*-D-*manno* configured compared to a D-*glycero*-D-*manno* configured heptose residue in *App*, *Hd*, *Mh* and some strains of *Hi*.

The substitution pattern of this heptose residue is considerably varied amongst these strains and it is at this point of the OS structure that the conserved inner core structural similarities between the various strains ends. In *Pm* the heptose residue is di-substituted with two glucose residues at the 4- and 6-positions, similar to *App* serotype 2 in which this heptose residue is di-substituted at the same locations, but with another heptose residue at the 4-position rather than a glucose residue. *Mh* also has a further D,D-heptose residue at the 4-position whereas *App* serotype 1, *Hd* and *Hi* also have further hexose extensions from this fourth heptose residue, but none have the extension observed here which terminates in the novel GlcNAc-GalNAc disaccharide unit.

Several candidate glycosyltransferases for the biosynthesis of the Pm70 OS were identified (Example 3, Fig. 8). Several putative heptosyltransferases were identified in the Pm70 genome sequence and included a Hep III Tase PM1294, a Hep II Tase PM1844, two Hep I Tases PM1302 and PM1843 and a Hep IV Tase PM1144.The best homologue of each of these genes in the databases are detailed in Table 3 and clearly suggests that the candidate PM gene would have the indicated function. Example 5 shows that PM1294 is the Hep III Tase in another *Pm* strain VP161. The gene that adds the α-glucose to the 6-position of Hep I is not known but there is a good homologue PM1306 to the β-glucosyltransferase that substitutes Hep I at the 4-position. Interestingly, several genes involved in the biosynthesis of the Kdo, Hep I, Glc I region are clustered in this region of the chromosome. Putative glycosyltransferases for the outer core region also appear to be clustered in a region of the chromosome ranging from PM1138 to PM1144. This clustering of glycosyltransferase genes is not always observed in this genus and indeed the glycosyltransferase for *Hi* OS are liberally scattered throughout the genome. Of course these homologues may not be the actual transferases but in all likelihood are. Another locus of glycosyltransferases can be found in another region of the *Pm* genome from PM506 to PM512. This locus lines up very well with the so-called lsg locus from both *Hi* and *Hd*. This study has structurally characterised the core OS region of the genome strain of *Pasteurella multocida* and identified putative glycosyltransferases for the complete biosynthesis of the core OS.

Example 3

MATERIALS and METHODS

Media and Growth conditions

Pm strain Pm70 (NRCC # 6232) was initially grown overnight on chocolate agar plates at 37°C and growths were used to inoculate 1 L of brain-heart infusion (BHI) medium supplemented with ∃ NAD (Sigma N-7004) to a final concentration of 5ug/ml, haemin (Sigma H-2250) to a final concentration of 5ug/ml and 1% glucose (10g). Cultures were then incubated at 37°C at 200 rpm for 6 hours and used to inoculate 24 L BHI medium (supplemented as above) in a 28 L NBS fermenter. The cultures were then grown at 37°C, with 24 $lmin^{-1}$ aeration and stirring at 200 rpm for 18 hours with 20% O_2 saturation. Following treatment with hyaluronidase (1g, Sigma,) cells were killed (2% phenol w/v, for 4 hours) and harvested by using a Sharples continuous centrifuge (~240g wet weight).

Isolation and purification of lipopolysaccharide

Following washing of the lyophilised cell mass (~ 70g) with organic solvents yielding ~ 50g, the lipopolysaccharide (LPS) was isolated from 10g of the washed, lyophilised cell mass by the hot water/phenol method. The aqueous phase was dialysed against water and lyophilised. The dried sample was dissolved in water to give a 1-2% solution (w/v) and treated with deoxyribonuclease I (DNase) (0.01 mg/ml) and ribonuclease (RNase) (0.01 mg/ml) for 3 hrs at 37°C, then treated with proteinase K (0.01 mg/ml) for 3hrs. The dialysed, dried sample was dissolved in water to make a 1 % solution and ultra-centrifuged at 45 K following a low speed spin at 8K to remove any insoluble material (124 mg). The LPS pellet from the 45K spin was redissolved in water and lyophilised (180 mg). Purified LPS (75 mg) was treated with anhydrous hydrazine with stirring at 37°C for 1 hr to prepare O-deacylated LPS (LPS-OH). The reaction was cooled in an ice bath and gradually cold acetone (-70°C, 5 vols.) was added to destroy excess hydrazine and the precipitated LPS-OH was isolated by

centrifugation (60 mg). The sample was then purified down a Bio-Gel P-2 column as described above. The core oligosaccharide (OS) was isolated by treating the purified LPS (100 mg) with 1 % acetic acid (10mgml^{-1}, 100°C, 1.5 hr) with subsequent removal of the insoluble lipid A by centrifugation (5000 g). The lyophilised OS (50 mg) was further purified down a Bio-Gel P-2 column with individual fractions lyophilised.

Analytical methods

Sugars were determined as their alditol acetate derivatives by GLC-MS. Samples were hydrolysed for 4 hrs using 4 M trifluoroacetic acid at 100°C, then reduced ($NaBD_4$) overnight in H_2O and acetylated with acetic anhydride at 100°C for 2h using residual sodium acetate as catalyst. The GLC-MS was equipped with a 30 M DB-17 capillary column (180°C to 260°C at 3.5°C/min) and MS was performed in the electron impact mode on a Varian Saturn II mass spectrometer. Methylation analysis was carried out by the NaOH / DMSO / methyl iodide procedure and analysed by GLC-MS as above.

Mass spectrometry

ESI-MS was performed in the negative ion mode on a VG Quattro Mass Spectrometer (Micromass, Manchester, U.K.) by direct infusion of samples in 25% aqueous acetonitrile containing 0.5% acetic acid. Capillary electrophoresis (CE)-ESI-MS was performed on a crystal Model 310 (CE) instrument (AYI Unicam) coupled to an API 3000 mass spectrometer (Perkin-Elmer/Sciex) via a microIonspray interface. A sheath solution (isopropanol-methanol, 2:1) was delivered at a flow rate of 1 □L/min to a low dead volume tee (250 □m i.d., Chromatographic Specialties). All aqueous solutions were filtered through a 0.45-□m filter (Millipore) before use. An electrospray stainless steel needle (27 gauge) was butted against the low dead volume tee and enabled the delivery of the sheath solution to the end of the capillary column. The separations were obtained on about 90 cm length bare fused-silica capillary using 10 mM ammonium acetate/ammonium hydroxide in deionised water, pH 9.0, containing 5% methanol. A voltage of 20 kV was typically applied at the injection

site. The outlet of the capillary was tapered to ca. 15 □m i.d. using a laser puller (Sutter Instruments). Mass spectra were acquired with dwell times of 3.0 ms per step of 1 *m/z* unit in full-mass scan mode. The MS/MS data were acquired with dwell times of 1.0 ms per step of 1 *m/z* unit. Fragment ions formed by collision activation of selected precursor ions with nitrogen in the RF-only quadrupole collision cell, were mass analyzed by scanning the third quadrupole.

Nuclear Magnetic Resonance

NMR experiments were acquired on Varian Inova 400, 500 and 600 MHz spectrometers using a 5 mm or 3mm triple resonance (^{1}H, ^{13}C, ^{31}P) probe. The lyophilised sugar sample was dissolved in 600 μL (5mm) or 140 μL (3mm) of 99% D_2O. The experiments were performed at 25°C with suppression of the HOD (deuterated H_2O) signal at 4.78 ppm. The methyl resonance of acetone was used as an internal reference at 2.225 ppm for ^{1}H spectra and 31.07 ppm for ^{13}C spectra. Standard homo and heteronuclear correlated 2D pulse sequences from Varian, COSY, TOCSY, NOESY, ^{13}C-^{1}H HSQC, ^{13}C-^{1}H HSQC-TOCSY and ^{13}C-^{1}H HMBC, were used for general assignments. The 1D ^{31}P experiment was carried out on a Varian Inova 200 spectrometer with a sweep width of 40 ppm, 20000 transients and acquisition time of 1.6 s. The 2D ^{1}H- ^{31}P HSQC experiment was acquired on a Varian Inova 400 spectrometer for 6 h. The coupling constant was optimised at 12 Hz by performing an array of 1D-HSQC experiments. The sweep width in the F2 (^{1}H) dimension was 6.0 ppm and in the F1 (^{31}P) dimension was 16.2 ppm. Water presaturation during the relaxation delay was 1.5 s, acquisition time in t_2 was 0.21 s, and 32 increments with 180 (HMQC) scans per increment were obtained. The 2D ^{1}H-^{31}P HSQC-TOCSY experiment was acquired on a Varian Inova 400 spectrometer for 8 h using the same parameters as the HSQC experiment with a TOCSY mixing time of 80 ms.

Example 3

FIGURE LEGENDS

Figure 1. Negative ion electrospray mass spectrum of *Pasteurella multocida* strain Pm70 core OS.

Figure 2. Positive ion capillary electrophoresis-electrospray mass spectrum of *Pasteurella multocida* strain Pm70 core OS MS/MS of *m/z* 1246.5^{2+}.

Figure 3. Positive ion capillary electrophoresis-electrospray mass spectrum of *Pasteurella multocida* strain Pm70 core OS precursor ion scan of *m/z* 316^{+}.

Figure 4. Anomeric region of the ^{1}H- NMR spectra of the core OS from *Pasteurella multocida* strain Pm70. The spectrum was recorded in D_2O at pH 7.0 and 25 ^{o}C.

Figure 5. Portion of the anomeric region of the TOCSY spectrum from the core OS from *Pasteurella multocida* strain Pm70. The spectrum was recorded in D_2O at 25^{o}C.

Figure 6. Portion of the anomeric region of the NOESY spectrum from the core OS from *Pasteurella multocida* strain Pm70. The spectrum was recorded in D_2O at 25^{o}C.

Figure 7. Anomeric region of the ^{1}H- ^{13}C HSQC NMR spectrum of the core OS from *Pasteurella multocida* strain Pm70. Inset is the region of the spectrum showing the diagnostic signals for the N-acetyl-amino sugars. The spectrum was recorded in D_2O at pH 7.0 and 25 ^{o}C.

Figure 8. Structure of the core oligosaccharide of *Pasteurella multocida* strain Pm70 with the putative glycosyltransferases indicated.

Example 3, Figure 1

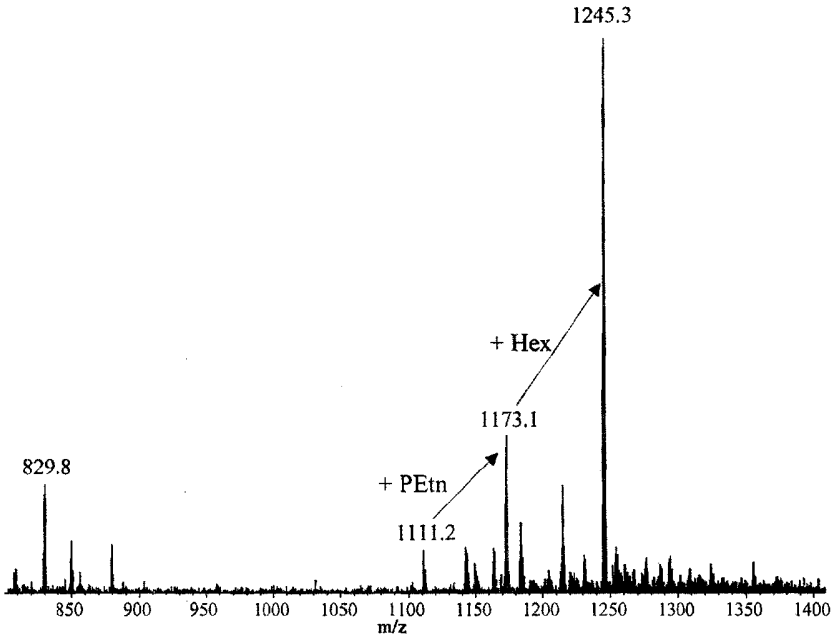

Example 3, Figure 2

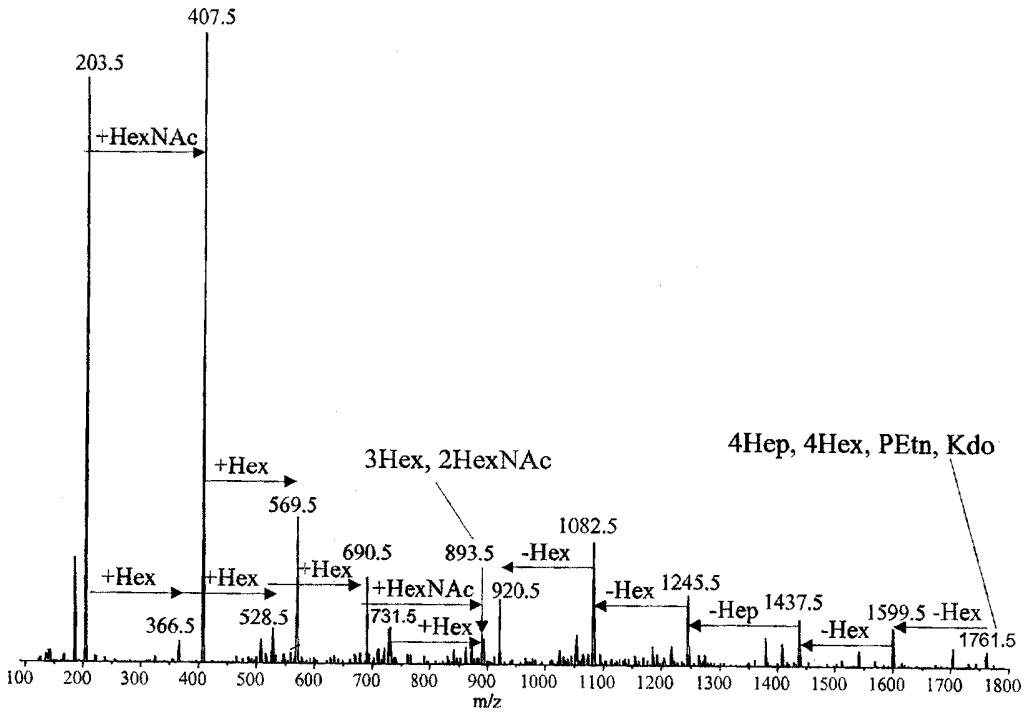

Example 3, Figure 3

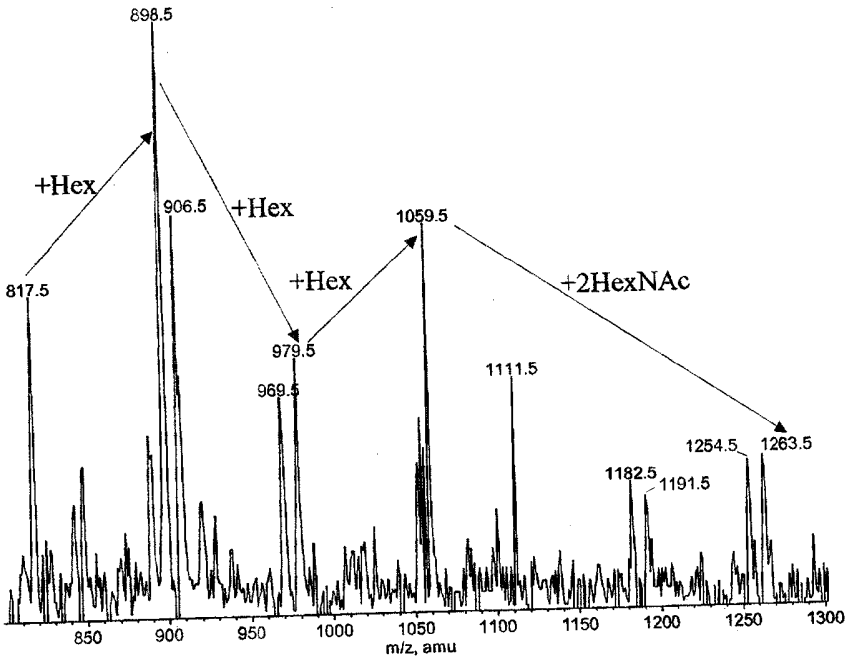

Example 3, Figure 4

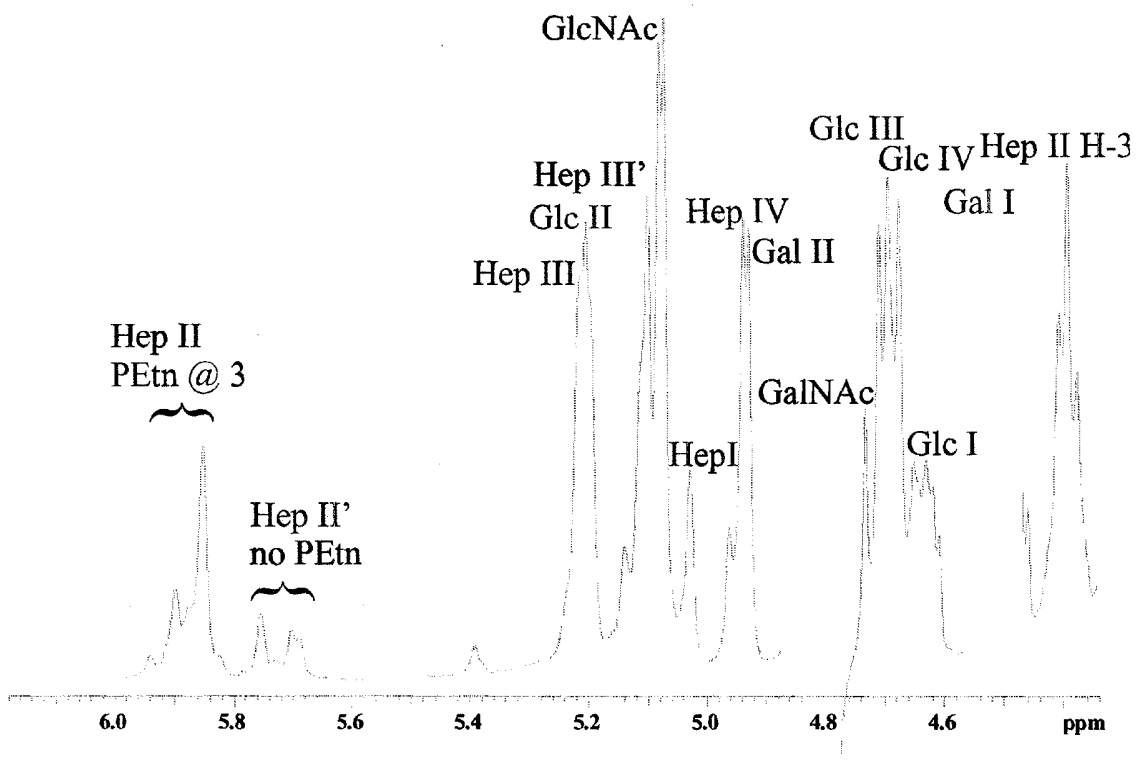

Example 3, Figure 5

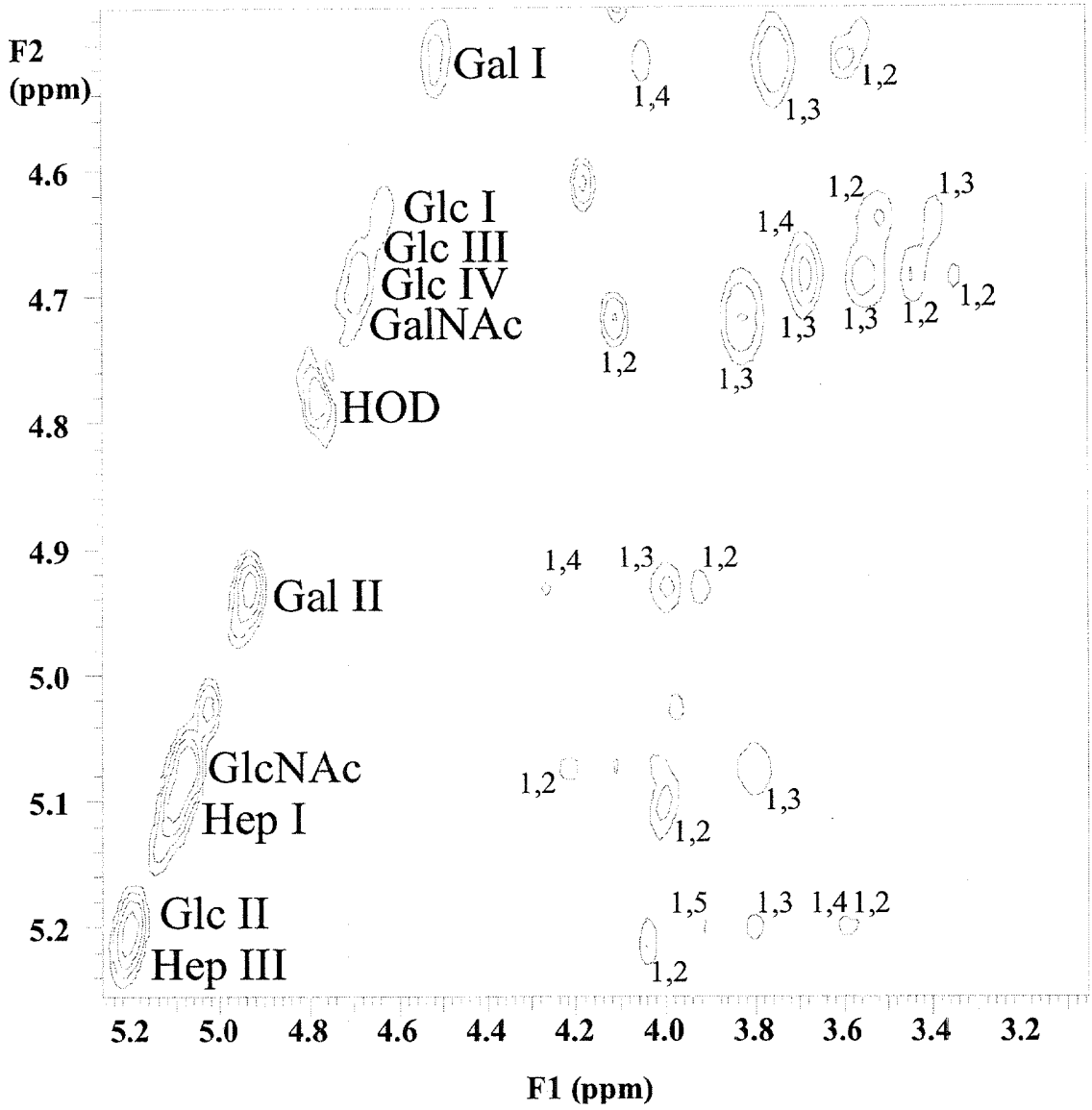

Example 3, Figure 6

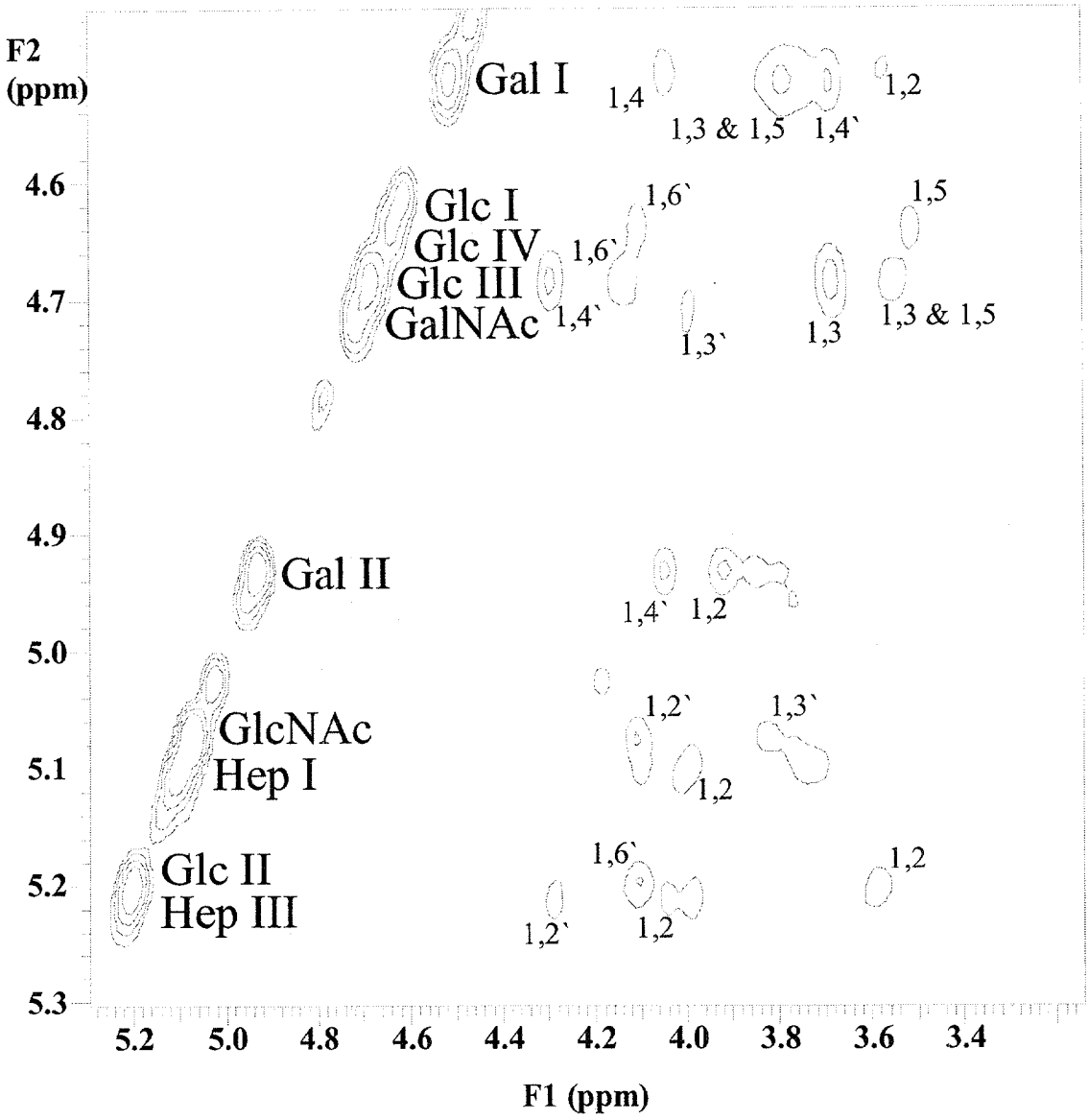

Example 3, Figure 7

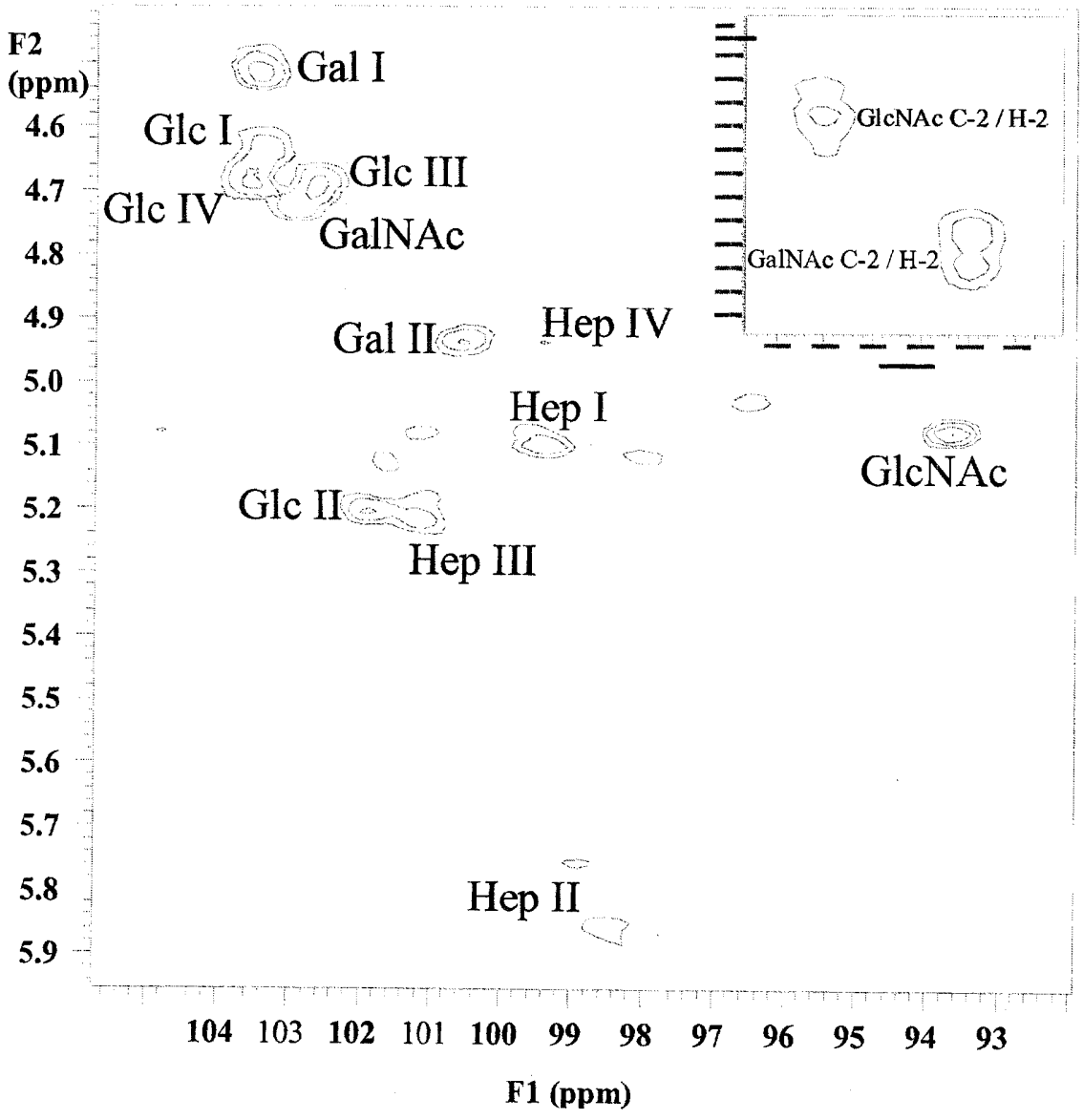

Example 3, Figure 8

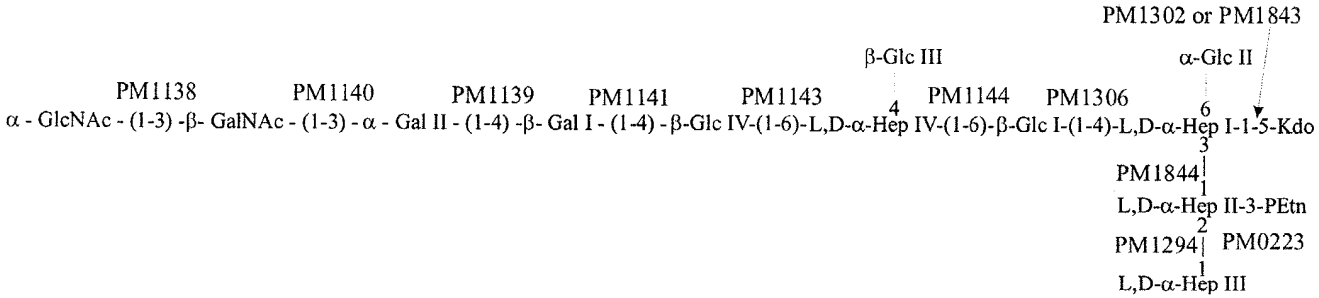

Example 3 Table 1: Negative ion CE-MS data and proposed compositions of core OS and O-deacylated LPS from *P. multocida* strain Pm70. Average mass units were used for calculation of molecular weight based on proposed composition as follows: Hex, 162.15; Hep, 192.17; Kdo, 220.18; HexNAc, 203.19; PEtn, 123.05.

Strain	$[M-3H]^{3-}$	$[M-2H]^{2-}$	Observed Molecular Ion	Calculated Molecular Ion	Relative Intensity	Proposed Composition
Pm70		1111.2	2224.4	2224.0	0.1	2HexNAc, 4Hep, 5Hex, Kdo
Core OS	-	1173.1	2348.2	2347.0	.25	2HexNAc, 4Hep, 5Hex, PEtn, Kdo
	829.8	1245.3	2492.5	2491.2	1.0	2HexNAc, 4Hep, 6Hex, PEtn, aKdo
Pm70	1132.9	1700.7	3402.5	3400.1	0.5	2HexNAc, 4Hep, 6Hex, Kdo, P, Lipid A-OH
O-deac	1173.8	1761.4	3524.6	3523.1	1.0	2HexNAc, 4Hep, 6Hex, PEtn, Kdo, P, Lipid A-OH
	1215.2	-	3648.6	3646.2	0.25	2HexNAc, 4Hep, 6Hex, 2PEtn, Kdo, P, Lipid A-OH

Example 3 Table 2: ^{1}H- and ^{13}C-NMR chemical shifts for the core OS from *Pasteurella multocida* Pm70 Fr 19.

	H-1	H-2	H-3	H-4	H-5	H-6	H-7	NOE's		
								Inter	Intra	Long Range
Kdo	-	-								
Hep-I	5.10	4.02	3.99	4.22		4.11	3.86	Kdo H-5	3.98 H-2	
	(99.4)	(70.6)	(78.9)	(73.9)	()	(79.5)	3.73	Kdo H-7		
							(62.1)			
Hep-II(PE@3)	5.85	4.29	4.39					5.22 Hep III H-1	4.29 H-2	3.77 Hep I H-5
	(98.6)	(79.2)	(75.4)	()	()	()		3.99 Hep I H-3		
							()			
Hep-III	5.22	4.04						5.85 Hep II H-1	4.04 H-2	
	(101.1)	(71.0)	()	()	()	()		4.29 Hep II H-2		
							()			
β-Glc (Glc-I)	4.64	3.53	3.40	3.60	3.52	4.06	-	4.22 Hep I H-4	3.52 H-5	5.21 Glc II H-1
	(103.3)	(73.5)	(77.2)	(69.7)	(73.8)	3.73		4.11 Hep I H-6	3.40 H-3	3.77 Hep I H-5

						(64.9)				
α-Glc (Glc-II)	5.20	3.59	3.80	3.59	3.92	3.95	-	4.11 Hep I H-6	3.59 H-2	4.64 Glc I H-1
	(101.9)	(72.3)	(73.1)	(68.7)	(71.7)	3.74				3.77 Hep I H-5
						(59.7)				
Hep-IV	4.96	4.18	3.93	4.14	4.11	4.30	3.96	4.06 Glc I H-6	4.17 H-2	
	(99.3)	(70.1)	()	(77.1)	(70.7)	(79.4)	3.77	3.73 Glc I H-6		
							(62.9)			
β-Glc(Glc-III)	4.69	3.37	3.56	3.41	3.56	3.94	-	4.14 Hep IV H-4	3.56 H-3	
	(102.6)	(73.3)	(75.9)	(69.7)	(75.8)	3.75		3.95 Hep IV H-3	3.56 H-5	
						(60.8)				
β-Glc(Glc-IV)	4.69	3.45	3.69	3.69	3.94	3.96	-	4.30 Hep IV H-6	3.69 H-3	3.94 Hep IV H-3?
	(103.6)	(73.2)	(74.5)	(78.8)	(70.4)	3.76		4.14 Hep IV H-4	3.94 H-5	
						(63.0)				
β-Gal (Gal-I)	4.52	3.60	3.76	4.05	3.79	nd	-	3.69 Glc IV H-4	3.76 H-3	
	(103.4)	(71.1)	(72.3)	(77.4)	(75.6)	nd			3.79 H-5	

						(69.5)				
	α-Gal (Gal-II)	4.93 (100.6)	3.92 (70.4)	4.00 (79.1)	4.27 (69.1)	4.08 (65.3)	3.70 nd (69.5)	-	4.05 Gal I H-4	3.92 H-2	3.79 Gal I H-5
	β-GalNAc	4.72 (102.8)	4.11 (51.0)	3.83 (74.8)	3.91 (63.7?, 73.1?, 77.0?)				4.00 Gal II H-3	3.83 H-3 H-5	
	α-GlcNAc	5.08 (93.7)	4.22 (49.5)	3.81 (67.9)	4.02 (70.8)	4.11 (63.8)			3.83 GalNAc H-3	4.22 H-2	4.11 GalNAc H-2
	PEtn	3.26 (40.1)	4.16 (62.2)								
	$CH_3C=O$	2.06 (22.4)									
	$CH_3C=O$	2.0 (22.1									

Example 3 Table 3. Putative glycosyltransferases for the LPS core biosynthesis in *Pasteurella multocida* genome strain Pm70.

P. multocida gene	Putative function	Best homologues	e-value
PM 1843	Hep I to Kdo α-1,5 heptosyltransferase	WaaC *Kp* WaaC *Ec*	e^{-96} e^{-94}
PM 1302	Hep I to Kdo α-1,5 heptosyltransferase	OpsX *Hi* (HI 0261)	e^{-149}
PM 1844	Hep II to Hep I α-1,3 heptosyltransferase	RfaF *Hi* (HI 1105) RfaF *Hd*	e^{-164} e^{-139}
PM 1294	Hep III to Hep II α-1,2 heptosyltransferase	OrfH *Hi* (HI 0523)	e^{-127}
PM 0223	PEtn to Hep II	Lpt3 *Nm* (NMB 2010)	e^{-154}
PM 1306	Glc I to Hep I β-1,4 glucosyltransferase	LgtF *Hi* (HI 0653)	e^{-108}
PM 1144	Hep IV to Glc I α-1,6 heptosyltransferase	LbgB *App* LbgB *Hd* (HD 1720)	e^{-93} e^{-87}
PM 1143	Glc IV to Hep IV β-1,6 glucosyltransferase	LbgA *Hd* (HD 1721) LbgA *App*	e^{-74} e^{-73}
PM 1141	Gal I to Glc IV	Lic2a *Hi* (HI 0550)	e^{-38}

	β-1,4 galactosyltransferase		
PM 1139	Gal II to Gal I α-1,4 galactosyltransferase	LgtC *Hi* (HI 0258) LgtC *Nm*	e^{-62} e^{-59}
PM 1140	GalNAc to Gal II α-1,3 N-acetylgalactosaminyltransferase	LgtD *Hi* (HI 1578)	e^{-83}
PM 1138	GlcNAc to GalNAc β-1,3 N-acetylglucosaminyltransferase	GTase *App*	e^{-62}

Example 4

Ap serotype 1

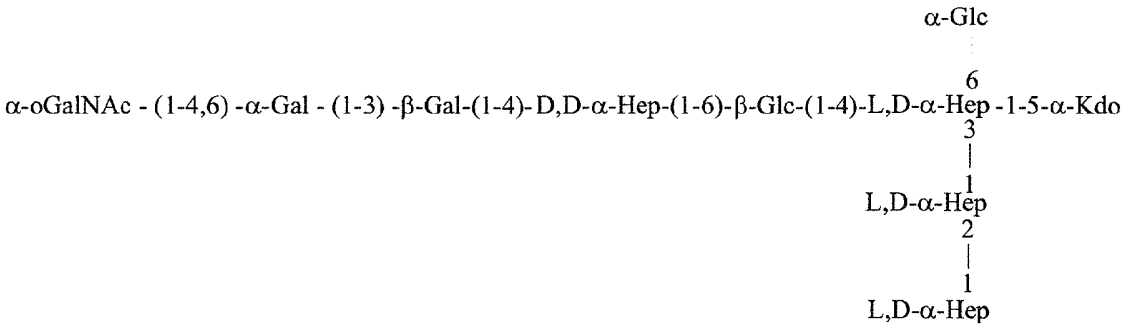

Ap serotype 2

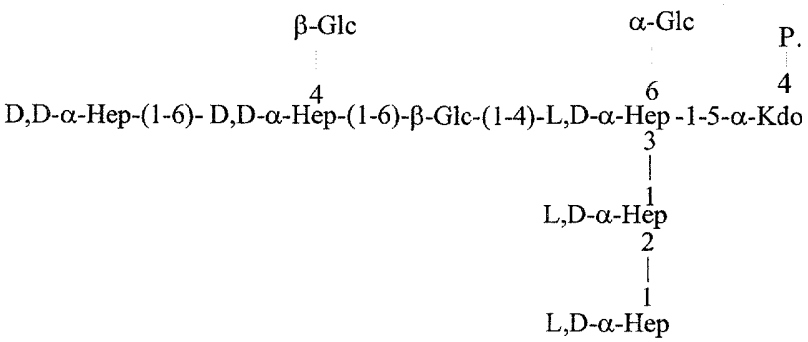

Ap serotype 5a/b

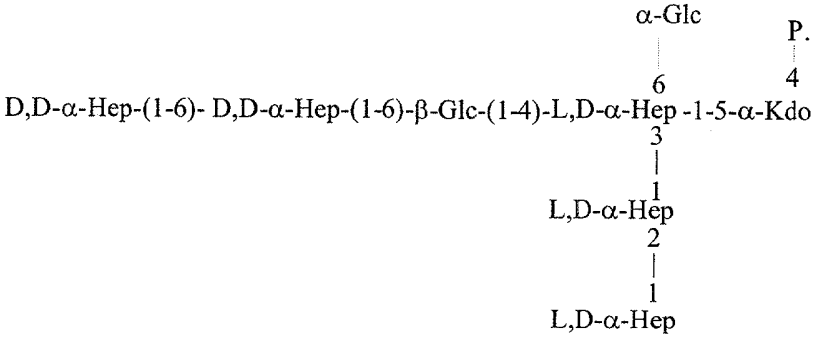

Mh serotype A1

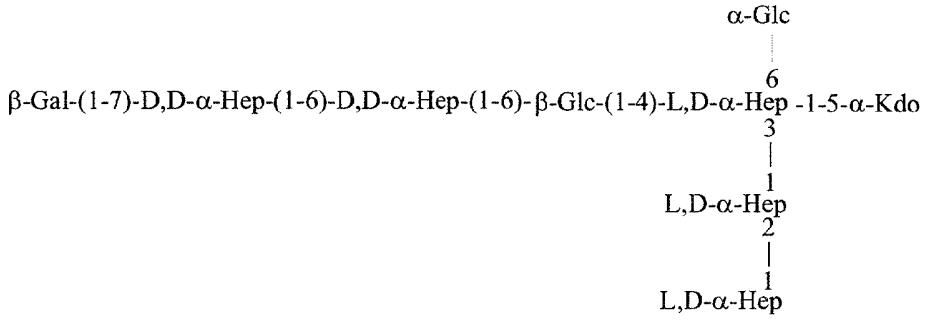

Pm genome strain Pm70

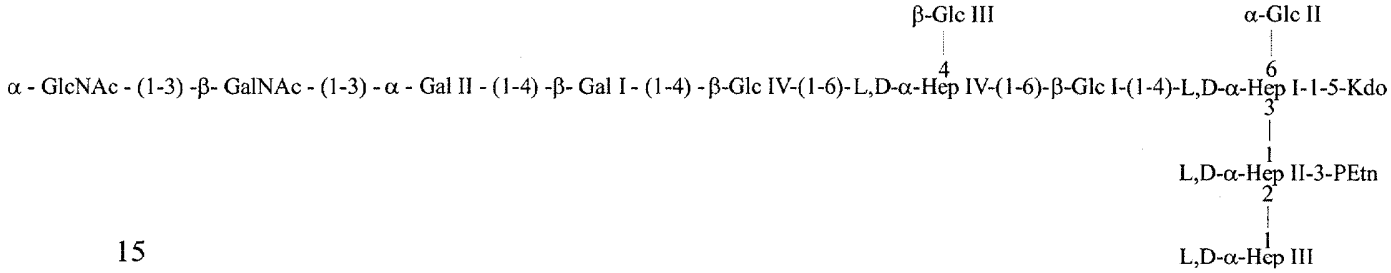

Pm strain VP161

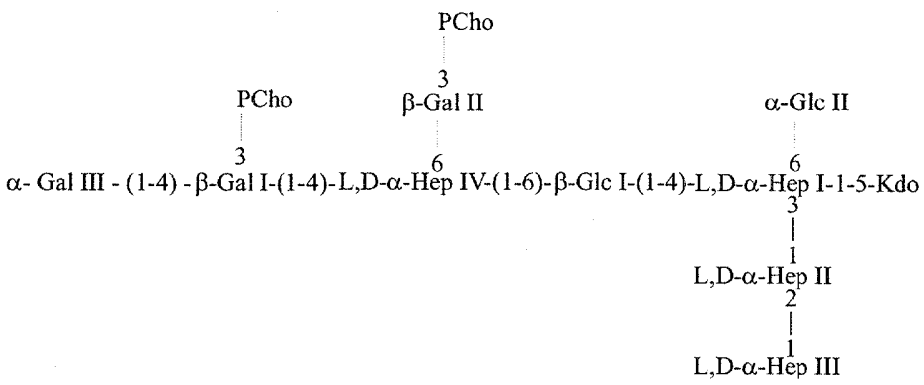

Inner Core Oligosaccharide Vaccine Candidate Antigen

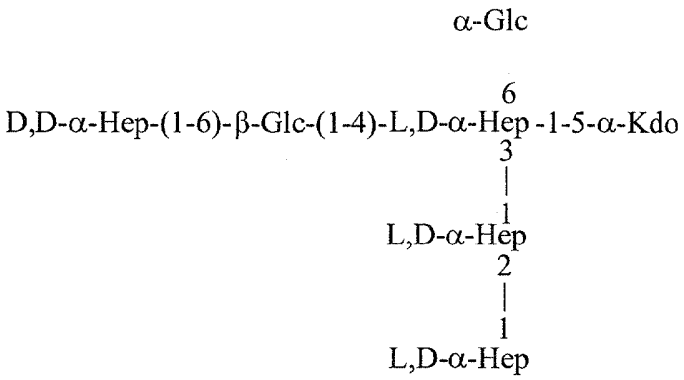

EXAMPLE 5

Analysis of the *P. multocida* VP161 wild type LPS indicated a "rough" LPS, similar to the LPS or lipooligosaccharide isolated from gram-negative mucosal pathogens such as *Haemophilus influenzae.*, *H. ducreyi*, *Neisseria meningitides*, and *N. gonorrhoeae*, with only a short nonrepeating polysaccharide unit attached to the lipid A. The inner-core structure of *P. multocida* LPS is similar to that described for *H. influenzae*, *Mannheimia haemolytica*, and *H. ducreyi* with a triheptose unit liked via a KDO residue to lipid A (Example 5, Fig. 4). In the AL251 mutant, inactivation of $waaQ_{PM}$ resulted in the expression of a highly truncated LPS that lacked the third heptose molecule (Hep III) in the inner-core region (Example 5). The most abundant glycoforms of LPS in the mutant also lacked all sugars distal to the first heptose, suggesting that the inactivation of $waaQ_{PM}$ prevented further sugar additions (Example 5). It is therefore probable that conformational changes in the LPS intermediates due to the lack of the third heptose largely prevented the action of subsequent transferases.

Example 5, Fig. 4

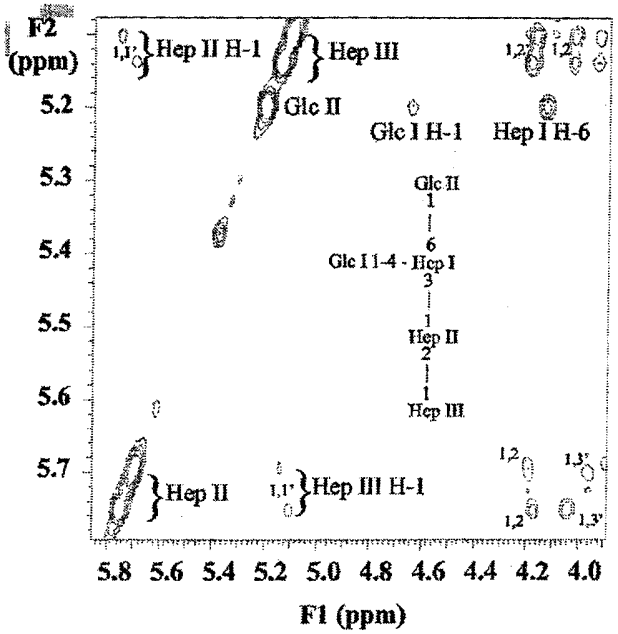

FIG. 4. Region of the NOESY spectrum of *P. multocida* VP161 core OS. NOE connectivities are as indicated. (Inset), Structure of the inner-core OS from VP161. The spectrum was recorded at 25°C and referenced against internal acetone at 2.225 ppm.

Example 5, Fig. 5

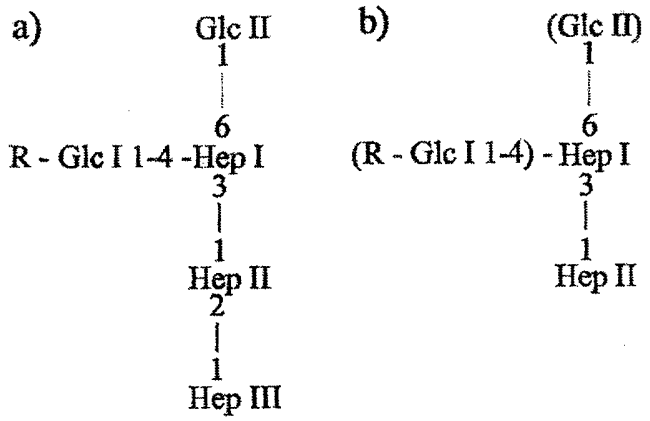

FIG. 5. Proposed structures of inner core LPS of *P. multocida* from parent strain VP161 (a) and mutant strain AL251 (b), where R is the OS chain extension beyond Glc. Based on negative-ion CE-MS data shown in Table 3, extension of the mutant LPS molecule to include the structures shown in parentheses occurs at only low frequency (less than 4%).

We Claim:

1. A lipopolysaccharide ("LPS") having the structure:

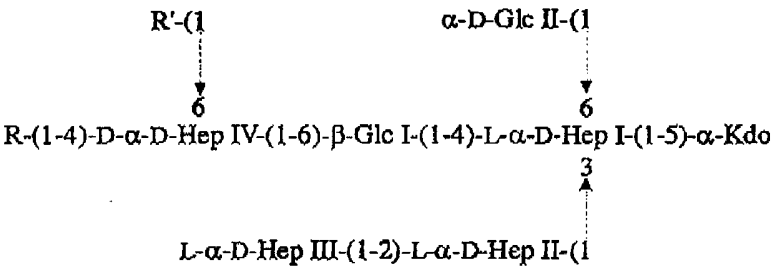

Where R and R' are variable outer core structures.

2. The LPS of claim 1 selected from at least one of:

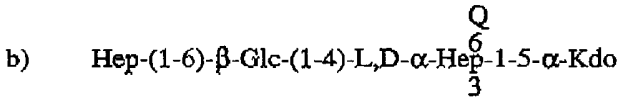

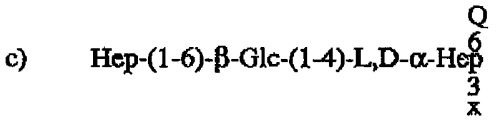

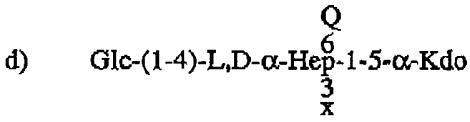

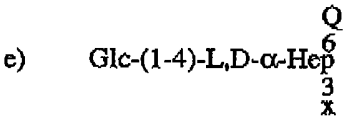

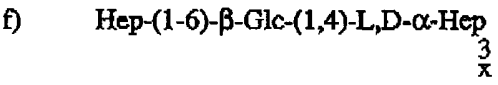

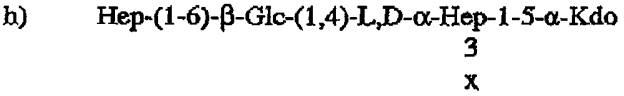

wherein:

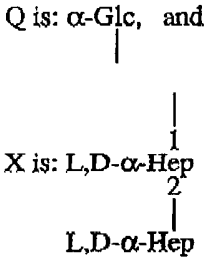

3. A method of making a vaccine comprising linking an LPS of claim 1 or a portion or variant thereof to an immunogenic carrier protein.

4. Use of the LPS of claim 1 in enhancing an immune response to bacterial infection.

5. A conjugate comprising an LPS f claim 1 or a portion thereof and an immunogenic carrier protein.

6. A vaccine comprising an LPS of claim 1 or a portion thereof.